Programa de Doctorado en Biociencias Moleculares

Departamento de Bioquímica

Facultad de Medicina

Universidad de Autónoma de Madrid

Understanding how Notch influences the development and fate of the hemogenic endothelium using genetic mosaics

Doctoral Thesis

Briane Danielle Laruy

Licenciada en Biología

Madrid, 2019

Director: Dr. Rui Benedito

Centro Nacional de Investigaciones Cardiovasculares (CNIC)

I am not here because I stood on the shoulders
of giants...

i stand
on the sacrifices
of a million women before me
thinking
what can i do
to make this mountain taller
so the women after me
can see farther

legacy - rupi kaur

SUMMARY

Notch is an important signaling pathway in the intraembryonic hematopoietic wave that occurs between E9.5-E11.5. Although most studies so far have claimed that its activity in endothelial cells (ECs) of the dorsal aorta (DA) is necessary for hematopoiesis, more recent evidence has suggested that Notch signaling must be downregulated for endothelial-to-hematopoietic transition (EHT) to occur. However, the exact molecular and cellular mechanisms are still not well characterized.

In this thesis we have used a wide range of novel genetic tools and imaging approaches to analyze the role of Notch in the EHT process with higher cellular, temporal, and molecular resolution. Our results show that embryos with increased Notch activity in the dorsal endothelium at E10.5 have a decrease in c-Kit^{+} hematopoietic stem progenitor cells (HSPCs). This is caused by a decrease in hemogenic specification, or CD31^{+}/Runx1^{+} cells. Additionally, HSPCs with high Notch activation presented proliferation defects as they tended to form unicellular clusters. We also found that embryos with loss of Jag1 in DA ECs had higher Dll4/Notch activity, which may explain why the loss of this Notch ligand also induces a decrease in hematopoiesis. This differential Jagged1/Dll4 Notch activity could be due to the known inhibitory role of Fringes on Jagged1/Notch signaling. Indeed overexpression of Manic Fringe in DA ECs resulted in a decrease in Dll4/Notch signaling and an increased number of HSPCs in the DA.

To determine the single cell-autonomous role of Notch during EHT, we induced Notch genetic mosaics in individual DA ECs. Single ECs with Notch loss-of-function (LOF) undergo EHT with more frequency compared to wildtype ECs. Comparative transcriptional profiling revealed that they had similar arterial endothelial identity (Sox17, Cx40) and hematopoietic progenitor (CD41) expression, however, we found that *Myc* and *Mycn* expression was significantly deregulated. Analysis of embryos with Myc and Mycn deletion in DA ECs surprisingly revealed that Mycn is a strong regulator of EHT, whereas Myc is dispensable. Mycn mutants presented a drastic loss of HSPCs in the DA whereas Myc mutants only displayed a late hematopoiesis progression phenotype.

Analysis of recently published single cell transcriptomic data allowed us to validate several of the experimental findings described above and to propose a model for the regulation of EHT by Notch. During EHT, most DA ECs have high Notch signaling induced by Jagged1 and Dll4 ligands and they are quiescent (KI67-). Among these cells, some upregulate Mfng, which decreases the signaling ability of the surrounding Jagged1 ligands and lowers Notch signaling cell-autonomously. These cells with lower Notch signaling upregulate Mycn, which is necessary to induce EHT. The Mycn induced EHT is associated with an entry into cell cycle which is subsequently maintained by the expression of the homologous gene Myc in the HSPCs.

RESUMEN

Notch es una vía de señalización importante en la onda hematopoyética intraembrionaria que se produce entre E9.5-E11.5. Aunque se especula que la señalización de Notch baja en las células endoteliales (EC) para que ocurra la transición endotelial-a-hematopoyética (EHT), el mecanismo molecular debajo de Notch en la aorta dorsal (DA) aún no está bien caracterizado.

En este tesis, hemos utilizado una amplia gama de herramientas genéticas novedosas.para analizar el papel de Notch en el prcoeso EHT con mayor resolución celular, temporal, y molecular. Nuestro resultados mostran quen en los embriones con mayor actividad de Notch en el endotelio dorsal tenían defectos en el sistema hemtopoyético definitivo en la aorta gonada mesonefros (AGM) en embriones de E10.5. Vimos una pérdida prejudicial de células madres progenitoras hematopoyético c-Kit+ (HSPC) en embriones con alta señalización de Notch. Los embiones con alta señalización de Notch tenían menos especificación hemogénica y un pequeño porcentaje de células endoteliales con alta activación celular autónoma de Notch también eran Runx1+. Además, las HSPCs con alta activación de Notch presentan defectos de proliferación. También hemos visto que en los mutantes Jag1 habia una alta tinción de Dll4/Notch1 y tiene un fenotipo similar a los embriones con alta señalización de Notch. Nosotros creiamos que los resultos implican un papel para Fringe. En efecto, sobreexpresión de Manic Fringe en el aorta bajan los niveles de la señalización de Dll4/Notch y suben los numeros de HSPCs en el aorta dorsal.

Utilizando mosaico genéticos de ratones para investigar el papel de Notch en el endotelio hemogénico (HE), hemos determinado que las ECs con pérdida de función de Notch (LOF) se someten a EHT con más frecuencia en comparación con las ECs de controles. Al asilar estas células, hemos encontrado que, aunque tenían una expresión de endotelio arterial (Sox17, CX40) y de progenitor hematopoyético (CD41+) similar a las ECs de controles, tanto Myc como Mycn se modificaron drásticamente. Utilizamos los mutantes Myc y Mycn para determinar si los dos factores de trascipción desempeñaron un papel en el desrrollo temprano del sistema hemtopoyético. Los mutantes de Mycn presentaron una pérdida drástica de HSPCs en la aorta, mientras mutantes de Myc tenian defectos hematoyecticos en adultos. El análisis de los datos transciptómicos de las células del aorta, tanto las HSPCs como las endoteliales, nos ayuda en proponer un modelo para la regulación de EHT por Notch. Durante EHT, la mayoría de las células del aorta dorsal tienen alta señalización de Notch inducido por los ligandos Jagged1 y Dll4 y bajo niveles de proliferación (Ki67-). Dentro de estas celulas, algunos suben la expresión de Manic Fringe y depués bajan los niveles de Notch en la celula de una forma autónoma. Estas celulas luego suben los niveles de Mycn, lo cual es necesaria para inducer EHT. El EHT inducido por Mycn se asocia con una entrada en el ciclo celular que posteriormente se mantiene mediante la expresión del gen homólogo Myc en las HSPCs.

TABLE OF CONTENTS

ABBREVIATIONS

AGM:	Aorta Gonad Mesonephros
Apln:	Apelin
AML:	Acute Myeloid Leukemia
BM:	Bone Marrow
BMP:	Bone Morphogenetic Protein
CB:	Cord Blood
CFU:	Colony Forming Unit
CFP:	Cerulean Fluorescent Protein
CLP:	Common Lymphoid Progenitors
CMP:	Common Myeloid Progenitors
DA:	Dorsal Aorta
dHSPCs:	Definitive Hematopoietic Stem Cells
Dll4:	Delta 4
DN-Maml1:	Dominant Negative Mastermind 1
EC:	Endothelial Cell
EHT:	Endothelial-to-Hematopoietic Transition
FL:	Fetal Liver
GFP:	Green Fluorescent Protein
GOF:	Gain of Function
GVHD:	Graft-versus-Host Disease
HE:	Hemogenic Endothelium
hESCs:	Human Embryonic Stem Cells
HH:	Hedgehog Signaling
HLA:	Human leukocyte antigen
HSC:	Hematopoietic Stem Cell
HSPC:	Hematopoietic Stem Progenitor Cells
IAHC:	Intraortic hematopoietic clusters
IF:	Immunofluorescence
Jag1:	Jagged1
LOF:	Loss of Function
LT-HSC:	Long-term Hematopoietic Stem Cells
Mfng:	Manic Fringe
NECD:	Notch Extracellular Domain
NICD:	Notch intracellular Domain
RFP:	Red Fluorescent Protein
Shh:	Sonic Hedgehog Signaling
ST-HSC:	Short-term Hematopoietic Stem Cells
TF:	Transcription factor
VA:	Vitelline artery
WT:	Wildtype

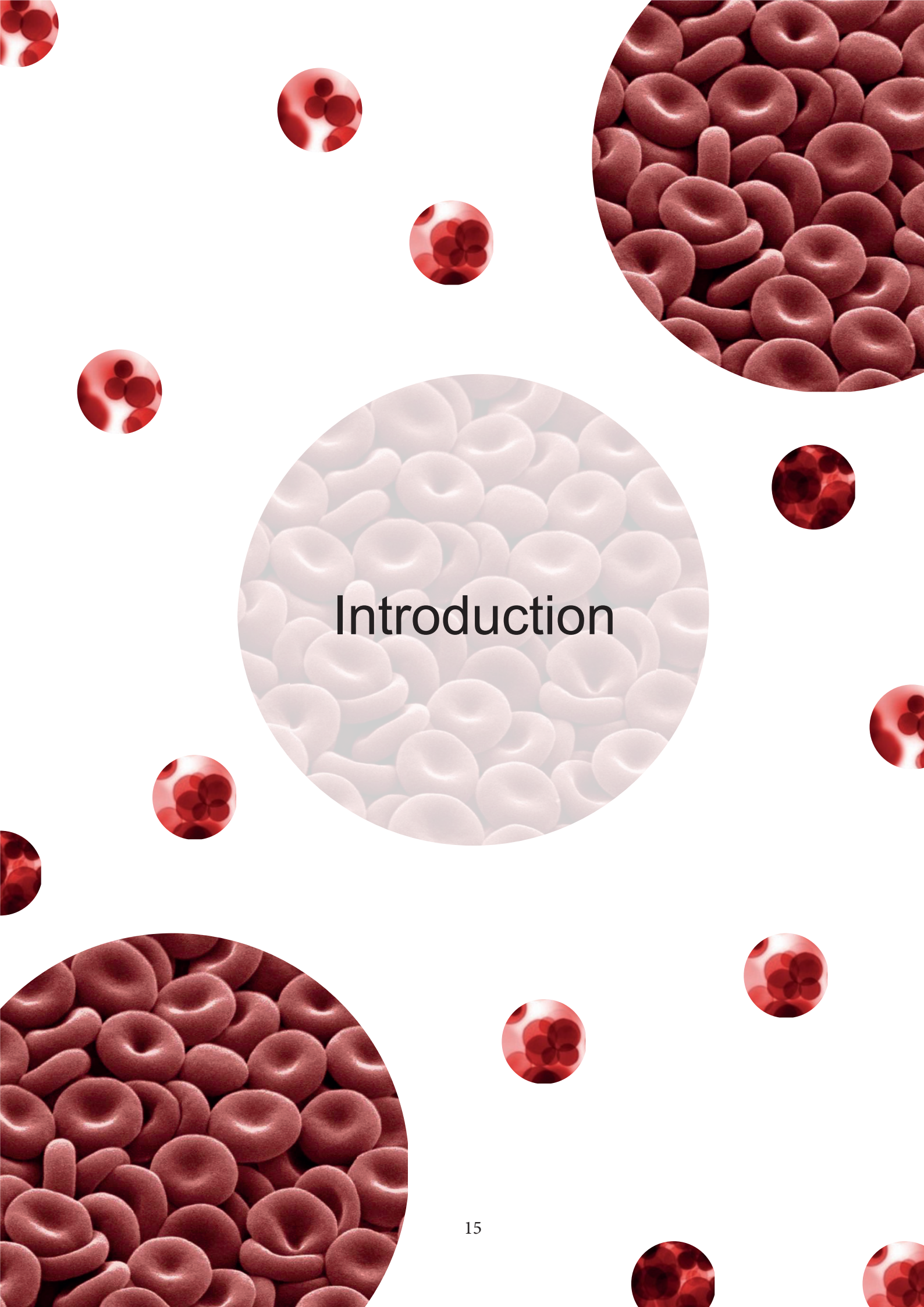

Introduction

INTRODUCTION

HISTORICAL BACKGROUND

"The blood is the life!" - Bram Stoker, Dracula (1897)

In CNIC, the heart may take center-stage, but in this text, it wins best supporting actor. This is not to declare the heart as unimportant, but its main responsibility- indeed, its whole reason for being - is to create a continuous stream of blood flow circulating through the body. From the beginning of life to the end of it, the heart allows the blood to bathe our cells with oxygen, to protect and mount a vicious war against invaders, and to control trafficking of impurities. In essence, the heart does its role to sustain life, but life itself is to be found in the blood.

It's fascinating to think that even before people knew about the concept of blood, it was known that the loss of this deep red liquid indicated potential peril or potential life. Even ancient civilizations understood this dichotomic role, embedding it into their culture through stories and myths. Medusa, the Gorgan monster with snakes for hair, was fabled to have blood that was both venomous and healing.

In 43 BC, Ovid crafted the bewitching tale of Medea and how she transfused blood into the aging King Aeson to cure him of his fading life, but it will not be until the 1600s that scientists would unlock the medicinal truth of transfusion. In the mid-19th century, Dr. James Blundell persisted in his quest to "turn the ebbing tide of life" in those at the "point of death from loss of blood" and performed the first documented (and successful) human blood transfusion. His early findings were later the foundations for modern day transfusions, and the knowledge built from this procedure prompted the idea for the transplantation of blood stem cells themselves.

Just as a boisterous war was booming in 1939, doctors attempted the first-ever human bone marrow (BM) transplant to treat WWII patients exposed to the radiation from atomic bombs. Today, BM transplants are the standard care technique for hematopoietic malignancies, congenital or acquired disorders, and as a therapeutic option in some solid tumors. As of 2012, 42% of all Hematopoietic Stem Cell Transplants (HSCT) are allogeneic, whereby patients receive stem cell grafts from a healthy donor (Henig and Zuckerman, 2014). However, only 30% of patients receive matched related donor transplantation, potentially leading to a serious medical problem known as Graft-versus-Host disease (GVHD) (Henig

and Zuckerman, 2014).

GVHD is an immune condition where the donor's immune cells attack the host tissue. Essentially, donor T-cells detect the human leukocyte antigen (HLA) class of the host as an invader and initiates an immune attack against them. It is a limitation of allogeneic HSCT and has a high rate of mortality and morbidity at 100 days post-transplant. Even if the patient remains disease-free for the first 2-years, disease relapse accounts for 41% of late mortality (Hierlmeier et al., 2018).

Besides the possibility of GVHD, another limitation of allogeneic transplantation is the short donor supply. A perfect candidate as a donor population is that of the umbilical cord blood (CB), a rich source of human embryonic stem cells (hESCs) with less stringent need for HLA matching (Park et al., 2015). However, its disadvantage is the low cell dose per CB unit that can be isolated. As scientists we can step in to ask: is there another possible donor source? Can we prevent GVHD? Is it possible to use the patient's own cells to reduce future complications?

Current research has tried to tackle such questions. Fibroblasts (the easiest cell type to isolate) could be taken from the skin of patients in need of a bone marrow transplant and it can be transdifferentiated into HSCs *in vitro* (Han et al., 2014; Rittie and Fisher, 2005). Recently, a new method was developed to expand (236-899 fold) *ex vivo* a small amount of functional HSCs and successfully transplant them into mice, a technique that holds great promise for HSC transplantation in humans (Wilkinson et al., 2019). From dish to bedside! However, as idealistic as this sounds, we still don't fully understand the molecular processes behind the initial development of the HSCs during embryogenesis, and even less on how to mimic those processes for therapeutic purposes. To discover these molecular cues, we must track and understand the humble beginnings of the HSCs.

DEVELOPMENT

"It is not birth, marriage, or death, but gastrulation, which is truly the most important time in your life..." Lewis Wolpert (1986)

Gastrulation to Mesoderm

After an oocyte is fertilized, cells rapidly divide and there will come a time when a seemingly chaotic event reaches a moment of critical decision-making. In mouse, by embryonic day (E) 6.5, the posterior region of the embryo undergoes gastrulation. Epiblast cells of the primitive streak form three primary germ layers: the ectoderm, the mesoderm, and the endoderm. It is within the mesoderm that our cells will begin its journey of potency restriction and lineage-gene activation to form structures such as muscle, bone, heart, and the blood vessels- the source of definitive hematopoietic stem cells (Rossant and Tam, 2002).

Blood Vessel formation

Blood vessels form through a process known as vasculogenesis. It was previously believed that a common endothelial and hematopoietic progenitor, the hemangioblast, leaves the primitive streak to form blood islands which then simultaneously differentiate into endothelial cells (ECs) and blood cells (Jaffredo et al., 2005). However, single cell genetic tracing experiments revealed that the progenitors of these blood islands first form ECs and some of these ECs will later differentiate into blood cells (Padron-Barthe et al., 2014). In amniotes, the formation of a vascular plexus (and later the blood tissue progenitors) occurs in two independent regions: extraembryonic vasculogenesis, in the yolk sac, and intraembryonic vasculogenesis, in the embryo proper (Adamo and Garcia-Cardena, 2012) (Figure 1).

Between E7.0 and E7.5, surface ectodermal cells undergo epithelial-to-mesenchymal transition and migrate to the extraembryonic region (Pardanaud et al., 1987). Within this region, cells form a mesodermal layer of blood islands, structures containing blood cells enclosed in a monolayer of ECs. These blood islands than grow and merge to form the primitive capillary networks of the yolk sac and the umbilical veins, structures necessary to bring nutrients from the mother to the growing fetus (Figure 1A). The blood cells that form in the extraembryonic region are mainly of the myeloid lineage, giving rise to nucleated erythrocytes and megakaryocytes (Medvinsky et al., 2011), a mostly primitive hematopoietic system that will sustain the growing embryo until intraembryonic hematopoiesis is established.

Intraembryonic vasculogenesis will form the vessels of the embryo proper as well as provide the foundations for definitive hematopoiesis. At around E7.5, two separate cords form underneath the lateral plate mesoderm. The cords, containing progenitors that gradually acquire an endothelial signature, will undergo a lateral-to-medial migration through the embryo. During this process, the somite and the splanchnic mesoderm contribute ECs to the initial vessel cords, thereby progressively increasing vessel diameter. By around E9.5, the two vessels will start to fuse in the posterior midline and form a single and larger dorsal aorta (DA) (Figure 1B). The anterior and bifurcated ends of the DA connects to the outflow tract of the heart and the posterior ends elongate towards the tail and connects with the vascular plexus in the splanchnic mesoderm (Sato, 2013). Angiogenic remodeling of the posterior vascular plexus will give rise to the vitelline artery (VA) (le Noble et al., 2004). The region where the DA and the VA organize themselves is known as the Aorta Gonad Mesonephros (AGM). It is within the DA of the AGM region where the main event and focus of this thesis occurs, the definitive hematopoiesis, or the origins of our beloved blood stem cells.

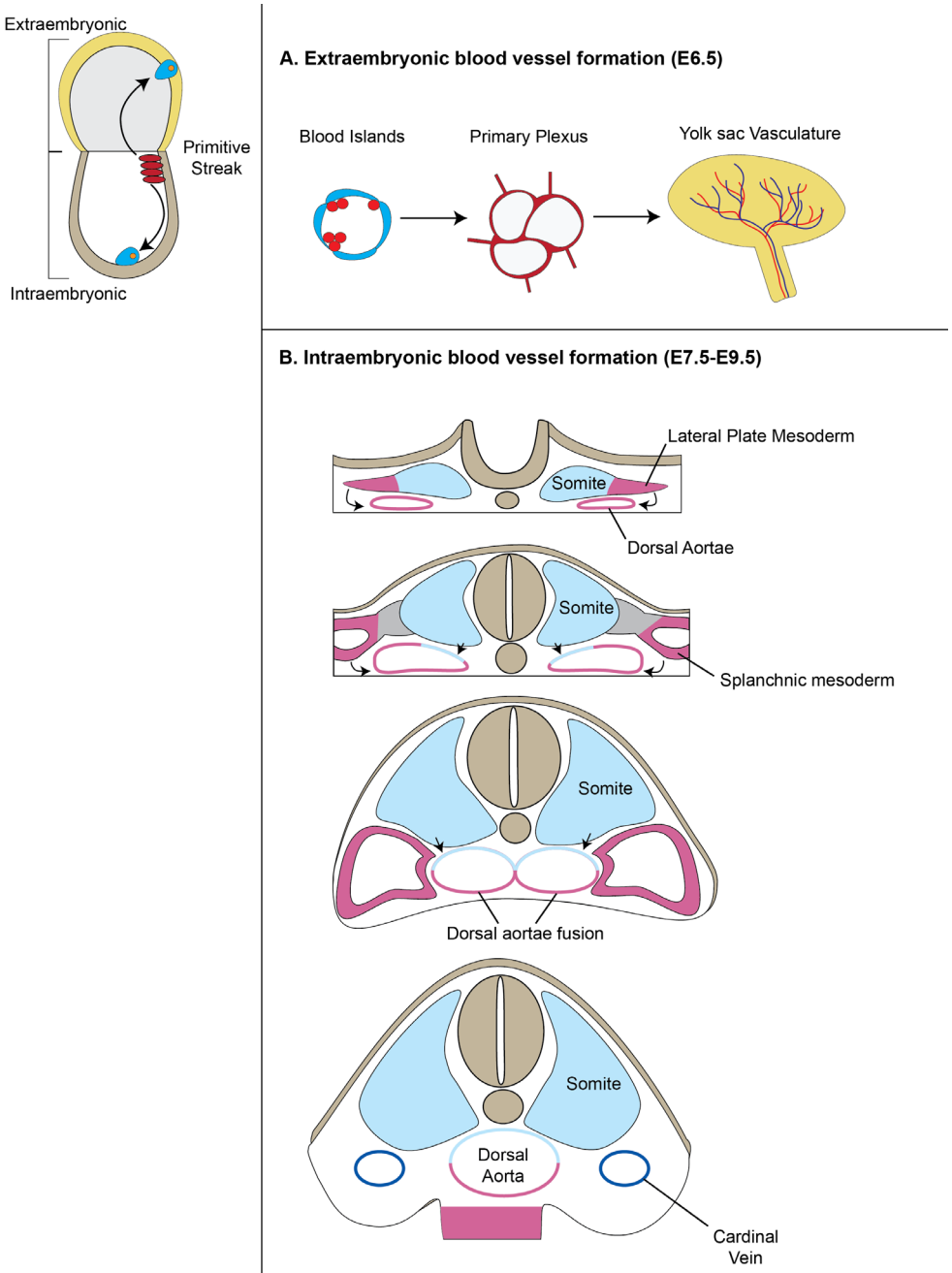

Figure 1 Intra and Extra-Embryonic formation of the Blood Vessels in Mouse Embryos. Blood vessels in the yolk sac and embryo proper evolve during two separate events. Hemangioblasts, cells that can give rise to both endothelial and blood lineages, migrate from the primitive streak to the yolk sac (E6.5) (**A**) and the blastula (E7.5-E9.5) (**B**) to form a primary vascular plexus. The rudimentary vasculature will then undergo remodeling and lumenized to become functioning blood vessels. Adapted from Sato (2013) and Park et al. (2013).

Definitive Hematopoiesis

Hemogenic Endothelium

Early investigation into the development of the definitive hematopoietic stem progenitor cells (dHSPCs) showed that the true HSCs only arise from arterial endothelium (Bertrand et al., 2010). Although many speculated that HSCs could arise from the mesenchyme underlying the DA, several studies have confirmed that all HSCs develop from a transient population localized within the endothelial layer of the DA (Bonkhofer et al., 2019; de Bruijn et al., 2002; North et al., 1999; Richard et al., 2013). By E9.5, scattered within the arterial endothelium of the DA is a Runx1-positive (+) endothelial cell population. These cells are a transient specialized population with a malleable identity that can give rise to multipotent HSPCs or commit to an endothelial existence (Dejana et al., 2017). This potential to acquire the hematopoietic fate is why these cells are considered to be the hemogenic endothelium (HE) (Chen et al., 2009; Lancrin et al., 2009; Yokomizo et al., 2001). Curiously, the HE is inconspicuous from the aortic endothelium, sharing arterial and endothelial marker genes such as Flk1 (VEGFR2), ERG, Dll4, and Notch (Gritz and Hirschi, 2016; Nikolova-Krstevski et al., 2009).

Although indistinct at a glance, Runx1^{+} HE is crucial for the development of the HSCs. Embryos completely deficient in Runx1 die before E12.5 with severe anemia (Samokhvalov et al., 2006). Runx1 null embryos develop CD41^{+} HSPCs (immature HSPCs) but these cells fail to express CD45^{+} (mature HSC marker) and therefore remain stunted from progressing to a more mature HSPC identity (Liakhovitskaia et al., 2014). The use of *VEC-Cre* to induce loss of *Runx1* specifically in ECs resulted in the absence of c-Kit^{+} cells in the DA (as well as in the vitelline and umbilical arteries) at E10.5, thereby leading to the conclusion that *Runx1* is necessary in the HE for the formation of c-Kit^{+} dHSPCs (Chen et al., 2009).

Runx1 expression occurs early during vascular development. In chicken embryos, *runx1* expression is seen in the lateral endothelium of the early-paired aortae stage- although expression is slight and seen in one cell (Richard et al., 2013). As the paired-aortae fuse into a single aorta, the number of cells expressing *runx1* substantially increases. Within the zebrafish embryo, *runx1* is also expressed early (highly expressed by 12 hours post fertilization (hpf)) in the paired aortae of the developing organism (Kalev-Zylinska et al., 2002). Interestingly, in the mouse embryo, the earliest expression was noted by E8.5 in the ECs of the VA and in the ventral portion of the paired DA. By E10.5, many ECs of the ventral AGM have *runx1* expression while expression is scant in the dorsal side of the DA. *Runx1* is also expressed in the mesenchymal cells underneath

the DA (North et al., 1999) which once led to the confusion about the Runx1+ origins of dHSPCs but which has since been settled as described before.

The molecular processes behind the specification of the HE are not very well understood but several signaling pathways such as Notch, c-Kit, p27, and retinoic acid are implicated (Gritz and Hirschi, 2016). Notch directly transcriptionally regulates several genes that are important for HSC formation such as *Hes1, Hes5*, and *Gata2,* but it does not directly regulate *Runx1* expression (Davis and Turner, 2001; Guiu et al., 2013; Robert-Moreno et al., 2005; Tsai et al., 1994). Instead Gata2 drives the expression of *Runx1* within the HE (Nottingham et al., 2007; Robert-Moreno et al., 2005). However, Runx1 induction but not Gata2 can rescue the defects associated with the absence of Notch signaling (Nakagawa et al., 2006). Therefore, it is speculated that Notch signaling must regulate Runx1 in other ways besides that of Gata2.

Prior to HE specification, arterial specification is a crucial first step of hemogenic potential. Endothelial-specific deletion of COUP-TFII (a venous gene) shows conversion of the venous structure into that of an arterial endothelium, with increased expression of arterial markers including *Nrp1, Hey1, Notch1*, and *Jag1 (*You et al., 2005*)*. This increased arterial identity was also accompanied by ectopic expression of *c-Kit* and *CD45* hematopoietic clusters. However, Notch is a unique component for the generation of the definitive HSCs. *In vitro* programmed HE deficient in Sox17 and Notch were able to generate erythroid and myeloid lineages but failed to maintain lymphoid potential (Clarke et al., 2013). Therefore, Notch signaling plays a key role in establishing hemogenic capacity of endothelial cells in the DA.

Endothelial to Hematopoietic Transition

Time lapse imaging of mouse transverse sections *ex vivo*, imaging of *in vitro* ESC culture differentiation, and *in vivo* 4D imaging of zebrafish embryos gave us the first “seeing is believing” evidence and morphological glimpses of the process of endothelial-to-hematopoietic transition (EHT) (Bertrand et al., 2010; Boisset et al., 2010; Eilken et al., 2009; Kissa and Herbomel, 2010; Lancrin et al., 2009). In mice and in humans, EHT most frequently occurs in the AGM region and not in the remaining DA. During this event, some Runx1^{+} ECs undergo a morphological change, going from a flat endothelial phenotype to a more rounded shape. Runx1^{+} rounded ECs bud into the lumen of the DA (or in the case of zebrafish embryo, will bud in the opposite direction), begin downregulating endothelial markers and upregulating the hematopoietic c-kit and CD41 surface markers, proliferate, and form grape-like clusters that remains adhered to the endothelial floor beneath (Figure 2) (Bertrand et al., 2010; Zape et al., 2017).

The definitive HSPCs primarily bud from the ventral side of the DA. As described before, ECs from the somite and the splanchnic mesoderm contribute to the EC population of the DA (Pardanaud et al., 1996). The dorsal/roof ECs are primarily somite-derived while the ventral/floor ECs derive from the splanchnic mesoderm. Therefore, dorsoventral asymmetrical contribution of ECs to the DA could have intrinsically different hematopoietic potential (Ambler et al., 2001; Esner et al., 2006; Pardanaud et al., 1996). Another reason behind greater ventral EHT (compared to EHT events on the dorsal side) is the molecular signaling niche asymmetry occurring near the AGM region. For example, during the time frame of E9.5-E11.5, bone morphogenetic protein (BMP) signaling from the developing gut induces the ventral HSC program of the DA while Hedgehog (Hh) signaling from the notochord specifies the dorsal cell fate of the DA (Crisan et al., 2016; Durand et al., 2007; Peeters et al., 2009; Wilkinson et al., 2009). As a result, the roof and the floor of the DA receive contradictory paracrine signaling molecules, all of which influence the EHT process in the ventral floor of the DA.

For EHT to occur, the endothelial genetic program of the Runx1^{+} cells must decrease (Gama-Norton et al., 2015) and the hematopoietic genetic program must increase. The mystery of this event is not fully understood, however, during EHT, there is signaling interplay between Sox17 and Runx1 (Bos et al., 2015). Sox17 marks the arterial endothelium and other hematopoietic sites within the embryo while Runx1 marks the HE (as previously mentioned). In the emerging HSPCs, Sox17 expression decreases while Runx1 levels relatively increase. Runx1 mechanistically facilitates EHT by repressing the endothelial program through the upregulation of Gfi1/Gfi1b (Lancrin et al., 2012). Thefore, endothelial markers (Cdh5 for instance) decreases in the emerging cells, but levels of decrease are only slight in comparison to the endothelial population. That is to say that, although these emerging cells are beginning to adopt another identity, they still retain the cloak of an endothelial one.

More factors contribute (and complicate) the EHT process. For example, Tal1 (also known as SCL) and GATA2 (previously mentioned in relation to Runx1 expression) are transcription factors (TFs) that are known to play an important role. Interestingly, in zebrafish two isoforms of *scl* exist in the HE. *scl-b* isoform is upstream of Runx1 but the *scl-a* isoform is the one upregulated after EHT and is critical for HSC maintenance (Zhen et al., 2013). Even further upstream is Gata2. Deletion of the *gata2* cis regulatory elements reduces expression of *Tal1* and *Runx1* and complete knockout of the gene in ECs prevent intraortic hematopoietic clusters formation (Gao et al., 2013).

The molecular process underlying EHT is not fully understood but the complex regulatory landscape present during fate determination offers a very interesting field of study. Recent single cell RNAseq analysis provided significant information on the genes and pathways

activated or inhibited during the EHT process (Baron et al., 2018; Bergiers et al., 2018; Zhou et al., 2016). The functional validation of the identified genes and networks will be of high relevance to the field.

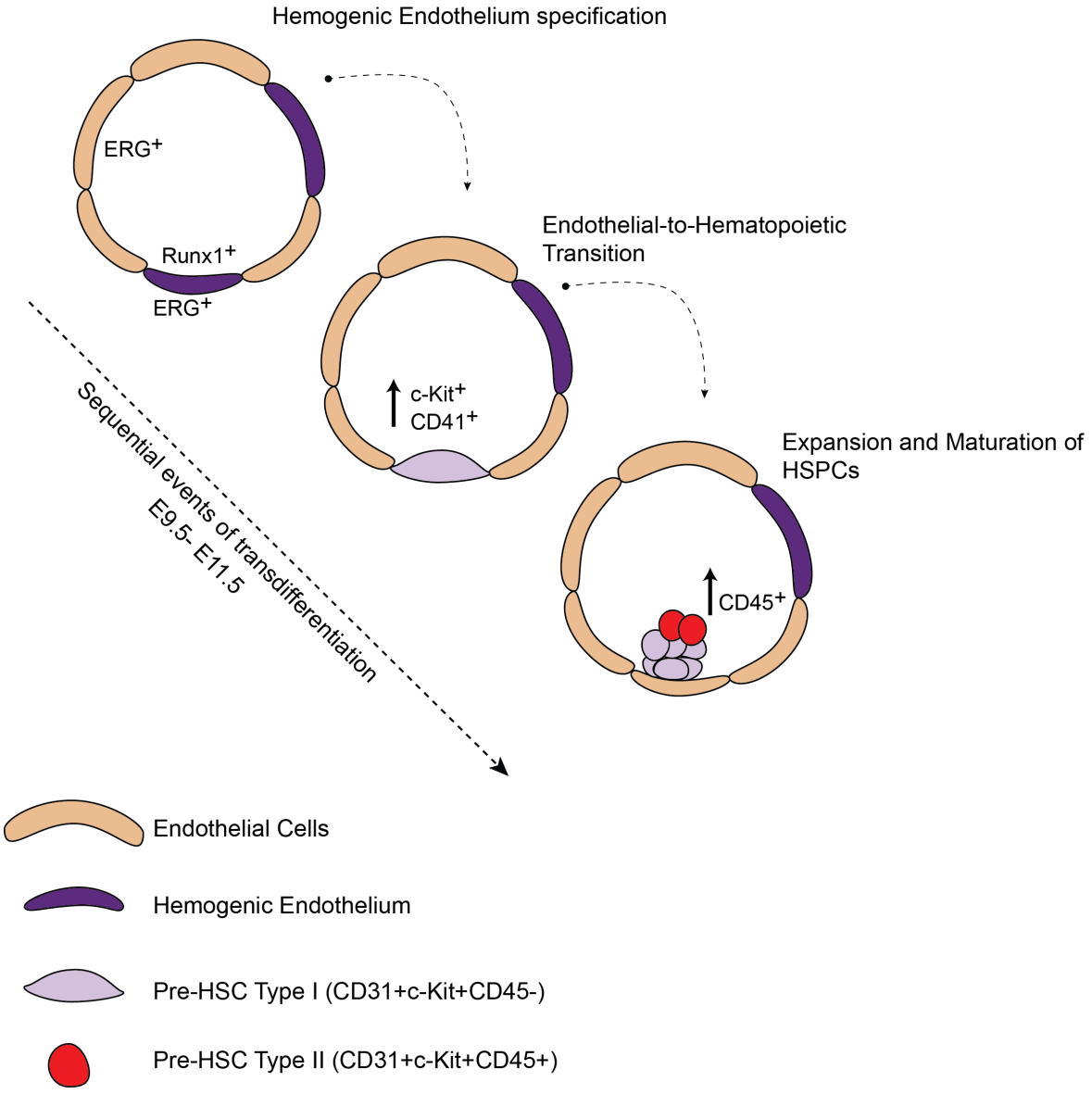

Figure 2 Sequential events of transdifferentiation in the DA. Within the DA, some cells of the hemogenic endothelium (Runx1^{+}) will undergo a lineage transition from endothelial to hematopoietic (EHT). These cells undergo a morphological change, going from a flattened phenotype to budding into the lumen of the DA. Finally, the now c-Kit cells proliferate and join other budded cells to form clusters. Within the cluster, by E11.5, some HSPCs begin to upregulate the mature HSC surface marker CD45. Adapted from Ottersbach (2019).

HSC maturation in the aortic niche

After EHT, c-kit^{+} cells will proliferate to form intraortic hematopoietic clusters (IAHC). Recent transcriptional profiling of the different cell populations have extended classification of dHSCs: pro-HSCs (CDH5^{+}CD41^{lo}CD43^{-}CD45^{-}) emerge at E9.5, pre-HSCs type I (CDH5^{+}CD41^{lo}CD43^{+}CD45^{-}) at E10.5, and pre-HSCs type II (CDH5^{+}CD41^{lo}CD43^{+}CD45^{+}) at E11.5 (Batsivari et al., 2017). By E11.5, cellular clusters will detach from the dorsal floor and travel to the secondary hematopoietic niche, the Fetal Liver (FL). While here, the cells will further mature and by E16.5, bona-fide HSCs will home to the Bone Marrow (BM) where it remains for the duration of the organism's life (Figure 3). During adulthood, BM progenitors also migrate to other hematopoietic sites such as the Thymus and Spleen (Babovic and Eaves, 2014). Accordingly, the proper establishment of early HSC development is imperative for a healthy hematopoietic system.

While the process of hematopoietic development is often described in the definitive wave within the AGM region, the AGM is not the only site of definitive hematopoiesis. Other embryonic sites where EHT occurs include: the vitelline artery, the placenta, the yolk sac, and the umbilical cord (Figure 3). Be that as it may, the AGM is considered the most important contributor to the final HSC pool of the BM and the only reported intraembryonic site that generates a large proportion of long-term multilineage HSCs (Ciau-Uitz and Patient, 2016; Cumano et al., 2001; Medvinsky et al., 2011; Muller et al., 1994).

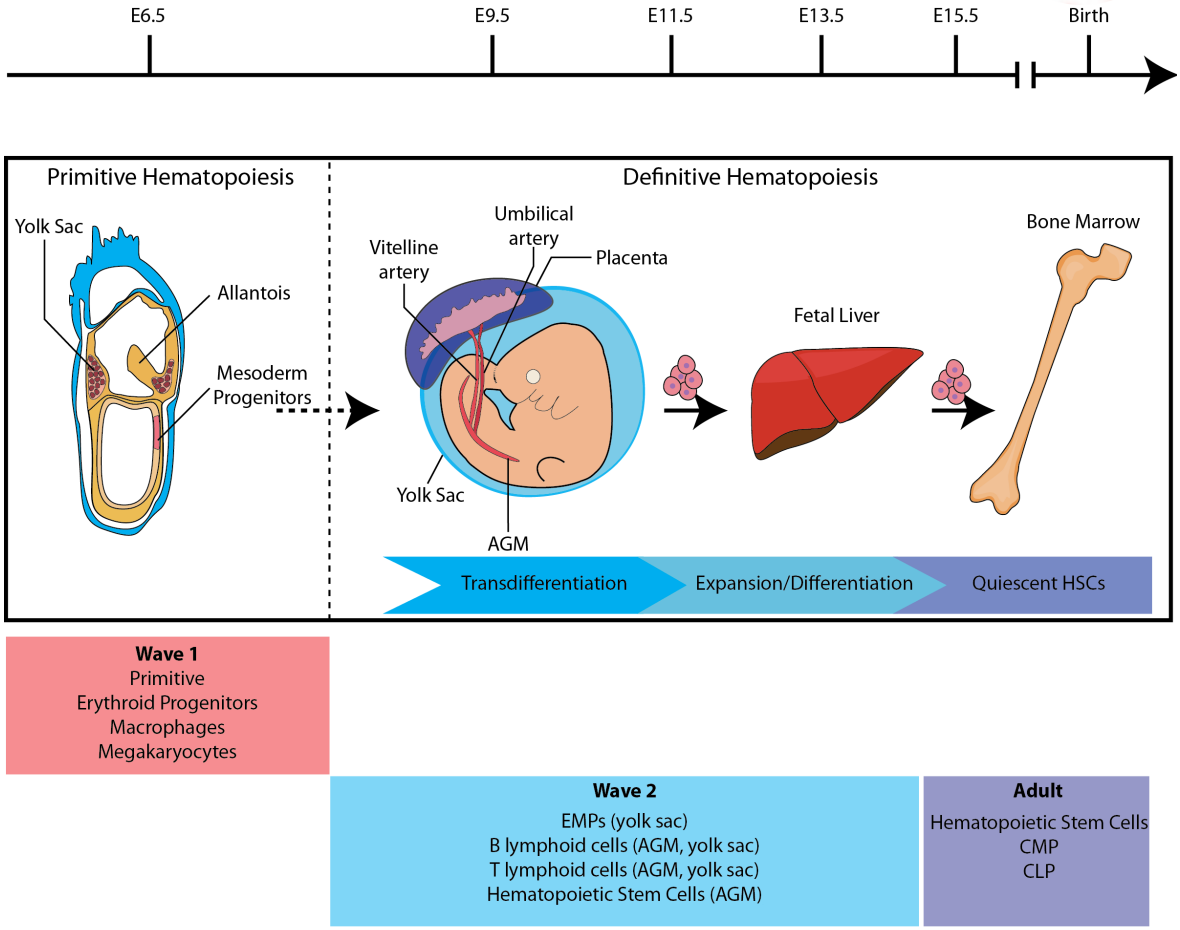

Figure 3 Two waves of hematopoiesis in the mouse embryo. Two distinct waves of hematopoietic development occur between E6.5 and E11.5. The primitive wave occurs in the yolk sac and will give rise to nucleated erythrocytes and other cells of the myeloid lineage. In the definitive wave, endothelial cells of the placenta, umbilical artery, vitelline artery, yolk sac, and AGM region will give rise to hematopoietic progenitor stem cells. These cells mature and further differentiate in the secondary hematopoietic niche- the fetal liver. Around the time of birth the mature HSC are located in the Bone Marrow. CMP = Common Myeloid Progenitors; CLP = Common Lymphoid Progenitors. Adapted from Yoder (2014) and Dzierzak and Bigas (2018).

Adult HSC lineages

The HSCs in the adult BM can be classified as long-term (LT-HSC) or short-term (ST-HSC). The LT-HSCs are the cells that can both self-renew and differentiate. These cells are mostly always dormant or quiescent and are normally activated to proliferate during extreme circumstances such as large-scope body damage, radiation, or various hematopoietic cancers (Hur et al., 2016; Sudo et al., 2012). In physiological conditions, LT-HSCs asymmetrically divide, producing one LT-HSC and one ST-HSC. ST-HSCs are more differentiated than their predecessor and have a limited capacity for self-renewal (Reya et al., 2001; Spangrude, 1994). ST-HSCs progressively divide and differentiate to become common myeloid or lymphoid progenitors, a more restricted cell type than those higher up in the hierarchy. Differentiation and proliferation proceeds in the peripheral blood to create more differentiated hematopoietic cell types. Ultimately, HSCs give rise to all of the cells in the hematopoietic tissue, from the oxygen-loving erythrocytes to the scanning guards of our system, the lymphocytes. They give rise to the system cleaners, the macrophages, and the dams of our system, the thrombocytes, and the vicious military agents, the basophils, neutrophils and eosinophils (Figure 4). It is therefore not difficult to appreciate how important these cells are for everyday life. (Imagine how else could we breathe and survive in a world full of bacteria, pollution, and viruses without them!)

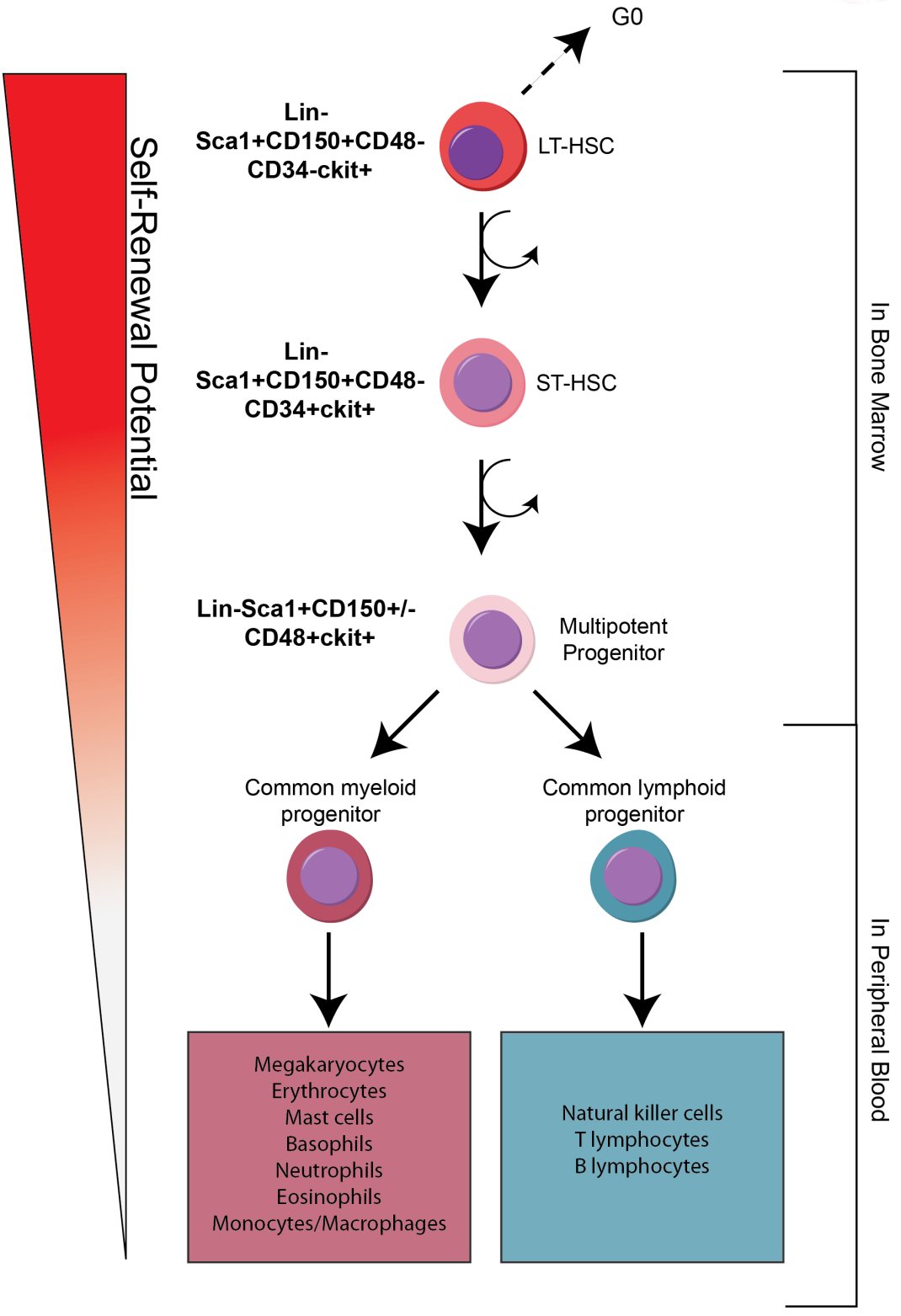

Figure 4 Hematopoietic Stem Cell Hierarchies in the Bone Marrow. In the bone marrow, LT-HSCs normally remain quiescent (G0 phase) and typically divide asymmetrically to give rise to 1 LT-HSC and 1 ST-HSC. The ST-HSC gives rise to both CMP and CLP. The CMP can differentiate into the vast array of myeloid cells while the CLP gives rise to lymphoid cells. As the cell progresses further down the hierarchy, they have a more stringent cell identity and less self-renewal ability. CMP = Common Myeloid Progenitors; CLP = Common Lymphoid Progenitors. Adapted from Bakhuraysah et al. (2016).

The role of Notch in HSC Development

Since HSCs develop from hemogenic arterial ECs, it can be difficult to separate the signaling pathways exclusively involved in endothelial and arterial specification versus the ones also involved in HSC development. Numerous arteriovenous signaling pathways -Vegfa, Bmp4, Shh, and Notch- have also been linked to the development of the dHSPCs in the AGM (Crisan et al., 2016; Durand et al., 2007; Jaffredo et al., 2013; McGarvey et al., 2017). Although there are other pathways implicated, my interest lies with Notch. Indeed, the cell-to-cell ligand-receptor interaction of the Notch signaling pathway plays an important role in fate determination of many different cell types (Bigas and Espinosa, 2012). Therefore, I will focus on the known role of the Notch signaling pathway for DA and HSC development.

The Notch pathway

First, a little background into the Notch signaling pathway would make the next section easier to understand. In mammals, there are 4 Notch receptors (Notch1, 2, 3 and 4). These receptors can interact with the ligands, of which there are 5: three of the Delta like family; Dll1, Dll3, Dll4; and two in the Jagged family of Serrate homologs; Jagged1 and 2. When the ligand comes into contact with the epidermal growth factor (EGF)-like repeats of the Notch receptor, an intracellular membrane bound metalloproteinase cleaves the S2 site of the Notch intracellular domain (NICD). The cleaved NICD will translocate to the nucleus of the cell and interact with other factors to form the nuclear Notch transcriptional complex (Figure 5). The canonical complex includes NICD, CSL/Rbpj and Mam/Maml, which will bind upstream to Notch target gene promoters allowing for the transcriptional activation of these genes. Rbpj is a corepressor of Notch target genes in the absence of Notch signaling and an activator in the presence of cleaved NICD. This is a simple overview of the pathway. Several Notch signaling modulators can alter the outcome of a given ligand-receptor interaction and the final signaling output are highly variable (Figure 5). For instance, Fringe proteins (Lunatic, Manic, and Radical) modulate Notch receptor activity by glycosylating the EGF repeats of the extracellular domain and modulating the ligand-receptor signaling ability (Bray, 2016; Kovall et al., 2017). In a situation where two or more Notch ligands are expressed in the same cell, as in the case of ECs during angiogenesis, the glycosylation acts as a positive regulator of Dll4 mediated Notch signaling while having a negative impact on Jag1-Notch signaling (Benedito et al., 2009) (Figure 5).

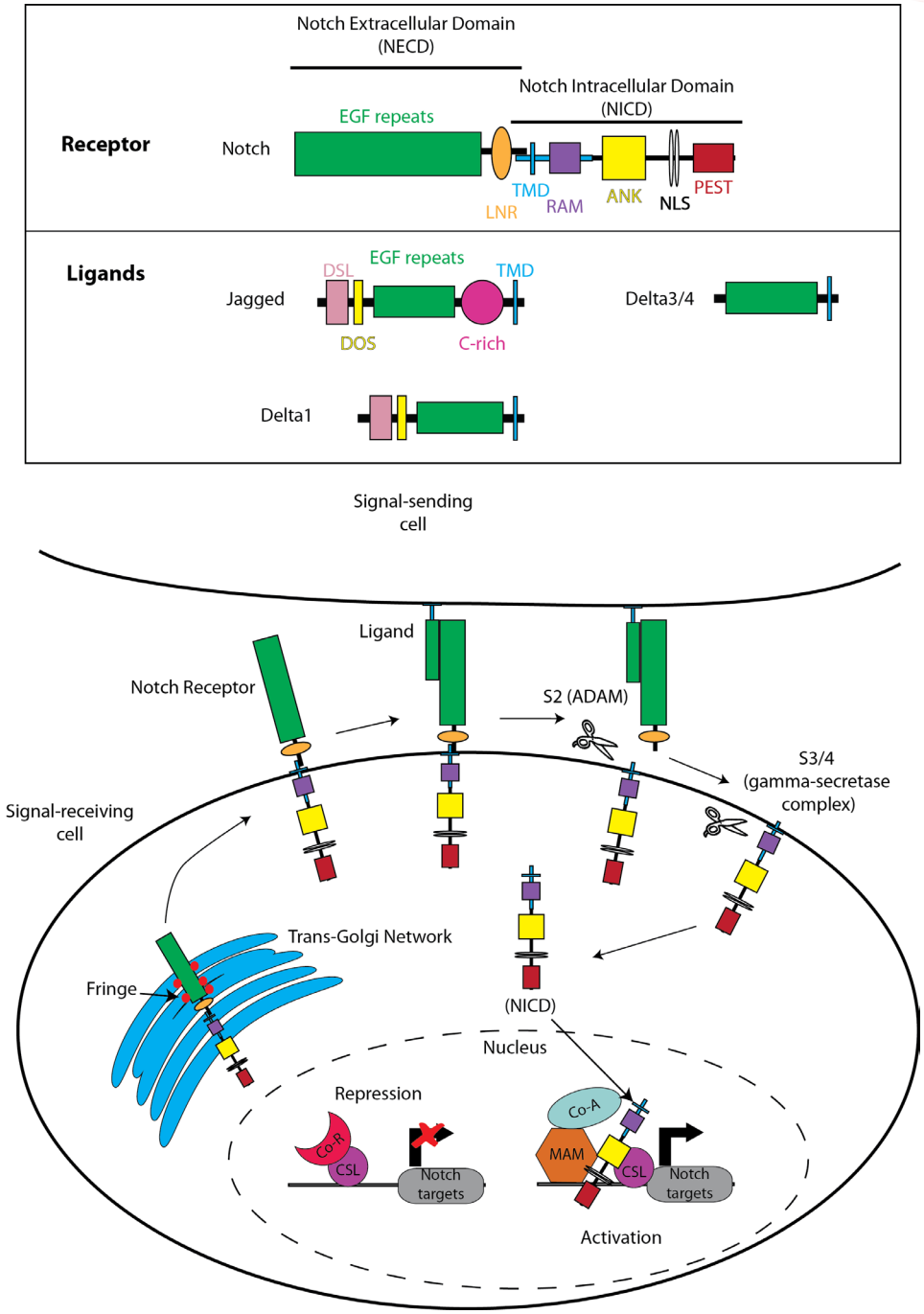

Figure 5 The Notch Signaling Pathway. The Notch signaling pathway is composed of Notch receptors (Notch1, 2, 3, and 4) and its ligands (Jag1, Jag2, Dll1, Dll3, and Dll4). Upon ligand/receptor interaction, the Notch intracellular domain (NICD) is cleaved and is translocated into the nucleus. In the nucleus, the NICD will form a nuclear complex with proteins CSL, Mam, and Rbpj to initiate gene expression of downstream Notch targets. Fringe proteins in the trans-golgi networks can modify the extracellular domain (NECD) to modify its affinity for the different ligands present. Adapted from Kato (2011).

Differences in ligand-receptor endocytosis, affinity and pulling strength can produce differences in the relative ligand-Notch signaling dosage (Bray, 2016). For example, it was proposed that in the mouse HE, low-strength Jag1 is necessary for specification of HSCs whereas Dll4 contributes to high-strength signal necessary for specification of endothelial

arterial cells (Gama-Norton et al., 2015). Notch dosage dependence is also very clearly illustrated in T-cell proliferation dynamics, whereby high dosage of Dll1 can suppress T-cell proliferation while at a low dose, T-cells produce IFN-y without growth suppression (Maekawa et al., 2003).

Notch and arterial-venous differentiation

Targeted mouse mutants of the Notch pathway demonstrated its essential role during vascular development as well as its role in arterial-venous specification. Endothelial specific loss of *notch1* or *dll4* resulted in severe angiogenesis and vascular developmental defects (Duarte et al., 2004; Gale et al., 2004; Krebs et al., 2010; Limbourg et al., 2005). Interdependence of the Notch and VEGF-A pathways in regulating the formation of large blood vessels, including the DA, demonstrated that deficiencies in VEGF and the subsequent Notch activation leads to the lack of arterial differentiation (Lawson et al., 2001; Lawson et al., 2002). In mice, mutants of most Notch signaling components (*Dll4, Rbpj,* and *Hey1/Hey2*) also showed loss of arterial marker gene expression (Duarte et al., 2004; Fischer et al., 2004; Gale et al., 2004; Kokubo et al., 2005). The arterial-venous differentiation genetic program consists in a large subset of differentially expressed genes, from which the arterial marker ephrinB2, and the venous marker EphB4, are among the most relevant (Adams, 2003; Wang et al., 1998). Notch promotes arterial specification mainly through the direct regulation of the arterial ligand EphrinB2 (Adams, 2003; Grego-Bessa et al., 2007). Likewise, overactivation of Notch can induce arteriolization of veins (Burns et al., 2005). Therefore, prior to HSC development, Notch is already a significant player for proper vascular formation and arterial specificiation.

Notch and HSC development

The study of the direct role of the Notch signaling pathway in HSC development was initially difficult due to the requirement for Notch in the early development of the vasculature and arteries, as mentioned above. Loss of *Notch1* or *Notch1/Notch4* or *Dll4* or *Rbpj* in ECs leads to severe arterial and vascular development defects and, consequently, loss of dHSCs formation (Hadland et al., 2004; Krebs et al., 2000; Kumano et al., 2003; Limbourg et al., 2005; Oka et al., 1995; Uenishi et al., 2018). Interestingly, nucleated erythrocytes are still present in embryos with loss of Notch, suggesting that Notch is irrelevant for the primitive hematopoietic wave (Limbourg et al., 2005). As HSPCs only arise in the arteries and Notch signaling specification of arterial endothelium is an imperative first step for dHSC development, does Notch play a role in the dHSC development apart from the initial

arterialization?

The first evidence that endothelial Notch signaling played a direct role in HSC development, independently of its role in arteriogenesis, came from the analysis of Jagged1 loss-of-function (LOF) mutants (Robert-Moreno et al., 2008). Embryos with loss of Jag1 unexpectedly formed normal arteries, but had impaired HSC development. At that time Jagged1 was always seen as a productive Notch ligand, therefore the authors concluded that the activation of Notch signaling by Jagged1 is necessary for and promotes HSC development. Mechanistically, they proposed that Jagged1/Notch signaling activity is essential to induce *Gata2* expression and the subsequent HSC development. Furthermore, *in vitro* data showed that treating AGM explants with y-secretase inhibitors (compounds that inhibit the final cleavage step and release of the intracellular domain of Notch) prevents formation of hematopoietic cell (CD45+) populations (Souilhol et al., 2016). In zebrafish embryos, overactivation of Notch was shown to increase *runx1* and *cmyb* expression, genes present in HSCs and progenitor cells (Burns et al., 2005). Altogether, the sum of these results favored a model in which endothelial Notch activation is required and induces hematopoiesis in the AGM.

In spite of previous data, more recent studies have instead shown that although Notch is indeed expressed in the arterial ECs of the DA and ectopic expression of Notch in the venous endothelium can confer expression of hematopoietic genes (Burns et al., 2005), the expression of Notch actually decreases in the emerging hematopoietic buds. When comparing arterial ECs ($CD31^{+}cKit^{-}CD45^{-}$) with HSPC clusters ($CD31^{+}ckit^{+}CD45^{-}$), it was observed that *Notch1*, *Jag1*, *RbpjK* and downstream target genes *Hes1* and *Hey1* are downregulated in the HSPC populations (Baron et al., 2018; Lizama et al., 2015). A very recent publication in zebrafish has shown that *dll4* expression is decreased in HE as *Runx1* expression increases and furthermore notes a repression of Notch signaling in the HE during hematopoietic development (Bonkhofer et al., 2019). In mouse embryos, loss of *Hes1* and *Hes5* have much larger hematopoietic clusters in the AGM (Guiu et al., 2013). In chicken embryos, there is a reduction of Notch signaling activity in hematopoietic clusters and blocking γ-secretase activity in aorta organotypic cultures was shown to promote hematopoietic production (Richard et al., 2013). Using Notch dosage-dependent Cre reporters *in vitro,* it was also concluded that endothelial progenitors with lower Notch activity may more frequently give rise to the dHSPC population (Gama-Norton et al., 2015). On the other hand, Notch overexpression in endothelial cells of the developing mouse embryo also leads to a substantial decrease of FL $CD45^{+}$ population and a reduced colony forming unit (CFU) potential (Tang et al., 2013; Venkatesh et al., 2008). These latest results challenge the previous model/assumption that endothelial Notch signaling positively regulates HSC development in the mouse and furthermore suggests that the manipulation of Notch in the whole blood vessel does not accurately reflect what occurs on a single-cell level in the DA.

Therefore, further investigation into the role of Notch during single-cell dynamics of dHSPC development is required to make sense of previously published works.

Besides the roles previously mentioned, Notch could be playing various and even opposing roles during the dHSC process in the aortic niche that is independent from the potential roles it has in liver hematopoiesis, bone marrow maintenance, and differentiation towards other hematopoietic lineages in adult organs (Bansal et al., 2015; Lampreia et al., 2017; Michalicka et al., 2017; Souilhol et al., 2016). The complicated nature of this process is made even more so because the dynamic single cell mechanism is studied using static images, and the manipulation of the whole vascular tissue complicates the efforts to unlink stages that occur before and after EHT. Due to the difficulty in distinguishing cell-autonomous and non-cell-autonomous effects with high temporal resolution, new genetic tools are required to accurately modulate Notch signaling and to understand its role during this multistep process.

MOSAIC GENETICS

One of the problems that we face in the vascular and Notch biology field is the ability to clearly distinguish a phenotype at the single cell level. Blood vessels are groups of tightly packed ECs that are adherent to each other. With standard live-imaging and antibody staining we have tissue resolution but no single cell resolution. The systematic analysis of gene function during vertebrate embryo development has mainly focused on understanding the phenotype caused by a mutation or deletion of one single gene at each time and in the entire embryo or vascular tissue. With classical genetics, it is difficult to assess the single-cell-autonomous effect of a given gene on blood vessels and HSPC development in the DA. In addition, deletion of important genes, such as those belonging to the Notch pathway, in the entire embryo or vascular tissue leads to developmental defects that can mislead the interpretation of a gene function in a given biological process.

Inducible genetic mosaics are powerful tools to study the biology of single cells and their organization in the tissue. One of the first and most brilliant inducible genetic mosaic mouse model was the Brainbow transgenic mouse line by Livet and colleagues (Livet et al., 2007). The technology is based on a Cre-dependent recombination of mutually exclusive LoxP sites that generates only one final outcome of multiple possible recombinatorial events. If one sees the images, they are spiraled into a world of psychedelic multispectral colors, but once the impact of these beautiful multicolored cells dwindle, one can see how powerful these tools are. They allow us to ask more complicated questions and quantify precisely how cells proliferate, migrate and differentiate over a given pulse-and-chase period of time.

Through single-cell progeny or clonal analysis we can understand the proliferation dynamics and differentiation potential of multiple cells in a given pulsed tissue.

Inspired by the potential of the Brainbow technology, our lab generated several new mosaic transgenic mouse lines (Pontes-Quero et al., 2017)(Garcia et al., unpublished) to study the development of tissues, and in the case of this thesis, the role of multiple genes and pathways in the endothelial-hematopoietic system at higher spatiotemporal resolution *in vivo*. These mouse lines allow the timely induction of genetic-fluorescent cellular mosaics that have normal, low, high or complete loss of a given gene or signaling mechanism. Unlike classical or conditional genetics, with this technology, tissues develop with a mix of mutant and wildtype cells that confront the same tissue microenvironment and experience exactly the same genetic induction and niche, allowing more precise quantifications of a given gene or pathway function. In addition, with this technology, the correlation between the expression of a given fluorescent protein and a given gene deletion or overexpression is 100% (Fernandez-Chacon et al., 2019) which enables a more reliable analysis of the cell-autonomous gene function.

OBJECTIVES

This doctoral thesis aims at understanding the role of Notch in the hemogenic endothelium. To do so, we used a novel Notch mouse genetic mosaic model to score the contribution of endothelial cells with differing Notch activation status to the clusters of hematopoietic stem and progenitor cells in the lumen of the dorsal aorta at E10.5. Although downregulation of Notch is proposed to be necessary for endothelial-to-hematopoietic transition to occur, mouse models of Notch loss of function produce detrimental vascular defects that precede the development of the definitive hematopoietic system thereby making the study of Notch in this context problematic. Therefore, the main objectives of this study are:

1) To determine how high activation of Notch in the aortic endothelium affects the development of the definitive wave at E10.5.

2) To use the genetic mosaic model to evaluate contribution of endothelial cells with varying Notch activation to the developing hematopoietic system.

3) To understand the downstream molecular processes regulating fate change in endothelial cells of the dorsal aorta.

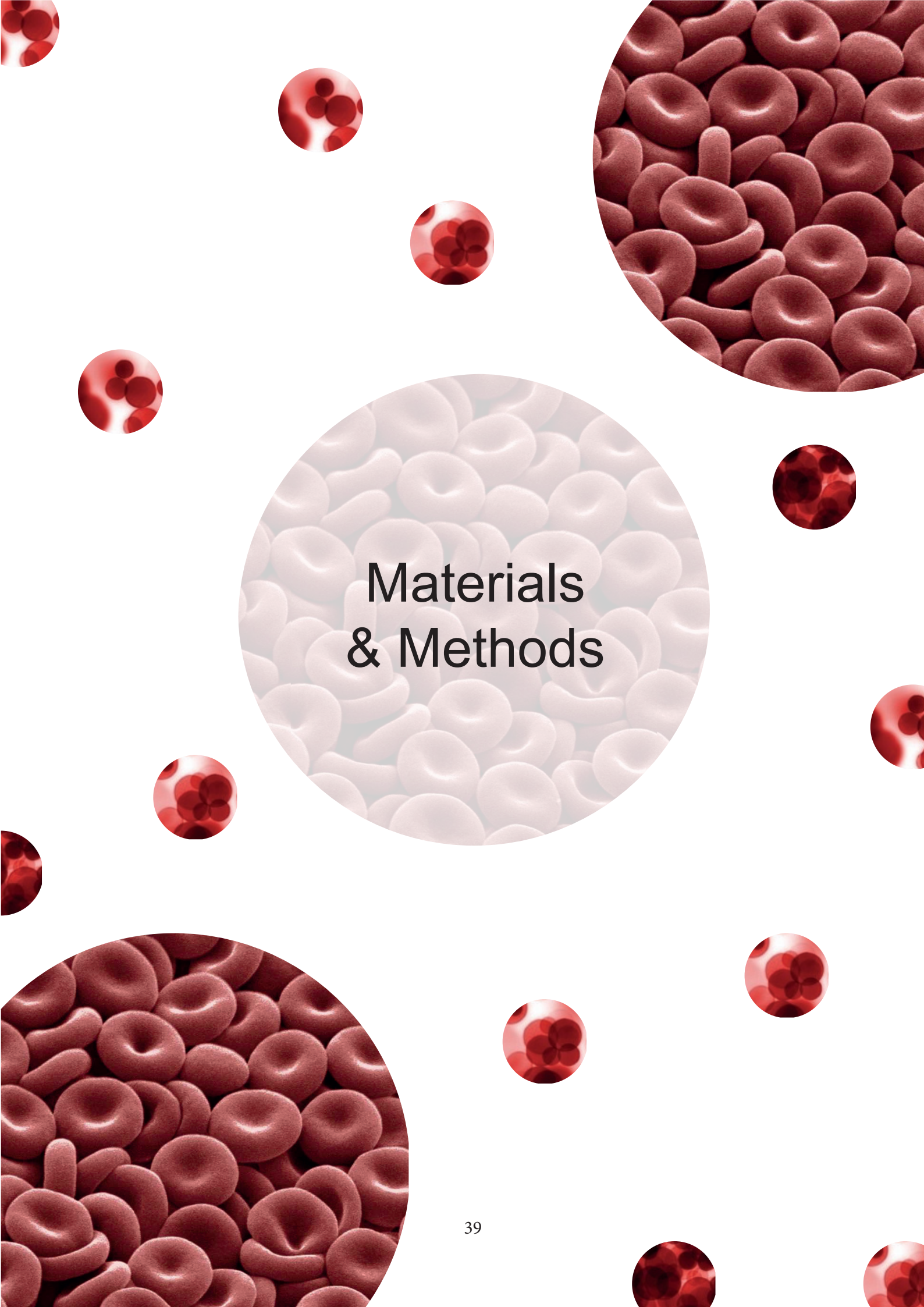

Materials & Methods

MATERIALS AND METHODS

Mouse lines

Experiments involving animals were conducted in accordance with institutional guidelines and laws, following protocols approved by local animal ethics committees and authorities. Mice were housed and maintained in the animal facility at the Centro Nacional de Investigaciones Cardiovasculares (CNIC, Madrid, Spain) in accordance with national and European Legislation. All mouse lines used are detailed in Table 1.

Table 1 Mouse Lines

Name	Official Strain Code	Reference	Primers
		Promoter driving Recombinase Expression	
Tie2-Cre	Tg(Tek-cre)1Ywa	Kisanki et al., 2001	5' GGGAAGTCGCAAAGTTGTGAGTT 3' 5' CTAGAGCCTGTTTTGCACGTTC 3'
Apln-FlpO	TBD	CNIC, R. Benedito	5' GCACTCACCTCCACAAACTG 3' 5' TCCCTGAACATGTCCATCAG 3' 5' GACCGAGTTGCAGCATGAAT 3' 5' GGGGCGGAAAGAGAGGAC 3'
		Mosaic Gene Expression	
iChr-Notch-Mosaic	Gt(ROSA)26Sor$^{tm1(iChr-Notch-Mosaic)}$	Pontes-Quero et al., 2017	5' ACGTGAAGCTGAGCAAGGAT 3' 5' CTTAGTCACCGCCTTCTTGG 3'
		Loss of Function	
Jag1^{lox}	Jag1^{CRUK}	Brooker et al., 2006	5' TGAACTCAGGACAGTGCTCT 3' 5' GTTTCAGTGTCTGCCATTGC 3'
Myc^{lox}	Myc^{tm2Fwa}	De Alboran et al., 2001	5' TTTTCTTTCCGATTGCTGAC 3' 5' TAAGAAGTTGCTATTTTTGGC 3'
Mycn^{lox}	Mycn^{tm1Psk}	Knoepfler et al., 2002	5' GTCGCGCTAGAAGAGCTGAGAT 3' 5' CACAGCTCTGGAAGGTGGGAGAAAGTTGAAGCGTCTCC 3'
		Gain of Function	
Mfng$^{EC-IGOF}$	Rosa26-MFng^{tg}	D'Amato et al., 2016	5´AAAGTCGCTCTGAGTTGTTAT 3´ 5´GCGAAGAGTTTGTCCTCAACC 3´ 5´AGGCTGCAGAAGGAGCGGGA 3'
N1CDP$^{EC-IGOF}$	Gt(Rosa)26Sor$^{tm(LSL-MbTomato-2A-H2B-GFP-NICD-PEST)}$	CNIC, R. Benedito	5' CGGGGTCATTAGTTCATAGCC 3' 5' CACCTCGACCATGGTAATAGC 3'
		Reporters	
iSuRe-Cre	iSuRe-Cre	Fernández-Chacón et al., 2019 (Nature Comm)	5' CCCCCTGAACCTAAACATA 3' 5' CCTTGCTCACCATGGTCTTG 3' 5' GTGTCTGTACCAGGTTGGTTTG 3' 5' GCTCTGCATGTTGCAAGAAA 3'
iFlp-Mosaic	iFlp$^{Mut/wt}$ Mosaic	Garcia-Gonzalez et al., TBD	5' GCACTTGCTCTCCCAAAGTC 3' 5' CTTTAAGCCTGCCCAGAAGA 3' 5' CGGGGTCATTAGTTCATAGCC 3' 5' CACCTCGACCATGGTAATAGC 3'

The *Tie2-Cre* line was used to achieve constitutive endothelial specific Cre recombinase activity during early embryonic development. We also used the *Apln-FlpO* line to recombine FRT sites of the *iFlp-Mosaic* line; recombination occurs primarily in endothelial cells.

To study the effects of the loss of gene function in the dorsal aorta, crosses were established to obtain embryos with Tie2-Cre^{+} and homozygous floxed of Jag1, Myc, Mycn, or double Myc/Mycn.

To study cell-autonomous effects of mosaic Notch expression of endothelial cells in the dorsal aorta, crosses were established to obtain embryos with Tie2-Cre^{+} and iChr-Notch-Mosaics$^{Ki/wt}$. An embryo needed to be heterozygous for the Mosaic construct to ensure only one cassette was recombined in a single cell.

Gain of gene function experiments using *Mfng*$^{EC\text{-}iGOF}$, or *N1ICDP*$^{EC\text{-}iGOF}$ were established by setting crosses to obtain embryos heterozygous for one of the mentioned lines and Tie2-Cre^{+}. We used heterozygous embryos to only create a moderate increase of the gene of interest in the endothelial and hematopoietic populations.

To investigate how loss of Myc, Mycn, or double Myc/Mycn effects the CD45^{+} population of the peripheral blood, embryos were generated to be floxed for the mentioned genes, Apln-FlpO^{Ki} and iFlp-Mosaic$^{Ki/wt}$. *Apln-FlpO* recombines the Rosa26 Ki *iFlp-Mosaic* construct to produce one of two possible outcomes: 1) recombination of the first FRT pair resulting in the cell having membrane RFP^{+} and a constitutively active Cre and subsequently loss of any floxed allele or 2) recombination of the second FRT pair resulting in a membrane YFP^{+} cell and a Flippase protein. For the purposes of use for this experiment, YFP^{+} cells are considered wildtype, as they are not crossed with any mice containing FRT sites.

To generate Apln KOs, only Apln Ki males or Apln$^{Ki/Ki}$ females were evaluated. The reason is because Apln is an X-linked gene so only Ki/Ki females or Ki/Y male were used. Full Apln KO mice are viable and fertile with slight vascular phenotype during development (Kuba et al., 2007; del Toro et al., 2010).

For blood analysis in adults Myc, Mycn, and double Myc/Mycn crosses were set up to generate Tie2-Cre^{+}, iSuRe-Cre$^{Ki/wt}$, homozygous floxed adults. The *iSuRe-Cre* line is a transgenic construct that upon recombination of its floxed PhiMut will produce a cell with Membrane Tomato fluorescence and a constitutive Cre, thereby labeling cells that have added Cre recombinase activity and a higher recombination assurance of any floxed allele (Fernández-Chacón et al., 2019). The theory of genetics behind this strategy is that Tie2-Cre recombines the iSuRe-Cre construct that will then recombine the floxed alleles.

Embryo generation and Genotyping

Embryos were generated from timed mating between transgenic, wildtype, or loxed females and males (>6 weeks). Pairings were crossed for collection of embryos at E10.5 whereby observation of vaginal plugs were considered as embryonic day E0.5 of development.

Embryos were collected in PBS and heads of the embryos were used for genotyping. Each embryo head was submerged into 150uL of genome extraction buffer (50mL Tris HCl Ph8; 5mL of 0.2% SDS; 5mL of EDTA; 20mL of NaCl; to 500mL with distilled H_2O) and 2uL of 20mg Proteinase K. After 1 hour in a Thermomixer (Sigma) at 55ºC and set for 700 RPM, 150uL of Isopropanol was added to precipitate DNA. Solution was then centrifuge at 15000 RPM at 4ºC for 25 minutes. One may observe a white pellet at the bottom of the Eppendorf (though not always the case) and solution was discarded and tubes were left to air dry. Once there is no evidence of liquid, 150uL of milliQ water was added and DNA was stored at 4ºC. Primers listed in Table 1 were used to genotype embryos.

Tissue processing and whole-mount immunofluorescence

Embryos were removed from the mother uterus and yolk sac was carefully removed. Embryos were staged according to the day of isolation and/or based on Thelier criteria. Once isolated, embryos were collected in PBS and fixed in 2% PFA for 20 minutes at 4ºC. Embryos were then washed three times for 15 minutes each round in PBS. They were then subjected to a serial dehydration with increasing methanol/PBS dilution (50%, 75%, 100%; 30 minutes each) and stored in 100% methanol until ready for processing. Embryos were then sectioned as described previously (Yokomizo & Dzierzak, 2010). Briefly, the rostral half of the body, limb buds and lateral body wall were removed and then rehydrated back to PBS using increasing PBS/methanol dilutions (25%, 50%, 75%; 30 minutes each). Embryos were blocked and permeabilized overnight at 4ºC in blocking solution (1% skim milk, 0.4% Triton, and 0.5% BSA in PBS). Primary antibodies (Table 2) were diluted in working solution (PBS, 1% skim milk, and 0.4% Triton) and tissue was incubated overnight at 4ºC. After three washes in working solution, each 30 minutes on ice, Alexa-conjugated secondary antibodies (Table 2) were incubated in working solution overnight at 4ºC. After three washes in PBS, embryos were subjected to serial dehydration in glycerol (20%, 40%, and 60%) and cleared in cubic 1 solution prepared as previously described (Susaki et al., 2014) for 24 hours. Embryos were then mounted in 1:1 cubic 1: glycerol solution on a FastWell chamber (FW20, Grace Bio-labs). A coverslip was placed on the FastWell and the sample was stored in 4ºC until ready for imaging.

Table 2 Antibody References		
Antibody	**Company**	**Reference**
Primary Antibodies		
Goat anti-GFP	Acris Antibodies	Cat# R1091P
Rabbit anti-DsRed	Clontech	Cat# 632496
Hamster anti-CD31	Millipore	Cat# MAB1398Z
Mouse anti-HA-AF647	Cell Signaling	Cat# 3444S
Rabbit-anti Connexin 40	Alpha Diagnostic	Cat # 28cx4029
Rabbit anti-RUNX1	Abcam	Cat# ab92336
Rabbit anti-Myc	Millipore	Cat# 06-340
Goat anti-Dll4	R&D	Cat# AF1389
Rabbit anti-Ki	Abcam	Cat# ab16667
Rabbit anti-ERG	Abcam	Cat# ab110639
Rabbit anti-ERG-AF647	Abcam	Cat# ab196149
Rat anti-CD117-APC	Tonobo Biosciences	Cat# 20-1172
Rat anti-mouse P21	CNIO	HUGO291
CD45.2-APC-Cyanine 7	Tonobo Biosciences	Cat# 25-0454-U025
Cd11b-APC	BD Pharmigen	Cat# 51_01712J
B220-Biotin	BD Pharmigen	Cat# 51_0122J
CD3e-Biotin	BD Pharmigen	Cat# 51_01082J
Secondary Antibodies		
Donkey anti-Goat AF488	Thermo Fisher	Cat# A-11055
Donkey anti-Rabbit AF594	Thermo Fisher	Cat# A-21207
Donkey anti-Rat AF647	Abcam	Cat# ab150155
Goat anti-Armenian Hamster AF680	Jackson Laboratories	Cat# 127-625-160
Donkey anti-Rat CF633	Biotium	Cat# 20137-1mg
Donkey anti-Rabbit CY3	Jackson Laboratories	Cat# 711-167-003
Streptavidin-BV421	BD Horizon	Cat# 563259

Image acquisition

Due to the complexity of the immunostainings and the combination of up to 5 different fluorophore signals per immunostaining, we used the Leica SP8 confocal. The confocal has a white laser that allows for excitation at any wavelength from 470nm to 670nm. Hybrid detectors were used for the 488/594/647/680 channels to allow for superior sensitivity during deep tissue imaging. Embryos were immobilized in the 1mm depth chamber made from FastWell (Grace Bio-Labs), and observed from the lateral side. Pinhole diameter was set at 2.5 Airy unit and steps were 5.5-7.0 μM per z-section. Images of the dorsal aorta (DA) were taken to the left of the vitelline artery (VA) using a 20x lens with glycerol as the immersion medium. All of the representative images shown represent the average of the results obtained from each group and experiment. Comparisons of phenotypes were obtained using the same laser excitation and confocal scanner detection settings. Z-stack thickness was determined manually for each embryo by scanning 594-Runx1 or 680-CD31

channels to ensure beginning and end slices covered the entire depth of the dorsal aorta.

Quantitative image analysis

Image processing and quantification was done using Fiji/ Image J (Schindelin et al., 2012).

For quantification of total hematopoietic stem progenitor cells in the dorsal aorta, the $CD117^+$ antibody was used to identify the cells on the dorsal floor. The ImageJ plugin *Cell Counter* (https://imagej.nih.gov/ij/plugins/cell-counter.html) was used for manual counting of $CD31^+$ and/or $Runx1^+$ and $CD117^+$ in each section of individual z-stacks and the total $CD117^+$ cells was determined per embryo. Transgenic embryos were compared with their wildtype littermate and each was quantified blindly based on randomly assigned codes.

In the case of quantifying GFP^+ versus GFP^- single cell (or monocluster) analyses, the ImageJ plugin *Cell Counter* was used to manually count single $CD31^+$ $CD117^+$ cells in each image of the DA z-stack. Cells were scored as either GFP^+ or GFP^- negative based on the clear intensity of the GFP signal.

To determine number of $Runx1^+$ $CD31^+$ $CD117^-$ cells present in the DA, five z-images in the z-stack where selected from each embryo. The picture had to have a complete lateral section of the DA. In each image, $RUNX1^+$ $CD31^+$ $CD117^-$ cells were manually counted.

For quantification of the ECs in the *iChr-Notch-Mosaics*, ECs in the 20x z stack images with RFP, GFP, or HA were manually counted. To determine if ECs were GFP^+ or CFP^+, cells that were detected with the GFP^+ antibody was also checked for positive HA staining. If a cell had signal in both channels, they were scored as CFP^+. For the HSPC quantification, $CD117^+$ cells in the 20x z stack images with RFP, GFP, or HA were manually counted. When determining if a cell was indeed GFP^+ or CFP^+, the same technique was used as that in the ECs.

Flow Cytometry

Embryo preparation

Embryos were collected in PBS, and dissected to only contain the trunk region of the embryo. Collectively, the embryos were manually disaggregated in sterile PBS using a

20-gauge syringe needle and then a 25-gauge syringe needle to create a homogeneous cell suspension. Cell suspensions were then passed through a 70 μM filter to remove any large clumps of tissue.

Isolation of Dorsal Endothelial Cells

To isolate embryonic endothelial cells from the DA region of E10.5 Notch mosaic embryos, cell suspensions were incubated with antiCD117^{+}-Biotin (Tonobo Biosciences 1:300) and Rabbit-anti-mouse Connexin 40 (Alpha Diagnostic, 1:200) as primary antibodies and finally with Streptavidin-BV421 (BD Horizon 1:300) and Alexa Fluor 647 conjugate Donkey anti-Rabbit (Jackson Laboratories, 1:200) as secondary antibodies. The flow cytometry analyses were performed in FACS Aria Cell Sorter (BD Biosciences). ECs were sorted from Cx40^{+}, CD117^{-} populations and separated according to their endogenous fluorescence (GFP, Cherry or Cerulean).

Peripheral Blood analysis

To analyze the CD45^{+} population of the peripheral blood, 150uL of blood was drawn from the submaxilar region of mice older than 6 weeks in tubes coated with EDTA to prohibit coagulation. Blood was transferred to a 15mL falcon tube and filled up to 14mL with PBS. Tubes were centrifuged at 400 RPM for 7 minutes at 4ºC. Liquid was discarded and cells were resuspended. Erythrocytes were lysed by introducing 2mL of distilled water and mixing for 10 seconds and then diluted with 12mL of PBS. Tubes were centrifuged with previously mentioned settings and liquid was discarded. Cells were then resuspended and then incubated with cd3e-Biotin (BD Pharmigen 1:100) and B220-Biotin (BD Pharmigen 1:100) for 30 minutes on a shaker at room temperature. Cells were then centrifuged as before, resuspended, and incubated with Streptavidin-BV421 (BD Horizon 1:100), cd11b-APC (BD Pharmigen 1:100), and CD45.2-APC/CY7 (Tonobo Biosciences 1:100) for 20 minutes on a shaker at room temperature. Cells were centrifuged and suspended in 50uL of PBS.

The flow cytometry analyses were performed in the LSRFortessa (BD Biosciences) SORP. Blood cells were gated with CD45.2 and myeloid/lymphoid populations were determined based on Side Scatter profile and surface labeling. When using *iSuRe-Cre* or *iFlp-Mosaic*, YFP and Tomato endogenous fluorescence was detected using laser 488 to excite YFP, detector 530/30, and laser 561 to excite Tomato, detector 610/20.

To determine the expression of Tie2 or Apln in normal mouse hematopoietic system Gene Expression Commons server (gexc.riken.jp) was utilized.

qRT-PCR

For quantitative real time PCR (qRT-PCR), ECs from E10.5 mouse embryos were sorted directly to RNeasy Mini Kit RLT buffer (Qiagen). RNA was extracted according to the Qiagen protocol. RNA was retrotranscribed with a High Capacity cDNA Reverse Transcription Kit with RNase Inhibitor (Thermo fisher, 4368814). cDNA was preamplified with Taqman PreAmp Master Mix containing a Taqman Assay based on pre-amplification pool which contained the following assays: ACTB, GAPDH, Hrpt1, Runx1, Gata2, CD41, Esm1, Hey2, Sox17, Cdh5, Numb, Apln, myc, mycn, Dll4, and Efrnb2 (Thermo Fisher). Preamplified cDNA was used to perform a standard qRT-PCR with gene-specific Taqman Assays (Thermo fisher) in an AB7900 machine (Applied Biosystems).

For the *iChr-Notch-Mosaic* endothelial cells, GFP^+ (Dnmaml) cells were compared with RFP^+ (Control) cells. For the *N1ICDP*$^{iEC\text{-}GOF}$ analysis, GFP^+ cells were compared with GFP^- cells from the same sorting session.

Single Cell Transcriptomics analysis

Published datasets (Baron et al., 2018) available in the Gene Expression Omnibus repository (series record GSE112642) was used to analyze single cells of the Dorsal Aorta at E10 and E11.

Single cell expression of aorta samples was sequenced using the CEL-Seq protocol. Paired end reads obtained by CEL-seq were aligned to the transcriptome using bwa (version 0.6.2-r126) with default parameters. The transcriptome contained all RefSeq gene models based on the mouse genome release mm10 downloaded from the UCSC genome browser and contained 31,109 isoforms derived from 23,480 gene loci. All isoforms of the same gene were merged to a single gene locus. The right mate of each read pair was mapped to the ensemble of all gene loci. Reads mapping to multiple loci were discarded. The left read contains the barcode information: the first eight bases correspond to a sample specific barcode. The remainder of the left read contains a polyT stretch followed by few (<15 transcript) derived bases.

To minimize the amount of low quality reads and to improve posterior normalization and analysis, a minimum total counts per cell of 1000 and a maximum of 13000 was applied. To minimize the amount of low quality cells we have applied also a minimum gene detection filter of 500 genes.

A simple PCA analysis using the most variable genes have been perform to QC the

experiment. Resolution set two 2 based on comparing unbiased clustering with supposed cell types.

To determine the top 20 genes expressed in each cluster, a MAST test was applied to each cluster. Only genes detected over 30% in the cells of any groups compared were analyzed. An adjusted p-value of 0.001 was used as a significance threshold.

To determine pseudotime, a Palantir trajectory/pseudotime analysis was performed to try to find a structure between the clusters. First a PCA was calculated and then a Diffusion Map based on the resulting PCA. The diffusion map components were reduced using tSNE for representation purposes. The Diffusion Map components were the used to extract pseudotime ordering of the cells with the differentiation potential, different terminal stages and the probability trajectories of the cells towards those terminal stages.

The gene expression trends on selected genes were computed across trajectories by fitting a generalized additive model. The trajectories were then clustered on a heatmap representation or co-paired by terminal stage on the mosaic plot. Gene trends across pseudotime trajectories were simplified into line plots to clearly illustrate trends.

To determine the average gene expression per cluster of Dll4 and Jag1, clusters were categorized as non-hemogenic (EC), hemogenic (HE), mixed HE and transition (HE/EHT), transitional (EHT), hematopoietic stem progenitor cell (HSPC), or hematopoietic stem cell (HSC) based on the majority presence of specified cell types in each cluster. Using the gene expression data taken from Baron et al., 2018, data was plotted to see the trend through pseudotime. A similar technique was used to determine the average gene expression throughout each group of genes implied in the cell cycle including Cdk1, Cdk2, Cdkn1a, Cdkn1b, Cdkn1c, Odc1, OAZ1 and OAZ2. To determine if there were any differences in the G1/S phase specific gene expression between clusters C1 and C0, genes specified in Torin et al., 2016 was cross-checked with the transcriptomics genes list and the average gene expression was represented in a heatmap. This gene list includes: *pcna, mcm5, tyms, fen1, mcm2, mcm4, rrm1, ung, gins2, mcm6, cdca7, dtl, prim1, uhrf1, mlf1ip, hells, rfc2, nasp, rad51ap1, gmnn, wdr76, slbp, ubr7, pold3, msh2, atad2, rad51, rrm2, cdc45, cdc6, exo1, tipin, dscc1, blm, casp8ap2, usp1, clspn, pola1, chaf1b, brip1,* and *e2f8*. Similarly, a GSEA study of RNA isolated from fetal hearts at E14.5 with loss of Dll4 in the endothelium showed enrichment in E2F target genes. These genes were cross-checked with the transcriptomics genes list and the average gene expression for clusters C1 and C0 were represented in a heatmap. This gene list includes: *pold1, kif18b, msh2, spag5, myc, cdc25b, mybl2, kif2c, mcm2, nup107, plk1, espl1, dnmt1, pold3, trip13, racgap1, aurka, tacc3, ncapd2, mcm4, melk, mlh1, brca1, bub1b, dlgap5, kpna2, mcm3, nup205, mcm5, dck, atad2, rrm2*, and

mthfd2.

Statistical analysis

Statistical analyses were performed in GraphPad (Prism 7.0). For comparisons of two samples with a Normal distribution we used the unpaired two-tailed Student *t*-test or, on the occasions when the standard deviation varied, we used the unpaired *t*-test with Welch's correction. Data is presented as means ± SEM. Population differences were considered statistically significant at $P < 0.05$. Since each tissue sample was given a code respective of its mother's code, samples were blind upon quantification. However, embryos were selected for immunostaining based on their genotype, whereby independent experiments had 2 wildtype and 2 mutants z stacks were analyzed at the same time and quantified then to their respective genotypes were assessed. The sample size was chosen for each experiment according to the observed statistical variation.

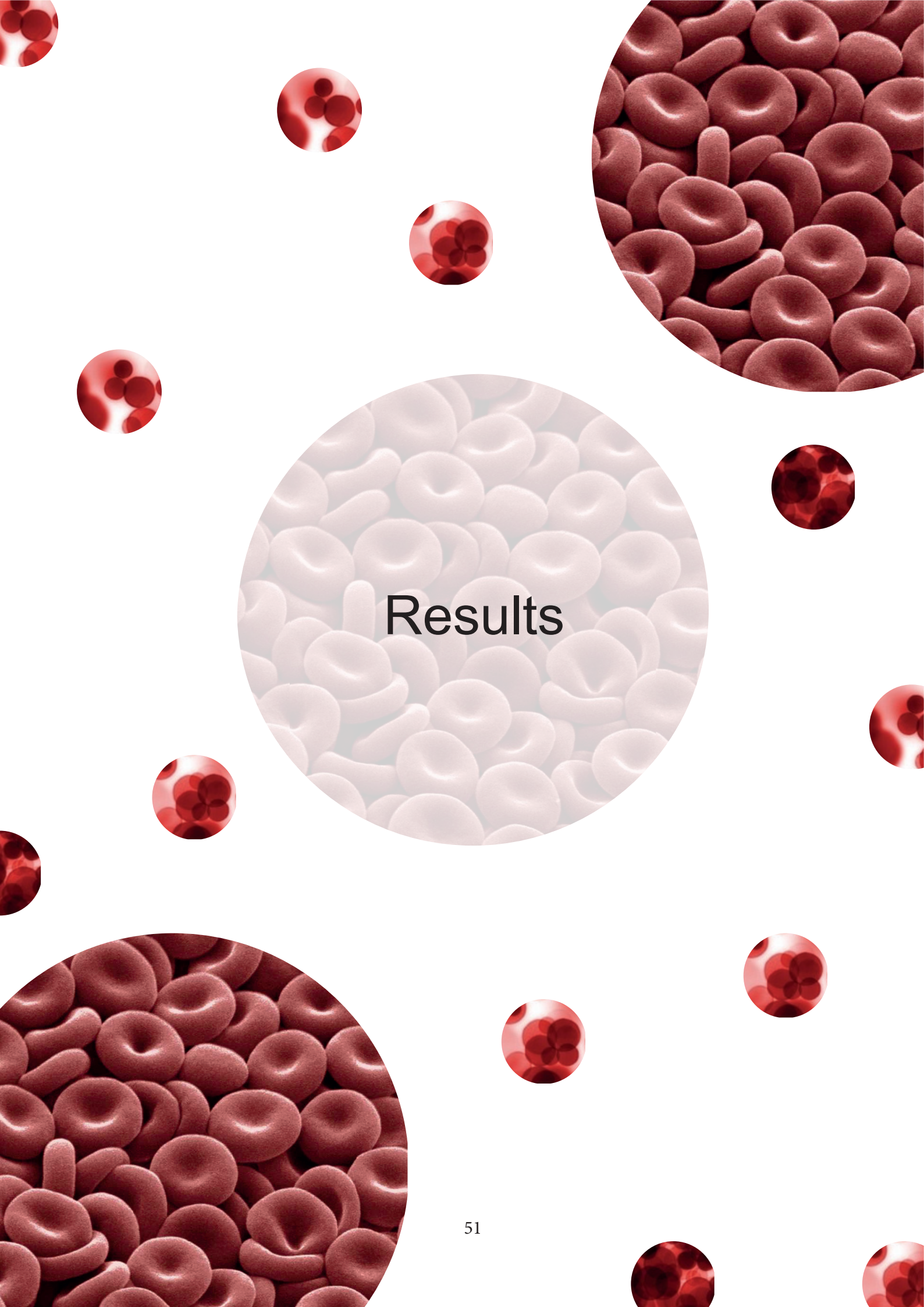

Results

RESULTS

4.1 Optimization of the mouse AGM wholemount immunofluorescence protocol

Immunofluorescence (IF) protocols previously done in embryos were normally done on thin cryo- or paraffin sections. In order to better visualize what is happening in the dorsal aorta (DA) it was necessary to set up a wholemount IF protocol that would allow for optical serial sections of the DA and deep imaging of immunostained tissue using antibodies conjugated with fluorophores. We used a modified version of a recently published protocol for high-resolution 3D wholemount imaging of the DA (Yokomizo and Dzierzak, 2010).

Figure 6A is an illustrated representation of how the E10.5 mouse embryos were microdissected in order to achieve the intended 3D imaging of the mouse DA. The protocols that were previously published needed to be optimized because many antibodies, for example anti-Dll4 and anti-N1CD, were sensitive to the dehydration method of methanol after the immunofluorescence protocol; signal was only detectable after using glycerol as a dehydration solution (Figure 6D, E). We also decided to use a modified version of the Cubic clearing method (Susaki et al., 2014) to clear the samples and obtain higher z-stack confocal microscopy resolution. Interestingly, the use of the Cubic solution on its own produced high autofluorescence from the circulating nucleated erythrocytes. Therefore, to decrease background, Cubic was diluted with glycerol to create a 1:1 clearing solution, the resolution results of which can be seen in Figure 6 (B-E).

An orthogonal z-stack view (Figure 6C) of a 260-micron thick DA sample shows that the entire diameter of the DA can be imaged, as orthogonal renderings of the z stack images shows a complete lumen surrounded by CD31 (Grey) ECs. Figure 6B shows immunostaining for CD31 (EC surface) and ERG (EC nuclei) of the imaged aorta.

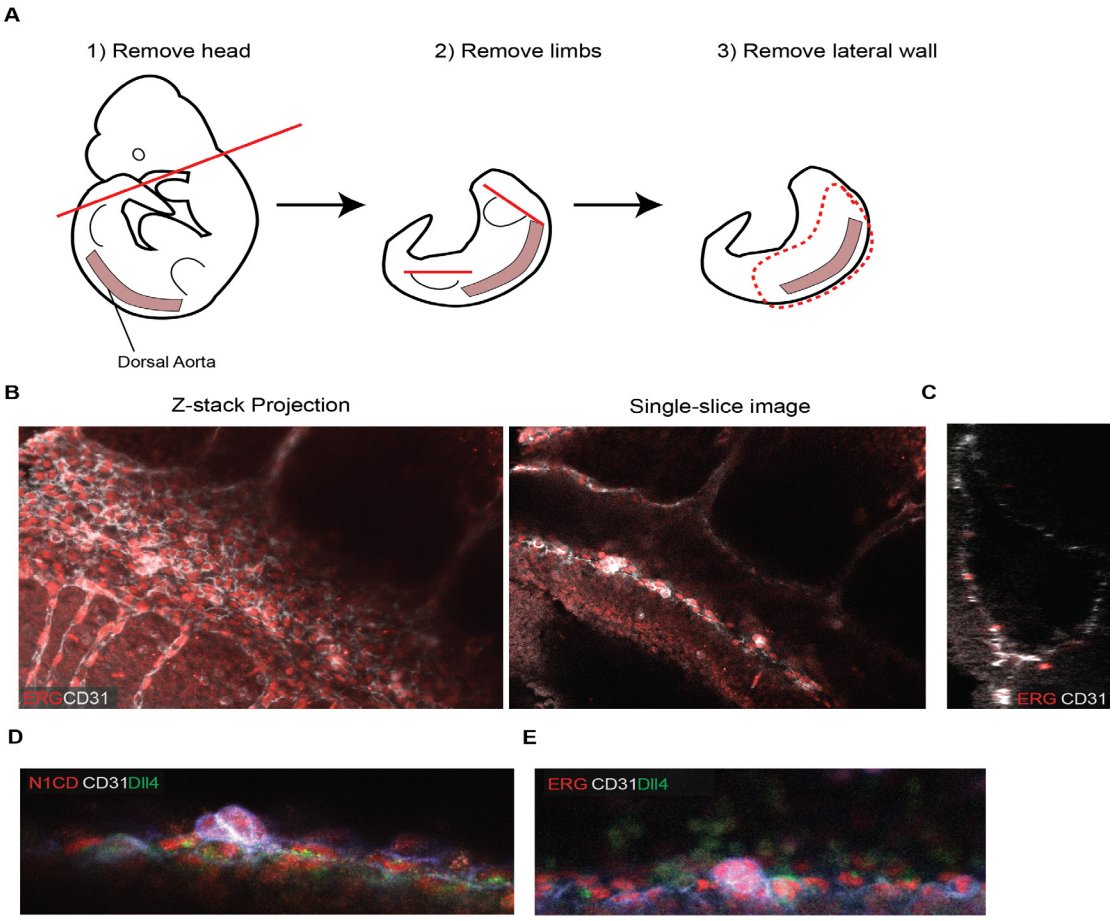

Figure 6 Optimization of the mouse AGM wholemount immunofluorescence protocol. A, Graphical representation of the E10.5 embryo dissection protocol to visualize the Dorsal Aorta. **B,** Representative photo of a confocal z-stack projection (STD DEV) (left) and a representative single-slice image (right) of a wildtype embryo at E10.5 immunostained with ERG (Red) and CD31 (Grey) **C,** Representative orthogonal slice image generated from the confocal z-stack projection to illustrate the lumen of the DA. **D,** Zoomed image of the dorsal floor stained with N1CD (Red), Dll4 (Green), and CD31 (Grey). **E,** Zoomed image of the dorsal floor stained with ERG (Red), Dll4 (Green), and CD31 (Grey).

4.2 Validation of a new Notch gain-of-function mouse model in the Dorsal Aorta

Previous studies in zebrafish have suggested that overexpression of Notch leads to an increase in *runx1* and *cmyb* expression, or an increased expression of HE genes (Burns et al., 2005). In order to determine if an increase of Notch signaling in the DA would induce more HSPC formation, we analyzed a new Cre-inducible Notch gain-of-function (GOF) mouse line (*Gt(ROSA)26Sor*$^{tm1(CAG\text{-}LSL\text{-}N1ICDP)Ben}$ - abbreviated as *N1ICDP*^{iGOF}) generated in

the lab (Fig. 7A). In embryos carrying the N1ICDP^{iGOF} and Tie2-Cre alleles (*N1ICDP$^{iEC\text{-}GOF}$*), ECs (Tie2-Cre^{+}) will express MbTomato (Membrane localized Tomato), H2B-GFP (Nuclei/Chromatin localized GFP), and the active Notch1 Intracellular domain containing its native PEST domain (N1ICDP) (Figure 7A, B). To validate that *N1ICDP$^{iEC\text{-}GOF}$* HE cells had increased expression of downstream Notch targets, I performed FACS of E10.5 hemogenic ECs (CD31^{+}/c-kit^{+}) that were Tomato positive (+) as well as Tomato negative (-). qRT-PCR analysis revealed that MbTomato^{+} ECs had increased expression of the canonical Notch downstream targets *Hey2*, *Dll4* and *Efnb2* (Figure 7C). Interestingly, less than half (45%) of the ERG^{+} cells were also N1ICDP$^{iEC\text{-}GOF}$/GFP^{+} (Figure 7D, E) showing that recombination or expression of the N1ICDP$^{iEC\text{-}GOF}$ allele with Tie2-Cre is not complete or that N1ICDP$^{iEC\text{-}GOF}$/GFP^{+} ECs are outcompeted during vascular development by non-recombined cells.

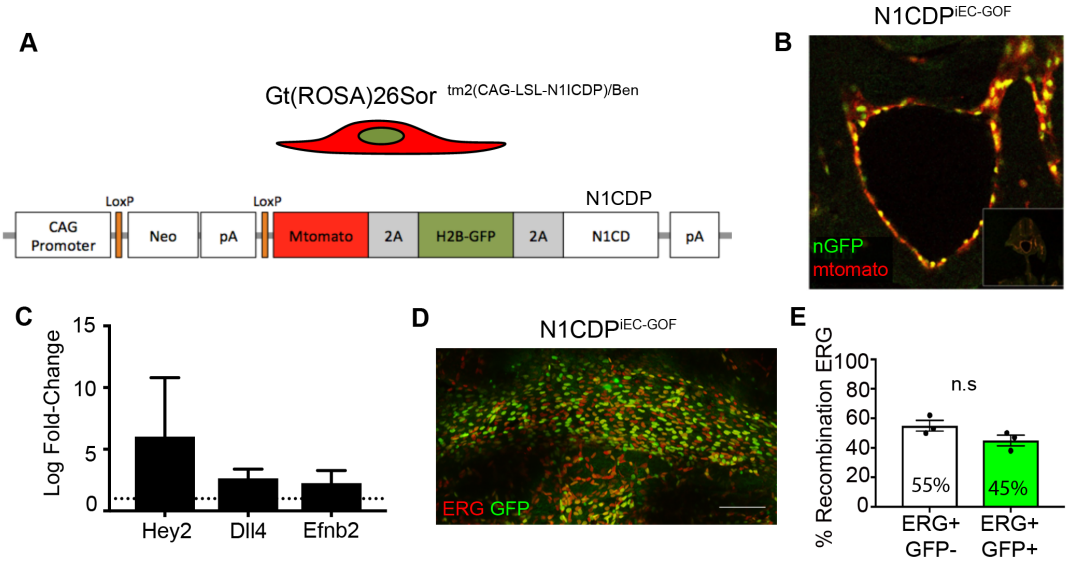

Figure 7 Validation of N1CDP$^{iEC\text{-}GOF}$ in E10.5 Dorsal Aorta. A, Diagram of the DNA construct inserted in the Rosa-26 locus, in which the nuclear expression of GFP and membrane expression of Tomato is associated with increased Notch expression. **B,** Cryosection of the AGM region of N1CDP$^{iEC\text{-}GOF}$ E10.5 embryos immunostained to show GFP in the nucleus and Tomato in the membrane. **C,** RT-qPCR analysis of fold change of *Hey2, Dll4*, and *Efnb2* expression in GFP^{+} ECs compared to GFP- ECs (dotted line) from N1CDP$^{iEC\text{-}GOF}$ **D,** Quantification of percent ERG^{+} cells that were positive for GFP; n=3 embryos. Error bars indicate SEM; n.s. indicates no statistical differences between the two groups in a two-tailed student t-test.

4.3 Notch GOF in the HE leads to fewer Runx1-positive cells and HSPCs in the dorsal floor.

Notch has been shown to promote arteriogenesis and block endothelial proliferation (Adams, 2003; Noseda et al., 2004; Sahara et al., 2014). We have observed that N1ICDP$^{EC\text{-}iGOF}$ embryos had a noticeably thinner aorta, even though it was lumenized (Figure 8A-C). This may indicate a decrease in EC proliferation in these mutants, and the consequent decrease in the number of ECs that form the DA. Interestingly, embryos with overexpression of N1ICDP in the dorsal endothelium showed a 64% decrease in the average number of HSPCs (c-Kit^{+}) present in the dorsal floor as compared to their control littermates (Figure 8D, E). This decrease in HSPC number is very significant since only 45% of the N1ICDP$^{EC\text{-}iGOF}$ aorta ECs are GFP^{+} (Fig. 7D, E).

To dissect if the impact of Notch on HSPC formation was at the step of endothelial commitment to the hemogenic lineage, we counted the number of CD31^{+} Runx1^{+} c-Kit^{-} cells that were present in serial sections of the dorsal floor of *N1ICDP$^{EC\text{-}iGOF}$* embryos. Embryos with Notch GOF had 40% fewer CD31^{+}/Runx1^{+} cells (average of 12 cells per section) as compared to their WT littermates (average of 20 cells per section) (Figure 8F, G). Consistent with this, only 30% of the CD31^{+} N1ICDP$^{EC\text{-}iGOF}$/GFP^{+} cells were also Runx1^{+} (Figure 8H, I).

Altogether, these results suggest that an increase in Notch signaling in the HE has a negative effect on the endothelial commitment to the hematopoietic lineage (Runx1^{+}) which results in a decrease to the number of hematopoietic progenitor stem cells (c-kit^{+}) in the DA at E10.5. Paradoxically, this N1ICDP$^{EC\text{-}iGOF}$ phenotype is also similar to the Jagged1/Notch LOF phenotype previously reported in mice (Robert-Moreno et al., 2008). The results suggest that contrary to what was previously published, cell-autonomous overactivation of Notch in ECs causes a decrease in the total number of Runx1 cells present in the dorsal floor as only a minor fraction of cells with increased Notch activity will upregulate Runx1.

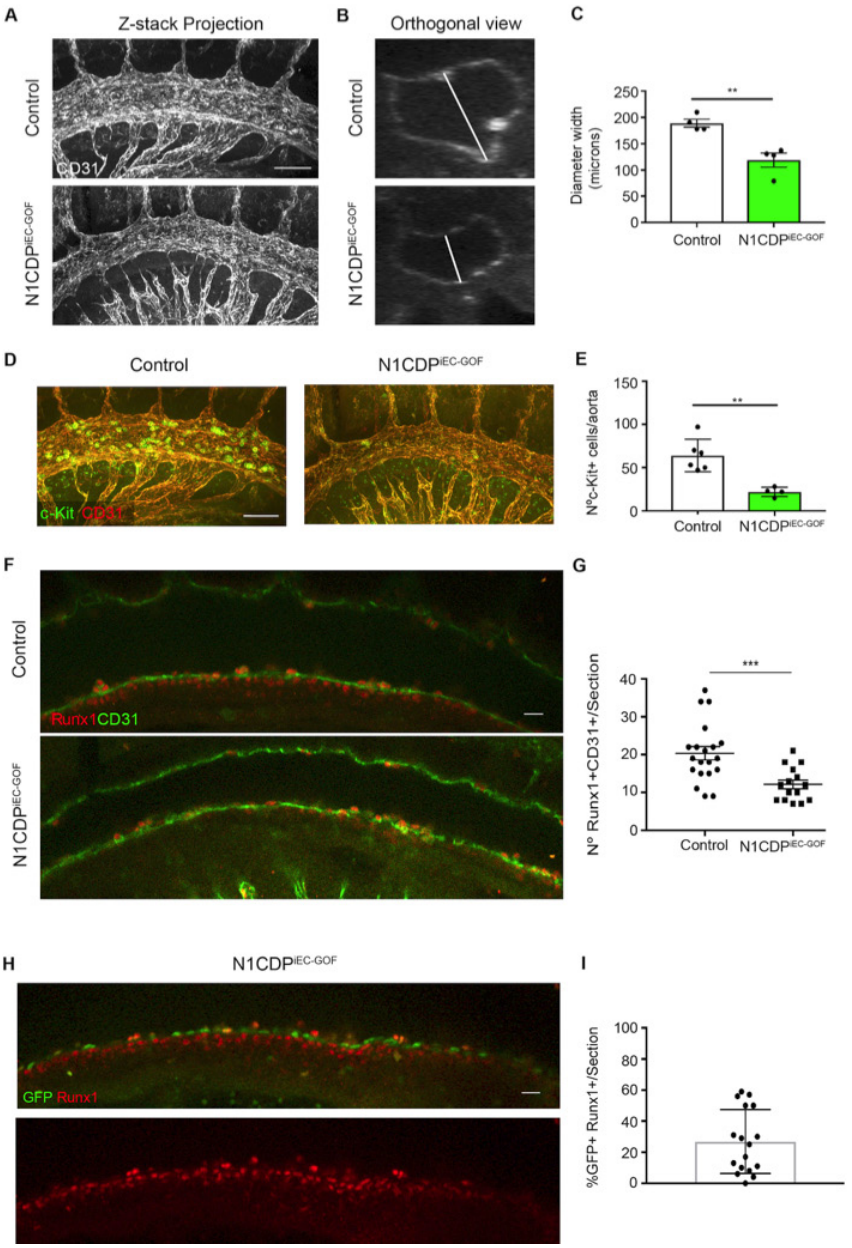

Figure 8 Notch GOF in the hemogenic endothelium leads to fewer Runx1-positive cells and HSPCs in the dorsal floor. A, Representative photo of a confocal z-stack projection of Control (Top) and N1CDP$^{iEC-GOF}$ (Bottom) DA at E10.5 immunostained with CD31 (Grey). White line on bottom right of top photo indicates 100µm. **B,** Orthogonal view of (A) z-stacked projections. White scale bar represents the longitudinal length of the dorsal lumen. **C,** Quantification of the diameter width (in microns) per aorta in both Control (n=4 embryos) and N1CDP$^{iEC-GOF}$ (n=4 embryos). **D Left,** Representative photo of a confocal z-stack projection (STD DEV) of Control DA at E10.5 immunostained for CD31 (Red) and c-Kit (Green). White scale bar on bottom right corner indicates 100µm. **D Right,** Representative photo of confocal z-stack projection of N1CDP$^{iEC-GOF}$ embryo DA at E10.5. **E,** Quantification of the number of c-Kit^{+} cells per aorta in both Control (n=6 embryos) and N1CDP$^{iEC-GOF}$ (n=4 embryos). **F,** Representative confocal slice images of the DA of Control (Top) and N1CDP$^{iEC-GOF}$ (Bottom) immunostained with CD31 (Green) and Runx1 (Red). White scale bar indicates 100µm. **G,** Quantification of the number of Runx1^{+} CD31^{+} cells per section in Control (n=4 embryos) and N1CDP$^{iEC-GOF}$ (n= 3 embryos); 5 sections per embryo. **H,** Representative confocal slice image of the DA of N1CDP$^{iEC-GOF}$ immunostained with GFP (Green) and Runx1 (Red). White scale bar indicates 100µm. **I,** Quantification of the % GFP^{+} of the dorsal floor that are also Runx1^{+} per section N1CDP$^{iEC-GOF}$ (n= 4 embryos); 3-5 sections per embryo; 264 cells quantified. Error bars indicate SEM; ** p value ≤ 0.01; *** p value ≤0.001 with a two-tailed student t-test.

4.4 Aorta ECs with an autonomous increase in Notch signaling have impairment in EHT and early HSPCs clonal expansion.

Given that only a fraction of the *N1ICDP*$^{EC\text{-}iGOF}$ aorta ECs (ERG^{+}) are GFP^{+} (Fig. 7D, E), we took advantage of this mosaicism to compare the frequencies of control (GFP^{-}) cells and cells with increased Notch signaling (GFP^{+}), in both the endothelial (ERG^{+}) and HSPCs (c-kit^{+}) populations. Examination of the percentage of cells that were GFP^{+} as compared to the total number of ERG^{+} or c-Kit^{+} cells showed that even though 45% of DA ECs were GFP^{+} (Figure 7E), only 27% of the DA c-Kit^{+} population was GFP^{+} (Figure 9B). This difference suggests that ECs with high Notch have either defects in undergoing EHT or proliferate less after they undergo EHT and become c-kit^{+} HSPCs. In order to distinguish the effect of Notch on these two consecutive events, we counted the frequency of GFP^{+} single endothelial budding c-kit^{+} cells. It was observed that only 29% of budding ECs were GFP^{+} (Figure 9C,D), which strongly indicates that Notch activation directly impacts EHT.

To determine if Notch activation would also impact the proliferation of HSPCs, we quantified all c-kit^{+}PECAM^{+} clusters and their size (number of c-kit^{+} cells per cluster) in control and *N1ICDP*$^{EC\text{-}iGOF}$ aortas. The results show that an increase in Notch activity leads to a significant reduction in the size of the HSPCs clusters. Most of *N1ICDP*$^{EC\text{-}iGOF}$ aortas clusters had between 1-4 cells per cluster, whereby 45% of clusters were formed by only 1 cell, whereas control aortas had a wider range of cluster sizes (Figure 9E, F). Upon examining cluster dynamics of monoclonal clusters (or clusters that were completely GFP^{+} versus those that were completely GFP^{-}) in the *N1ICDP*$^{EC\text{-}iGOF}$ aortas, it was calculated that GFP^{+} clusters were most often found in the 1 cell state while GFP^{-} clusters had a wider range of cluster sizes (Figure 9H, I).

The data therefore indicates that Notch activation inhibits both the initial EHT transition (Runx1^{+}) and the later HSPCs (c-kit^{+}) expansion in the dorsal aorta floor.

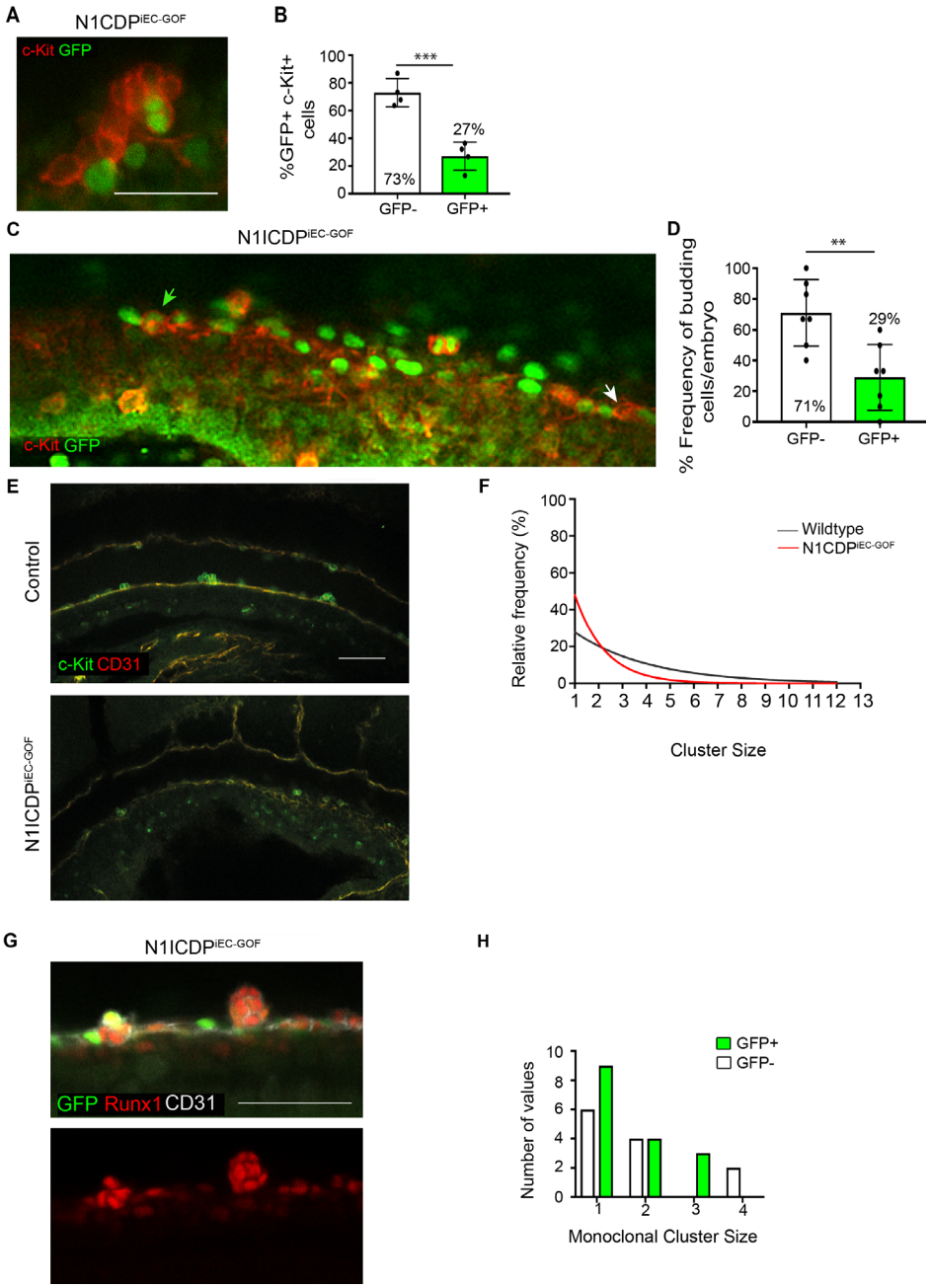

Figure 9 Aorta with endothelial autonomous increase in Notch signaling have impairment in EHT and early HSPCs clonal expansion. A, Zoom image of HSPC clusters in DA of an E10.5 N1CDP$^{iEC-GOF}$ embryo immunostained c-Kit (Red) and GFP (Green). White scale bar in bottom right corner indicates 50μm **B,** Quantification of the percent GFP^{+} versus GFP^{-} contribution to the total number of c-Kit^{+} cells present in the DA of N1CDP$^{iEC-GOF}$ embryos at E10.5; n= 4 embryos. **C,** Zoom of the dorsal floor of an E10.5 N1CDP$^{iEC-GOF}$ embryo immunostained c-Kit (Red) and GFP (Green). White arrow points to a budding GFP^{-} c-Kit^{+} HSPC while the green arrow indicates a budding GFP^{+} c-Kit^{+} HSPC. White scale bar in bottom right corner indicates 50μm. **D,** Quantification of the percent GFP^{+} versus GFP^{-} frequency of budding cells per embryo; n= 7 embryos. **E,** Representative slice image of Control (Top) and N1CDP$^{iEC-GOF}$ (Bottom) immunostained with CD31 (Red) and c-Kit (Green). White scale bar indicates 100μm. **F,** Line graph indicating the relative frequency in percentages of clusters sizes found in Control embryos (black line) versus N1CDP$^{iEC-GOF}$ (red line) embryos. **G,** Zoom of two different clusters in the dorsal floor of N1CDP$^{iEC-GOF}$ embryos. Immunostained GFP (Green), Runx1 (Red), and CD31 (Grey). White scale bar line measures 53μm. **H,** Bar graph showing the number of values of GFP^{+} versus GFP^{-} monoclonal cluster size. Error bars indicate SEM in all quantifications; *** p value ≤0.001; ** p value ≤ 0.01 with a two-tailed student t-test.

4.5 Using ifgMosaics to understand the cell-autonomous requirement for Notch in EHT

One of the technical issues related with the use of classical genetics to study the role of genes or pathways in the EHT process *in vivo* is that the loss of any gene required for arteriogenesis or vascular development will also affect EHT and the subsequent development of HSPCs. This occurs even if HSPC development is not the primary function of the gene. As the loss of Dll4/Notch1/Rbpj has been shown to severely impact the development of the DA (Duarte et al., 2004; Gale et al., 2004; Krebs et al., 2010; Limbourg et al., 2005), we sought to overcome the problem of lack of arteriogenesis in mutants by instead analyzing genetic mosaics in compound mutants having the *Tie2-Cre* and *iChr-Notch-Mosaic* alleles (Pontes-Quero et al., 2017).

The *iChr-Notch-Mosaic* allele has three distinct cassettes flanked by mutually exclusive LoxP sites. Upon Cre recombination of the flanking Lox sites, only one of three possible events can occur in a given cell (Figure 10A). Due to the different genetic distances between LoxP sites, the most frequent event is the recombination of the first LoxP1 cassette inducing the expression of H2B-Cherry which will label the control cells with normal levels of Notch signaling. The second most frequent event is the recombination of the LoxP2 flanked cassette that induces expression of H2B-GFP and Dominant Negative (DN)-Mastermind (Maml1) at equimolar levels. Expression of this version of Maml1 has been shown to inhibit Notch signaling cell-autonomously (Maillard et al., 2004). The third and less frequent recombination event, leads to the expression of HA-H2B-Cerulean and N1ICDP to induce Notch overactivation. Published qRT-PCR of Notch target genes in FACS sorted ECs from *Tie2-Cre* and *iChr-Notch-Mosaic* E10.5 embryos revealed the expected downregulation of Notch target genes in H2B-GFP^{+} cells and upregulation of Notch target genes in HA-H2B-Cerulean^{+} cells (Pontes-Quero et al., 2017). Fig. 10B is an illustration to depict how ECs in the DA are predicted to recombine and how labeled HSPCs will be scored to determine how different cell-autonomous Notch signaling levels affects the biology of these cells during EHT and HSPC expansion.

To analyse how cells with different Notch levels behaved over time, we determined the intial frequencies of the *iChr-Notch-Mosaic* cells in Tie2-Cre^{+} ECs and HSPCs. At E9.5, the DA endothelial Cherry: GFP: Cerulean frequency was 70%: 20%: 10%, likely reflecting not only the lower recombination efficiency of the second and third cassettes but also the lower tendency of cells with low Notch (DN-Maml1^{+}/GFP^{+}) to become incorporated in arteries and the lower proliferation of ECs with high Notch (N1ICDP/Cerulean^{+}) (Fig. 10C-E).

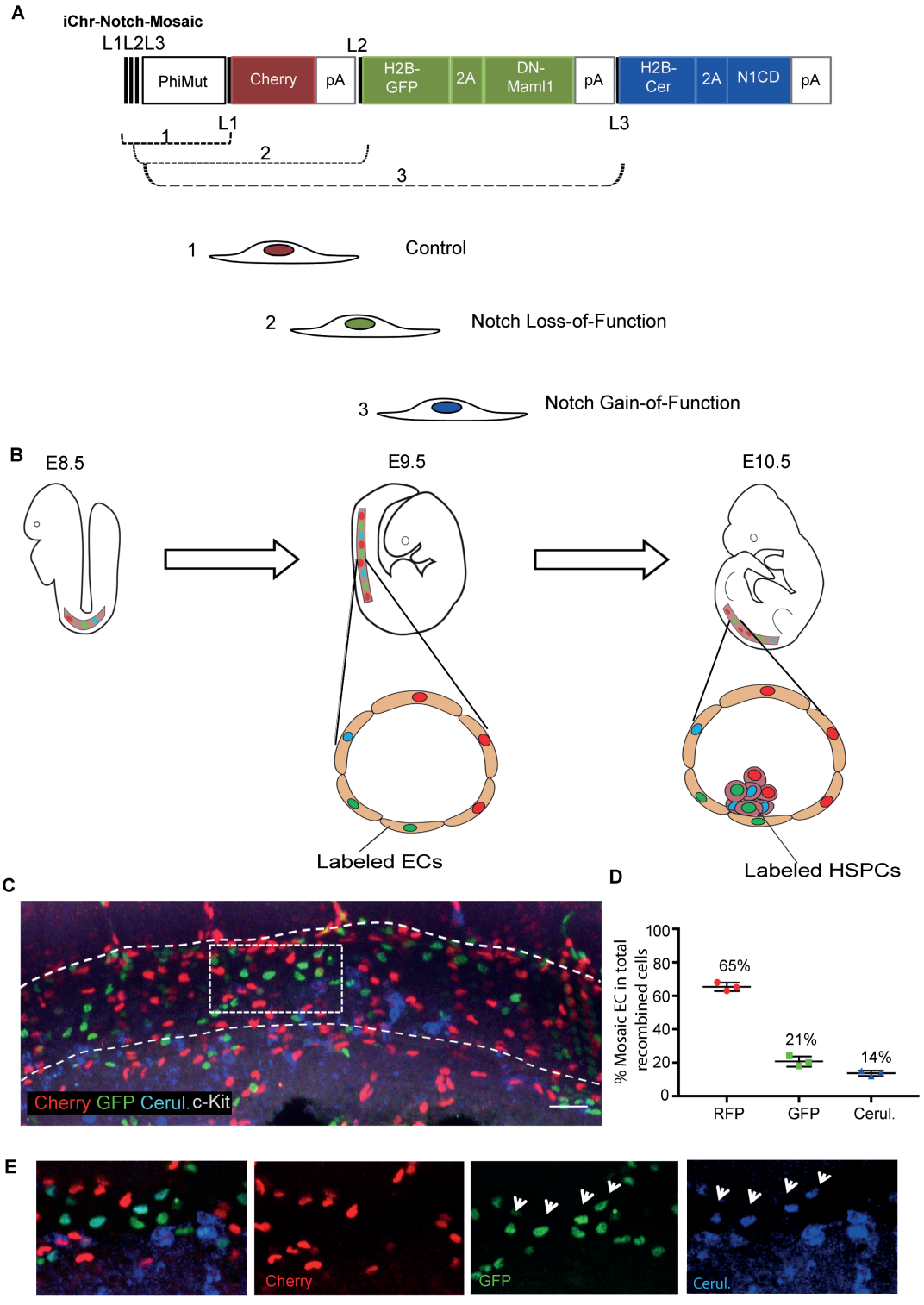

Figure 10 Endothelial Recombination of iChr-Notch-Mosaic at E9.5. A, The mosaic genetic construct is illustrated at the top. ECs of the Dorsal Aorta recombine to produce one of the three fluorescent proteins: nuclear Cherry nuclear Control cell (1), nuclear GFP Notch loss-of-function cell (2), or nuclear Cerulean Notch GOF cell (3). **B,** Between E8.5 and E10.5, ECs of the Dorsal Aorta recombine to have one of the three fluorescent proteins labeled in the endothelial cell. The left DA shows labeled ECs according to predicted recombination events. The Dorsal Aorta on the right represents potential labeled HSPC population in the lumen of E10.5 embryos.

C, Representative photo of a confocal z-stack projection (STD DEV) of Tie2-Cre; iChr-Notch-Mosaic embryos. Cherry (RFP); GFP (Green); CFP (Light Blue); and c-Kit (white). White scale bar indicates 100μm. The DA is indicated to be between the two parallel dotted white lines. White dotted rectangle within this area is to highlight where the zoomed photos in (**E**) are located. **D,** Quantification of the percent mosaic recombination (RFP, GFP, or CFP) in endothelial cells of the DA in recombined endothelial cells (n= 3 embryos). **E**, Zoomed images of a section in (**C**). White arrows indicated ECs that are Cerulean but also are stained GFP. Error bars indicate SEM.

Next, we checked the frequencies of ECs with the different labels at E10.5. The frequency of the Cherry$^+$ population slightly increased from E9.5 to E10.5 (65% to 74% respectively) while the GFP$^+$ and Cerulean$^+$ frequencies decreased to 16% and 10% respectively (Figure 10D & Figure 11B).

Interestingly, when we examined the frequency of mosaic contribution to the c-Kit$^+$ HSPC population, we saw that the GFP$^+$ population became 40% more frequent (from 16% of ECs to 27% of HSPCs) while the Cerulean$^+$ population became 60% less frequent (from 10% of ECs to 4% of HSPCs) (Figure 11B, D, E).

Contrary to published data using zebrafish genetics or mouse classical genetics, our inducible fluorescent genetic mosaics (*ifgMosaics*) data suggests that endothelial cells with lower Notch activity have an advantage in undergoing endothelial to hematopoietic transition and becoming hematopoietic progenitor cells. On the other hand, cells with higher Notch activity have a disadvantage. Therefore, even though in our work we are only analyzing Notch mosaic mutant behaviours, our results suggest that within a wildtype/normal developing aorta, the arterial ECs with lower Notch signaling will more likely undergo fate transition. Our data also suggests that higher Notch signaling is initially required to specify the arterial fate, and once this is acquired, a decrease in Notch signaling is required or facilitates EHT.

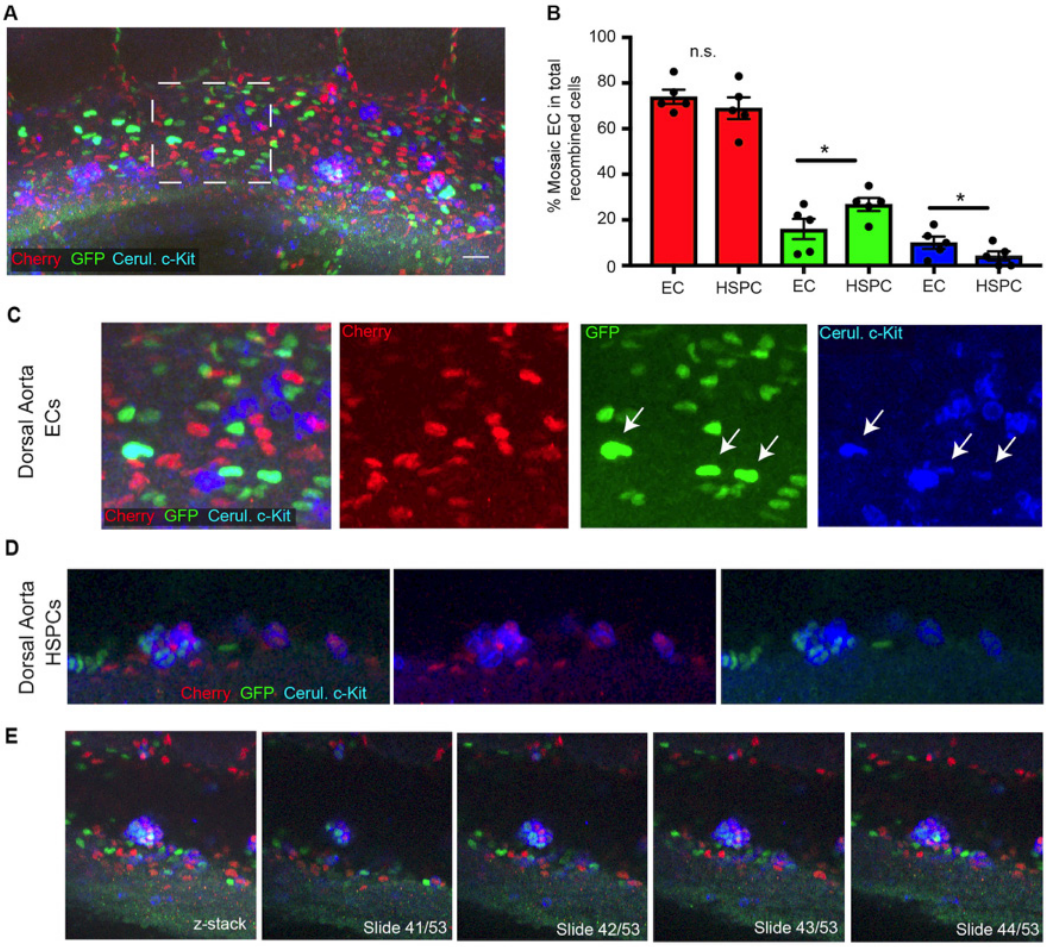

Figure 11 iChr-Notch-Mosaic Endothelial Recombination at E10.5 shows ECs with less Notch activity become HSPCs. A, Representative photo of a confocal z-stack projection (STD DEV) of Tie2-Cre; iChr-Notch-Mosaic embryos. Cherry (RFP); GFP (Green); CFP (Light Blue); and c-Kit (white). White scale bar indicates 100μm. The DA is indicated to be between the two parallel dotted white line. White dotted rectangle within this area is to highlight where the zoomed photos in (**C**) originates in the original z stack. **B,** Quantification of the percent mosaic recombination (RFP, GFP, or CFP) in Endothelial cells and Hematopoietic Stem and Progenitor Cells of the DA in the total recombined cells (n= 5 embryos) * p value ≤0.05; n.s. means not significant in one-tailed student t-test. **C,** Zoomed image of selected area in (**A**). White arrows indicated ECs that are Cerulean but also are stained GFP. **D,** Zoomed image of a HSPC cluster in E10.5 iChr-Notch-Mosaic embryos with Cherry and GFP c-Kit^{+} cells. **E,** Images of serial images of a z-stack to show the single cell resolution at 20x magnification.

4.6 Endothelial loss of Jagged1 phenocopies N1ICDP overexpression during definitive hematopoiesis

Previous research has tried to circumvent the detrimental vascular phenotype and lack of arteriogenesis associated with Notch1/Dll4/Rbpj loss of function by generating mutants with loss of the Notch ligand Jagged1 (Robert-Moreno et al., 2008). Global loss of the Jag1 ligand does not affect arteriogenesis but results in a specific impairment in AGM hematopoiesis, a phenotype that was attributed to the loss of Jagged1-Notch activation in DA ECs located in the AGM, even though Notch activity differences were not reported in these mutants (Robert-Moreno et al., 2008). However, these mutants lack Jag1 ligand expression in all embryo cells since conception. Therefore, to evaluate the phenotype of Jag1 LOF specifically in ECs, we generated compound Tie2-Cre; $Jag1^{fl/fl}$ embryos and counted the number of c-kit^{+} cells present in the DA at E10.5. We observed a 60% reduction in the number of HSPCs present in the DA of Jag1 mutants as compared to control littermates (Fig. 12A-C). These results are in agreement with previous results obtained in embryos with global Jagged1 deletion and clearly point towards the endothelial origin of the Jag1 LOF phenotype. Since *Dll4* expression is induced after Notch activation in ECs (Fig.7C), we stained with a Dll4 antibody to investigate if there was a difference in Notch activation levels in the DA of these embryos. When quantifying the % of DLL4 in CD31 (endothelial) area we saw that in Jag1 mutants, Dll4 immunosignals were significantly increased (Figure 12E, F). This data suggests that loss of endothelial Jag1 in the DA induces an increase in Notch activation in the endothelium and that the reduction in the number of HSPCs that was previously associated with the loss of the ligand-receptor signaling can be, in fact, due to increased Notch signaling.

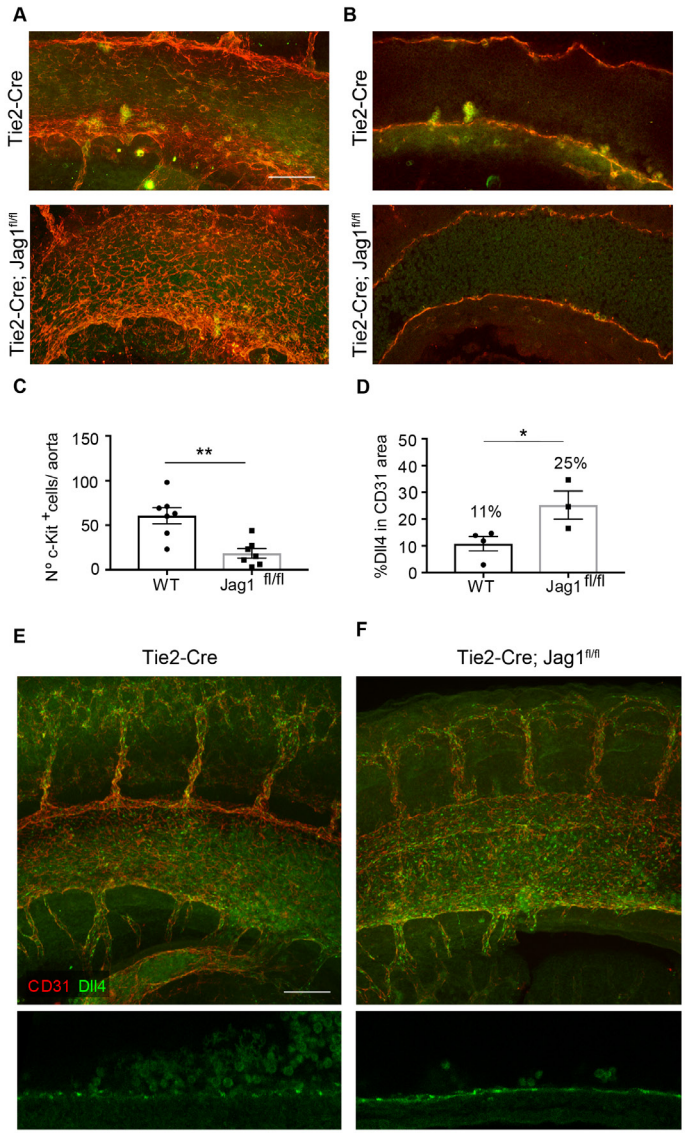

Figure 12 Loss of Jagged1 in Endothelial Cells of the Dorsal Aorta leads to decreased c-Kit⁺ cells and increased whole tissue Notch activation. A, Representative photo of a confocal z-stack projection (STD DEV) of Tie2-Cre (top) and Tie2-Cre; Jag1$^{fl/fl}$ (bottom) DA at E10.5 immunostained for CD31 (Red) and c-Kit (Green). White scale bar on bottom right corner indicates 100µm. **B,** Tie2-Cre (top) and Tie2-Cre; Jag1$^{fl/fl}$ (bottom) DA at E10.5 immunostained for CD31 (Red) and c-Kit (Green). **C,** Quantification of the number of c-Kit+ cells per aorta of wildtype (n=7 embryos) and Jag1$^{fl/fl}$ (n=7 embryos). **D**, Quantification of the percent Dll4 in CD31 area in wildtype (n=4 embryos) and Jag1$^{fl/fl}$ (n=3 embryos) embryos. **E**, Representative photo of the Dll4 (Green) and CD31 (Red) immunostaining in Tie2-Cre. Top is a full z-stack projection of the DA and bottom is a zoom photo of the dorsal floor and only the Dll4 (Green) immunostaining. **F**, Representative photo of the Dll4 (Green) and CD31 (Red) immunostaining in Tie2-Cre; Jag1$^{fl/fl}$. Top is a full z-stack projection of the Jag1$^{fl/fl}$ DA and bottom is a zoom photo of the dorsal floor immunostained for Dll4 (Green). White scale bar indicates 100µm. Error bars indicate SEM in all quantifications; * p value ≤0.05; ** p value ≤ 0.01 with a two-tailed student t-test.

4.7 Overexpression of Manic Fringe in the DA endothelium leads to increased numbers of c-Kit^{+} cells by decreasing Jagged1-Notch signaling

Fringes are glycosyltransferases that have been shown to be able to glycosylate the Notch extracellular domain and regulate the Notch ligands signaling ability (Kakuda and Haltiwanger, 2017). Three Fringes proteins exist in mammals (Lfng, Mfng and Rfng) and they are broadly expressed in the organism. Fringe proteins are partially functionally redundant (Moran et al., 2009a) and it was shown that they can inhibit the signaling ability of Jagged ligands while promoting the signaling ability of Delta ligands (Benedito et al., 2009; Yang et al., 2005).

To understand the biological impact of Fringes in EHT, we crossed *Tie2-Cre* with a (*Mfng*$^{EC\text{-}iGOF}$) line to generate *Manic Fringe*$^{EC\text{-}iGOF}$, and counted the number of c-Kit^{+} cells present in the aorta of E10.5 embryos. Embryos with an endothelial increase in Mfng expression had more c-Kit^{+} cells present in the DA as compared to their control littermates (Figure 13A, B). This suggests that the final output of Mfng expression in the DA is of Notch signaling inhibition and not Notch GOF. Since aorta ECs express both Jagged1 and Dll4 ligands and Fringes inhibit Jagged signaling while promoting Delta signaling (Kakuda and Haltiwanger, 2017), this data suggested that Jagged1 ligands could be more expressed than Delta4 ligands in the aorta endothelium. We suspect that, based on our phenotype, Jagged1 mRNA levels should be significantly higher than that of Dll4 in the *Mfng*$^{EC\text{-}iGOF}$ endothelium. Immunostaining for Dll4 protein, an endothelial Notch target gene (Benedito et al., 2009), also showed a significant reduction of this protein in *Mfng*$^{EC\text{-}iGOF}$ E10.5 embryos (Figure 13C, D). These results indicate that overexpression of Manic Fringe in the endothelium leads mainly to a loss of Jagged1-Notch signaling ability, which likely masks the eventual and less pronounced Fringe-mediated increase in Dll4-Notch signaling.

In conclusion, the overall consequence of Mfng overexpression is of a decrease in Notch signaling output in the AGM. We therefore hypothesize that during EHT, Mfng or the other three Fringes are required to modulate Notch signaling and promote EHT. This hypothesis could only be confirmed by analysis of single or compound mutants for Fringe genes.

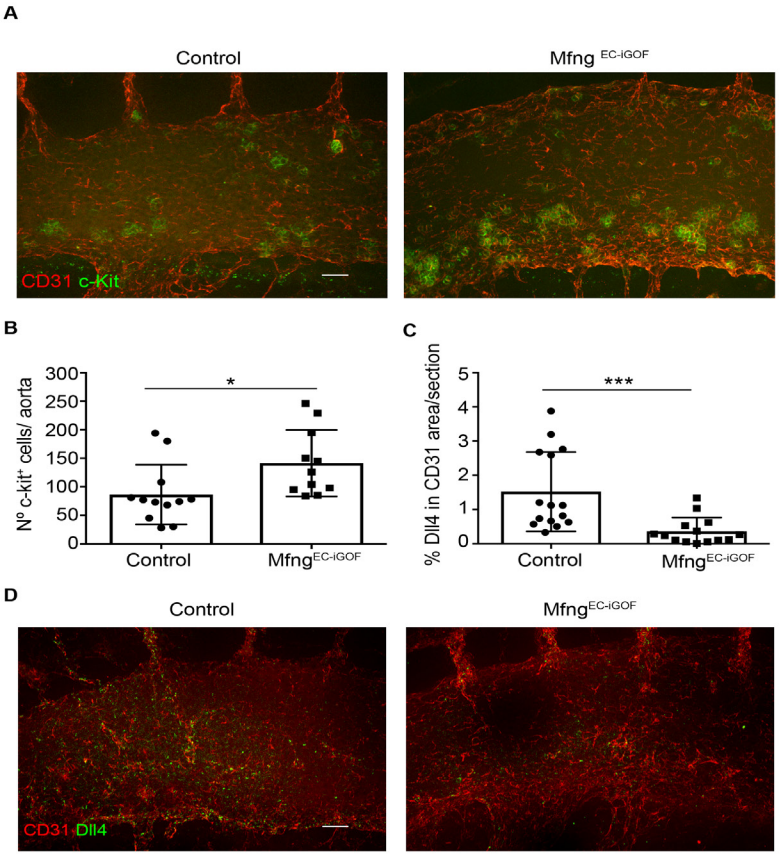

Figure 13 Overexpression of Manic Fringe in Endothelial Cells of the Dorsal Aorta leads to more c-Kit⁺ cells and overall lower endothelial Notch activation in the DA. A, Representative confocal z-stack projection (STD DEV) of Tie2-Cre (left) and Tie2-Cre; Manic Finge^{GOF} (Mfng$^{EC\text{-}iGOF}$) (right) immunostained with CD31 (Red) and c-Kit (Green). White scale bar indicates 100μm. **B,** Quantification of the number of c-Kit⁺ cells per aorta in WT (n= 12 embryos), and Mfng$^{EC\text{-}iGOF}$ (n= 11 embryos) embryos. **C,** Quantification of the percent Dll4 staining in the CD31 area per section (n=3 embryos; 3 sections per embryo). **D,** Representative confocal z-stack projection (STD DEV) of Tie2-Cre (left) and Mfng$^{EC\text{-}iGOF}$ (right) immunostained with CD31 (Red) and Dll4 (Green). White scale bar indicates 100μm. Error bars indicate SEM. * p value ≤0.05; *** p value ≤0.001 two-tailed student t-test.

4.8 qPCR analysis of ECs with lower Notch signaling shows an increase in tip cell genes and mycn expression

Because our data suggested that ECs with low Notch had a higher chance to undergo EHT and form the aorta HSPC population, we decided to isolate arterial Cx40^{+}/c-kit^{-}/Cherry^{+} and Cx40^{+}/c-kit^{-}/GFP^{+}-DN-Maml ECs from a pool of E10.5 DAs to do a qPCR analysis of several genes of interest (Figure 14A, B). Compared to normal ECs, ECs with lower Notch signaling (H2B-GFP^{+}/DN-Maml1^{+}) showed a decrease in *Hey2* expression. Both CD41, an early marker of hematopoietic progenitor cells, and Sox17, a marker of arterial endothelium, did not differ between the two populations. Interestingly, Numb, an antagonist of Notch (McGill and McGlade, 2003) has a 2-fold increase in the ECs with Notch LOF. Numb plays an important role in cell fate determination in development and, at least during neurogenesis, asserts this role by inducing asymmetrical cell division (Wakamatsu et al., 1999).

Lastly, since previous electron microscopy imaging of the DA determined that Runx1^{+} ECs undergoing a characteristic morphological change indicative of EHT upregulate lamelipodia-like projections on their surface (Bos et al., 2015), we wondered if arterial ECs with downregulation of Notch would upregulate tip-cell genes. We also hypothesized that this may be relavent since it has been shown that Notch inhibition induces a tip-cell sprouting phenotype and the expression of tip cell enriched transcripts (Hellstrom et al., 2007; Pontes-Quero et al., 2019). We found Esm1, a known tip cell marker (del Toro et al., 2010), to be highly upregulated in Dorsal ECs with Notch LOF (Fig. 14C).

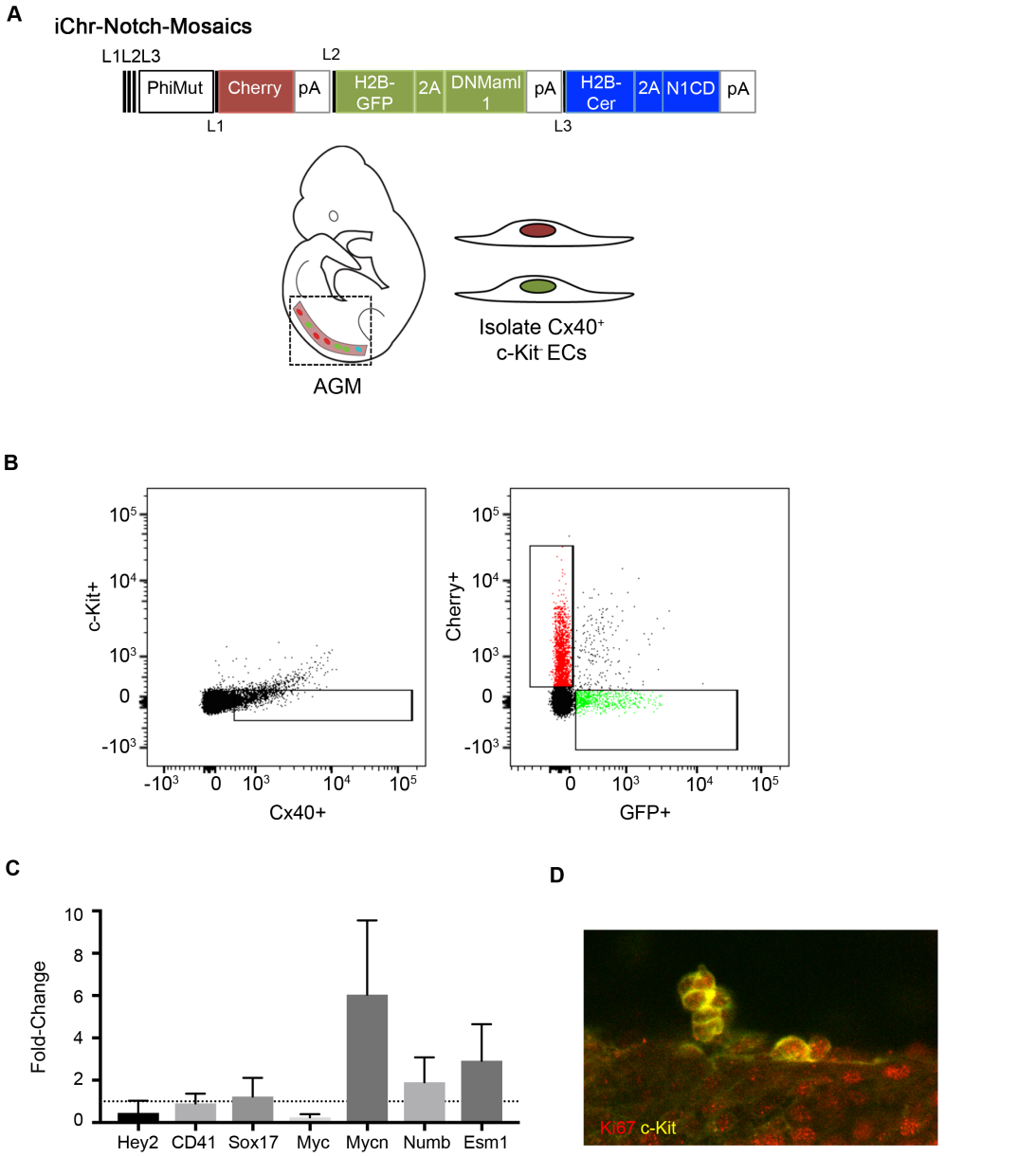

Figure 14 Qualitative PCR analysis of DN-MAML ECs shows increased mycn expression. **A,** Graphical representation of the iChr-Notch-Mosaic construct. Drawing represents the two endothelial cell populations (Cherry$^+$ or GFP$^+$, Cx40$^+$ c-Kit$^-$) isolated from E10.5 AGM. **B,** Cytometry dot plots indicating the isolated ECs (left) and the separation of the two fluorescent ECs (right). **C,** Bar graph showing the changes, in fold-change, of the mRNA expression of genes (*Hey2, CD41, Sox17, Myc, Mycn, Numb, Esm1*) in the GFP$^+$ population compared to the baseline Cherry$^+$ population (indicated on the chart as a black dotted line at Y=1). (n=2-3 pools of embryos containing 6-8 embryos each). **D,** Zoomed image of proliferative (Ki67$^+$) HSPCs (yellow) in the dorsal floor.

However, when we analyzed embryos with full loss of *Apelin (Apln*), another tip cell gene required for endothelial sprouting (del Toro et al., 2010), we saw that Apln KOs had statistically more c-kit$^+$ HSPCs in the DA as compared to the control littermates (Figure 15A, B). We could not investigate this data further but we thought it interesting to note in this document.

Because budding HSPCs in the DA are highly proliferative (high Ki67 staining)(Figure 14D)

as compared to the underlying ECs (Batsivari et al., 2017; Zape et al., 2017) and since Myc has been shown to be a positive regulator of proliferation and regulated by Notch in hematopoietic cells (Bretones et al., 2015; Sanchez-Martin and Ferrando, 2017), we analysed if its expression was deregulated in GFP$^+$ cells during EHT. Surprisingly, *Myc* expression went down considerably in GFP$^+$-DN-Maml1$^+$ ECs while *Mycn* expression, the closely related homologous gene capable of substituting Myc function in some biological contexts (Malynn et al., 2000), increased by an average 6-fold (Figure 14C).

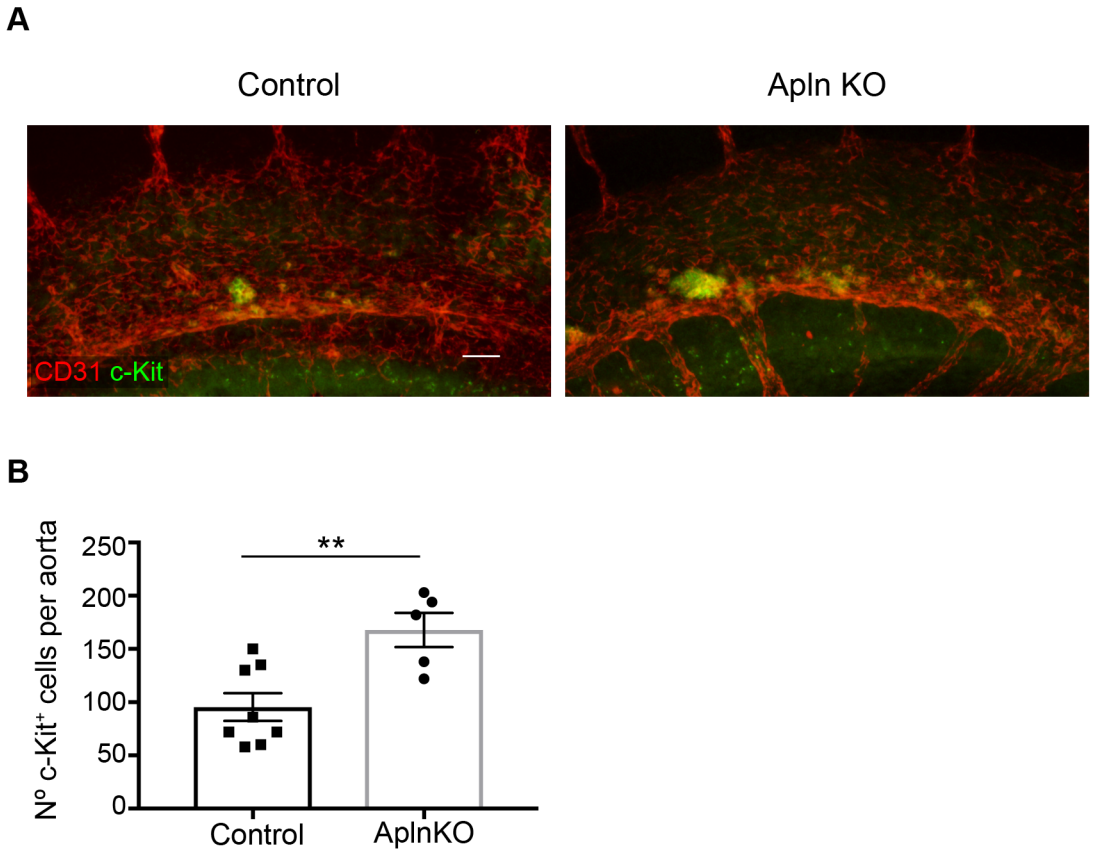

Figure 15 Loss of Apelin in Endothelial Cells of the Dorsal Aorta leads to increased c-Kit$^+$ population in the DA. A, Representative confocal z-stack projection (STD DEV) of Wildtype (left) and Apelin knockouts (Apln KO) (right) immunostained with CD31 (Red) and c-Kit (Green). White scale bar indicates 100µm. **B,** Quantification of the number of c-Kit$^+$ cells per aorta in WT (n=8 embryos) and Apln KO (n= 5 embryos). Error bars indicate SEM. ** p value ≤ 0.01 two-tailed student t-test.

4.9 Mycn, not Myc, is a key regulator of EHT

Previous publications on the role of *Myc* in definitive hematopoiesis have demonstrated opposing results when using Tie2-Cre;Myc$^{fl/fl}$ (*Myc^{iDEC}*) (Dubois et al., 2008; He et al., 2008). Dubois and colleagues found that E11 embryos had a decrease in CD45^{+} blood population but had a relatively high stem/progenitor population. However, He and colleagues, using a similar model, found no clusters in the *Myc^{iDEC}* embryos concluding a diminished HE in the DA. Yet, in neither of the aforementioned studies did they specifically look into the process of DA EHT. Therefore, we decided to further investigate the role of Myc in the process by using the *Tie2-Cre* allele to recombine the floxed *Myc* gene (Figure 16A). We observed no difference in the number of c-kit^{+} cells present in the DA of *Myc^{iDEC}* mutants when compared with control littermates (Figure 16B). Since Mycn is known to be able to compensate for the loss of Myc in developing embryos (Malynn et al., 2000), we analyzed embryos that had lost both *Myc* and *Mycn* in the dorsal endothelium. In contrast to single *Myc^{iDEC}* mutants, dual floxed *Myc/Mycn^{iDEC}* embryos showed a significant reduction in the number of c-kit^{+} HSPCs in the DA endothelium. Surprisingly, the single loss of Mycn in the endothelium also resulted in a drastic reduction in the average number of HSPCs present on the dorsal floor (Figure 16C, D). We also checked HSPC cluster dynamics in these embryos and saw that *Mycn^{iDEC}* embryos had clusters with an average of 2 cells per cluster, instead of 6, with a great proportion of c-kit^{+} clusters being only single cells, and the largest clusters reaching a maximum of 5 cells, instead of 30 (Figure 16E, F). These results indicate for the first time that *Mycn,* not *Myc,* is a key driver of EHT.

This *Mycn^{iDEC}* EHT phenotype is similar, although more pronounced, than the *N1ICDP$^{iEC\text{-}GOF}$* phenotype described above. Given that GFP^{+}/DN-Maml1^{+} cells upregulate *Mycn* (Figure 14C), we checked if aorta ECs with higher Notch signaling in *N1ICDP$^{iEC\text{-}GOF}$* mutants had a decrease in *Mycn* expression. For that, we isolated Cx40^{+}/c-kit^{-} and Cx40^{+}/c-kit^{-}/Tomato^{+} ECs from control and *N1ICDP$^{iEC\text{-}GOF}$* embryos. Indeed, when compared to control littermates, *Mycn* expression decreased 3 log-fold in arterial ECs (Cx40^{+}) with increased Notch activity in 2 out of the 3 litters analyzed (Figure 16G).

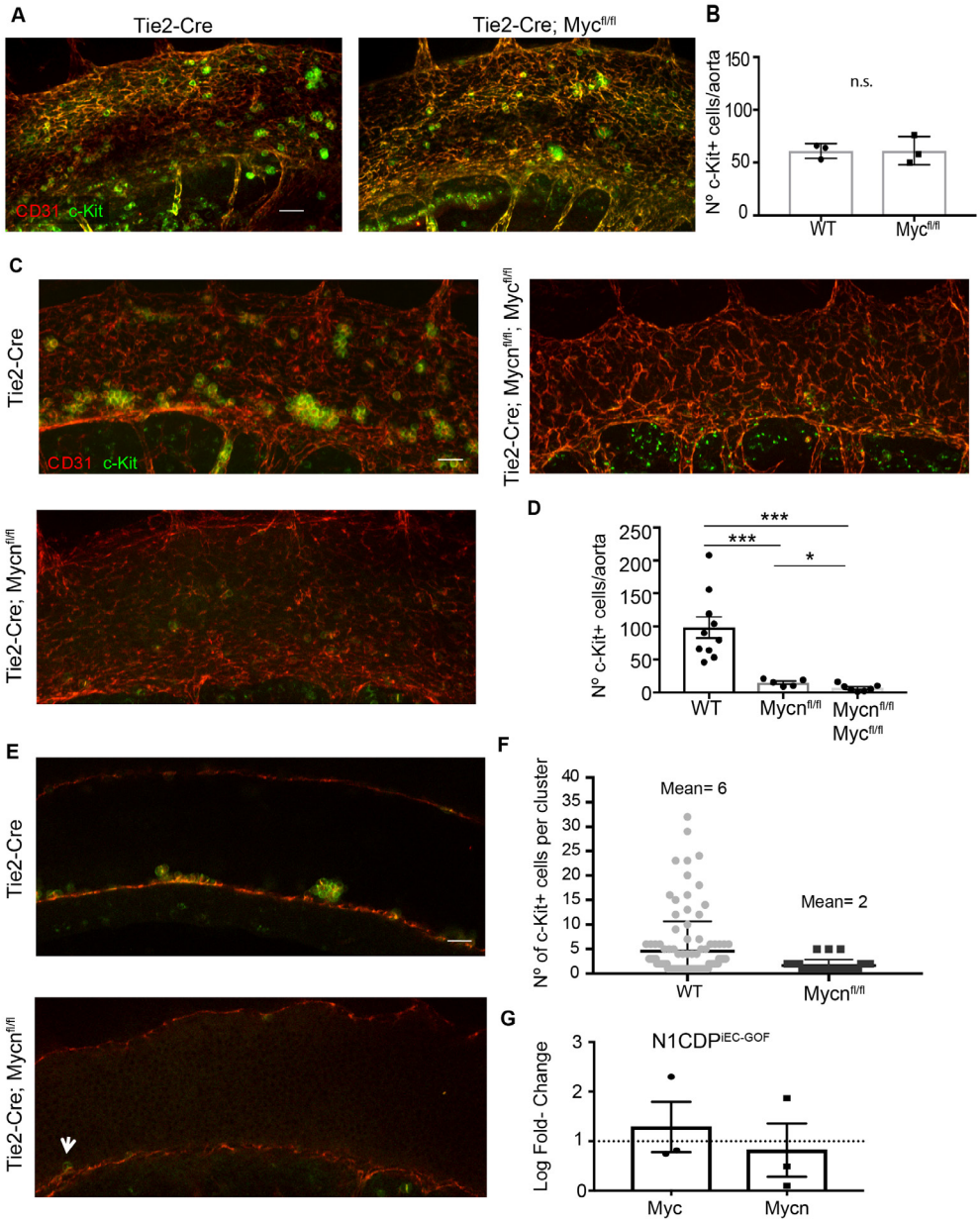

Figure 16 Loss of Mycn but not Myc leads to detrimental loss of the HSPC population in the DA at E10.5. **A**, Representative photo of a confocal z-stack projection (STD DEV) of Tie2-Cre (**left**) and Tie2-Cre; Myc$^{fl/fl}$ (**right**) DA at E10.5 immunostained for CD31 (Red) and c-Kit (Green). White scale bar on bottom right corner of the top image indicates 100µm. **B**, Quantification of the number of c-Kit+ cells per aorta in both WT and Myc$^{fl/fl}$ embryos (n=3 embryos). **C**, Representative photo of a confocal z-stack projection (STD DEV) of Tie2-Cre (**top, left**), Tie2-Cre; Mycn$^{fl/fl}$ (**bottom, left**), and Tie2-Cre;Mycn$^{fl/fl}$; Myc$^{fl/fl}$ (**top, right**) DA at E10.5 immunostained for CD31 (Red) and c-Kit (Green). White scale bar on bottom right corner of the top image indicates 100µm. **D**, Quantification of the number of c-Kit+ cells per aorta in WT (n= 10 embryos), Mycn$^{fl/fl}$ (n= 5 embryos), and Myc$^{fl/fl}$;Mycn$^{fl/fl}$ (n= 7 embryos) embryos. **E**, Representative slice image of Tie2-Cre (**top**) and Tie2-Cre; Mycn$^{fl/fl}$ (**bottom**) immunostained with CD31 (Red) and c-Kit (Green). White scale bar indicates 100µm. White arrow in bottom image points a weakly stained c-Kit+ cell attached to the dorsal floor. **F**, Quantification of the number of c-Kit+ cells per cluster in WT (n= 6 embryos; 116 clusters) and Mycn$^{fl/fl}$ (n= 4 embryos; 32 clusters). **G**, RT-qPCR analysis of log fold-change of Myc and Mycn expression in GFP+ ECs compared to GFP- ECs (dotted line) from *N1CDP$^{iEC-GOF}$* (n= 3 litters); Error bars indicate SEM. * p value ≤0.05; *** p value ≤0.001; n.s. not significant; two-tailed student t-test.

4.10 Loss of Mycn prevents EHT of DA ECs, particularly the cells with lower Notch signaling

We then wanted to determine if the *Mycn* upregulation seen in DA ECs with lower Notch signaling (GFP^+/DN-$Maml1^+$) is indeed a key event for these cells to undergo EHT. For that, we interbred *Tie2-Cre* with *iChr-Notch-Mosaic* and *Mycn* floxed mice, and in this way we were able to quantify how the different mutant aorta ECs differentiated and expanded in the absence of *Mycn*. As predicted and shown above, the number of c-Kit^+ cells per aorta was decreased in the Tie2-Cre; iChr-Notch-Mosaic; $Mycn^{fl/fl}$ embryos as compared to the control Tie2-Cre; iChr-Notch-Mosaic embryos (Figure 17A).

Then, we compared the c-kit^+ cluster dynamics between the two experimental groups and among the cells with different levels of Notch signaling. iChr-Notch-Mosaic embryos had a mean of 1.87 $Cherry^+$ cells per cluster but iChr-Notch-Mosaic;$Mycn^{fl/fl}$ embryos had a mean 64% fewer (Figure 17B). GFP^+/DN-$Maml1^+$ cells, after Mycn deletion, had an even more significant decrease (75%) in the number of cells per cluster (Figure 17C). On the other hand, unlabeled cells, or cells that were not recombined for the *iChr-Notch-Mosaics* and assumed to also have no recombination of the floxed *Mycn* allele, showed no differences between the two groups (Figure 17D).

These results show once again that Mycn is important for EHT and the development of the dHSC during early embryonic development. Results also indicates that cells with lower Notch signaling within the DA and higher *Mycn* expression (Fig. 14C – qPCR data), are the most sensitive to Mycn deletion.

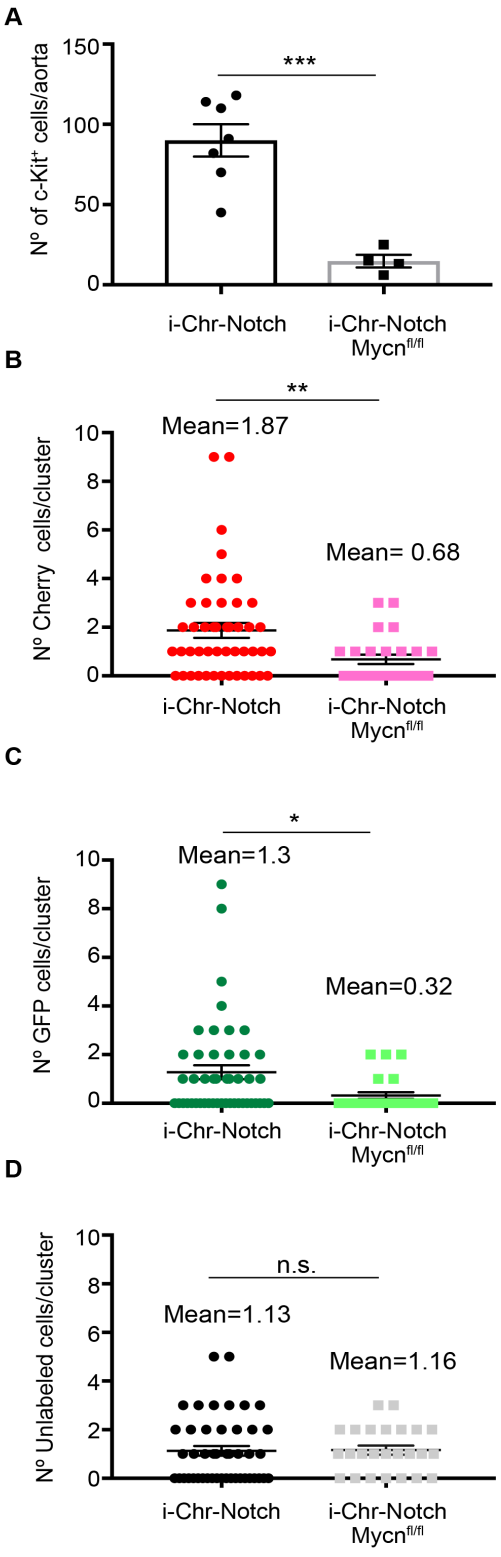
A
Nº of c-Kit+ cells/aorta
150
100
50
0
***
i-Chr-Notch
i-Chr-Notch Mycnfl/fl
B
Nº Cherry cells/cluster
10
8
6
4
2
0
**
Mean=1.87
Mean= 0.68
i-Chr-Notch
i-Chr-Notch Mycnfl/fl
C
Nº GFP cells/cluster
10
8
6
4
2
0
*
Mean=1.3
Mean=0.32
i-Chr-Notch
i-Chr-Notch Mycnfl/fl
D
Nº Unlabeled cells/cluster
10
8
6
4
2
0
n.s.
Mean=1.13
Mean=1.16
i-Chr-Notch
i-Chr-Notch Mycnfl/fl

Figure 17 ECs with loss of Mycn show decreased HSPC contribution in the iChr-Notch-Mosaic line. A, Quantification of the number of c-Kit$^+$ cells per aorta in iChr-Notch Mosaic (n=7 embryos) and iChr-Notch Mosaic; Mycn$^{fl/fl}$ (n= 4 embryos). **B,** Quantification of the number of RFP$^+$ c-Kit$^+$ cells per cluster in iChr-Notch Mosaic (n=2 embryos; 46 clusters) and iChr-Notch Mosaic; Mycn$^{fl/fl}$ (n=3 embryos; 25 clusters). Mean number of RFP$^+$ c-Kit$^+$ cells per group are identified above. **C,** Quantification of the number of GFP$^+$ c-Kit$^+$ cells per cluster in iChr-Notch Mosaic (n=2 embryos; 46 clusters) and iChr-Notch Mosaic; Mycn$^{fl/fl}$ (n=3 embryos; 25 clusters). Mean number of GFP$^+$ c-Kit$^+$ cells per group are identified above. **D,** Quantification of the number of unlabeled c-Kit$^+$ cells per cluster in iChr-Notch Mosaic (n=2 embryos; 46 clusters) and iChr-Notch Mosaic; Mycn$^{fl/fl}$ (n=3 embryos; 25 clusters). Mean numbers of unlabeled$^+$ c-Kit$^+$ cells per group are identified above. Error bars indicate SEM. * p value ≤0.05; ** p value ≤ 0.01; *** p value ≤0.001; n.s. = no statistical significance two-tailed student t-test.

4.11 HSPCs with early loss of Myc or Mycn do not contribute to the adult HSC system

The strong EHT defect identified in *Mycn*^{iDEC} E10.5 embryos led us to hypothesize that *Mycn* deletion was not compatible with the development of the hematopoietic system. However, published data on *Mycn* knockouts have only suggested early embryonic lethality by E11.5 due to diverse organ tissue defects including: deficiency in neuron maturation, defect in heart remodeling, underdeveloped lungs, enlarged encephalic walls, and issues in the organization of the mesonephros in the genitourinary system (Charron et al., 1992; Moens et al., 1992; Moens et al., 1993; Sawai et al., 1991; Sawai et al., 1993; Stanton et al., 1992). Perhaps, the role of Mycn in the DA has eluded notice before. Indeed, we also found that *Mycn*^{iDEC} adult mice were viable and fertile. Given that *Tie2-Cre* seems to recombine floxed genes only in a fraction of arterial ECs (Fig. 7E), we hypothesized that the survival of *Mycn*^{iDEC} mice could be due to the incomplete expression of Tie2-Cre and Mycn deletion in aortic ECs during EHT as some HSPCs did form and expand in *Mycn*^{iDEC} aortas (Figure 16D and 17A).

A new Dual Cre-Reporter line generated by the group, *iSuRe-Cre* (Fernandez-Chacon et al., 2019) (Figure 18A), allows us to follow cells that have 100% deletion of any floxed gene. We decided to use this line to track if cells with early loss of Mycn contribute to the adult hematopoietic system. Surprisingly, Tomato$^+$ hematopoietic cells having Mycn deletion were present at a high rate (almost 98% of total CD45$^+$ population) in *Mycn*^{iDEC} adult mice. This rate was similar to their control littermates (Figure 18B). Upon further analysis of the blood cells types, we determined that adults with full loss of Mycn in their HSCs seemed to have a lower percentage of Lymphocytes in the total CD45$^+$ population (almost half) and inversely, an increase in the percentage of myeloid cells present in the total blood (Figure 18D- F).

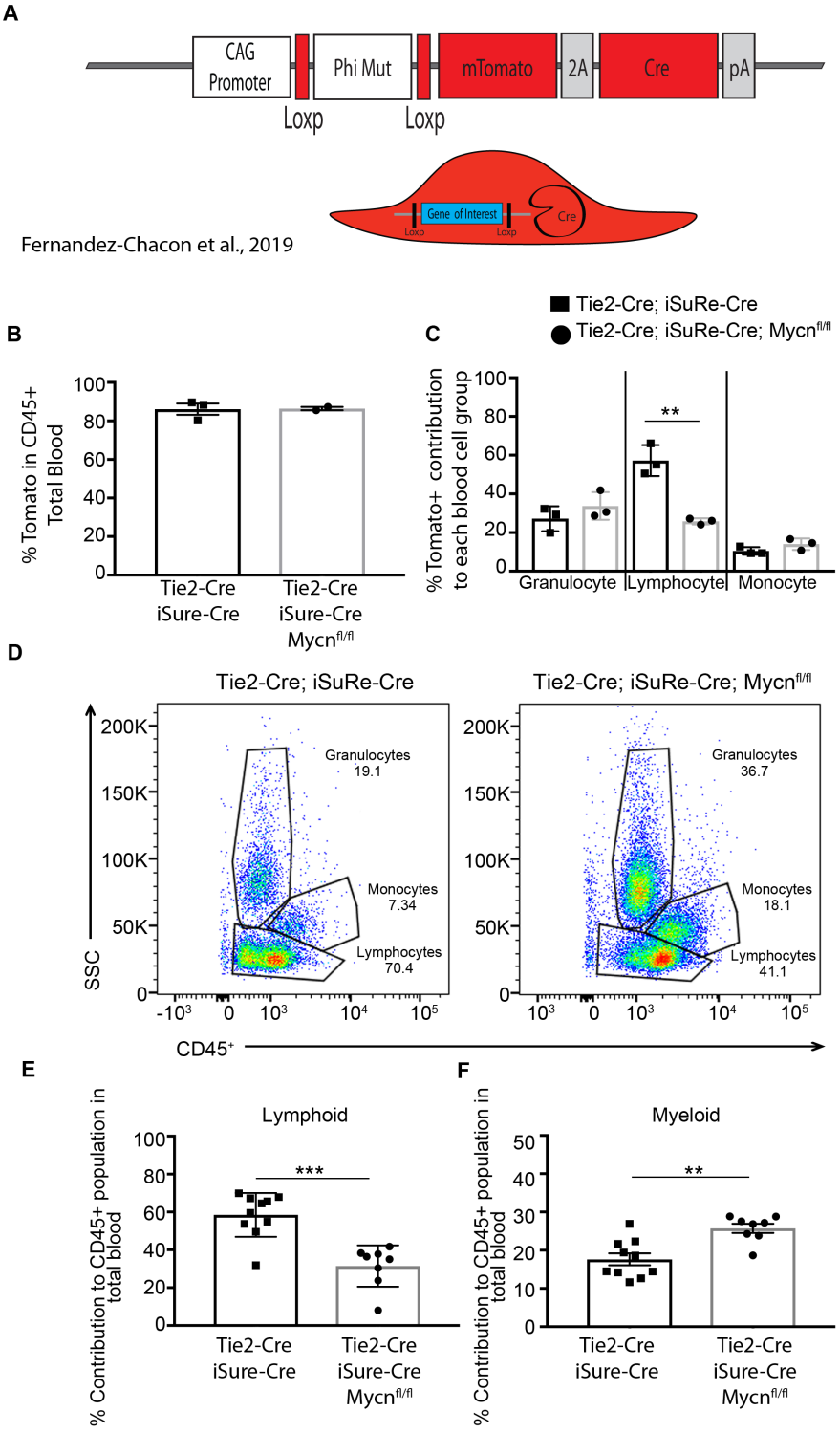

Figure 18 Blood analysis using *iSure-Cre* shows slight myeloid bias in adult HSC system. **A,** Graphical scheme of the *iSuRe-Cre* line. **B,** Quantification of the percent RFP present in the CD45⁺ population of the total blood in Tie2-Cre; iSuRe-Cre (Black squares; n=3) versus Tie2-Cre; iSuRe-Cre; Mycn$^{fl/fl}$ (black circles; n=3) adults. **C,** Quantification of the percent RFP distribution to the three blood cell groups (Granulocytes, Lymphocytes, and Monocytes) of the two groups. **D,** Representative dot plot of cytometry analysis of Tie2-Cre; iSuRe-Cre (left) and Tie2-Cre; iSuRe-Cre; Mycn$^{fl/fl}$ (right). The cells were plotted in side-scatter (SSC) versus CD45⁺ to determine the three main blood cell groups (Granulocytes, Lymphocytes, and Monocytes) and their respective percent to the total CD45⁺ blood population. **E,** Quantification of the percent contribution to the lymphoid population of the total blood in Tie2-Cre; iSuRe-Cre (Black squares; n=10 adults) and Tie2-Cre; iSuRe-Cre; Mycn$^{fl/fl}$ (black circles; n=8 adults). **F,** Quantification of the percent

contribution to the myeloid population (Monocytes + Granulocytes) of the total blood in Tie2-Cre; iSuRe-Cre (Black squares; n=10 adults) and Tie2-Cre; iSuRe-Cre; $Mycn^{fl/fl}$ (black circles; n=8 adults). Error bars indicate SEM. ** p value ≤ 0.01; *** p value ≤0.001 two-tailed student t-test.

Since this adult mice data was apparently not compatible with our earlier embryo studies, we used a public server (gexc.riken.jp) to check the expression of Tek (Tie2) in normal mouse HSCs. We saw that this gene is expressed not only in EC, but it is also highly expressed in adult LT-HSCs and other hematopoietic cells. Therefore, the high percentage of $Tomato^{+}$ cells in the $CD45^{+}$ blood population of $Mycn^{iDEC}$ adult mice could reflect the recombination of the *iSuRe-Cre* reporter, and subsequent loss of *Mycn,* in late embryonic stages or adult HSCs and not in early HE cells. Yet, the data from this experiment suggests that loss of Mycn in adult HSCs may be essential for HSC differentiation or expansion, though more work needs to be done on the subject.

Since the previous model was not conclusive about the contribution of HSPCs with loss of Mycn, we decided to perform inducible genetic mosaics with new mouse lines that would be more restricted to the EHT lineage, and would allow us to clearly induce a mosaic of control/wildtype and mutant cells with full loss of the *Myc* genes. To achieve this, we used a novel *iFlp-Mosaic* allele (Garcia-Gonzalez et al., unpublished) generated in the lab whereby instead of Cre recombinase, Flippase is used to induce recombination of a set of mutually exclusive Flp sites that produce either one of two possible independent recombination events (Fig. 19A). One event leads to the expression of YFP in a cell that acts as a control cell and the other event will induce expression of Tomato-2A-Cre. Similar to the *iSure-Cre* model, Tomato-2A-Cre^{+} cells have recombination or deletion of any floxed allele (Fig. 19A). To induce this allele, the group generated *Apln-FlpO* mice, in which the Flippase (FlpO) is expressed by ECs in the DA at E10.5 (Fig. 19B), and not in the following hematopoietic progenitors or blood lineages (Apln expression from gexc.riken.jp). In control mice having the *Apln-FlpO* and *iFlp-Mosaic* alleles, the Tomato-2A-Cre^{+} cells contributed to about 80% of the total recombined cells while YFP^{+} cells only contributed to about 20% (Figure 19D). This Tomato:YFP ratio was very consistent from animal to animal (n=4 adults). When examining the Tomato:YFP ratio in $Myc^{fl/fl}$, $Mycn^{fl/fl}$, and $Myc/Mycn^{fl/fl}$, we saw a very significant detrimental loss of the Tomato-2A-Cre^{+} population; almost 90-95% of the total recombined $CD45^{+}$ cells were YFP^{+} (Figure 19D).

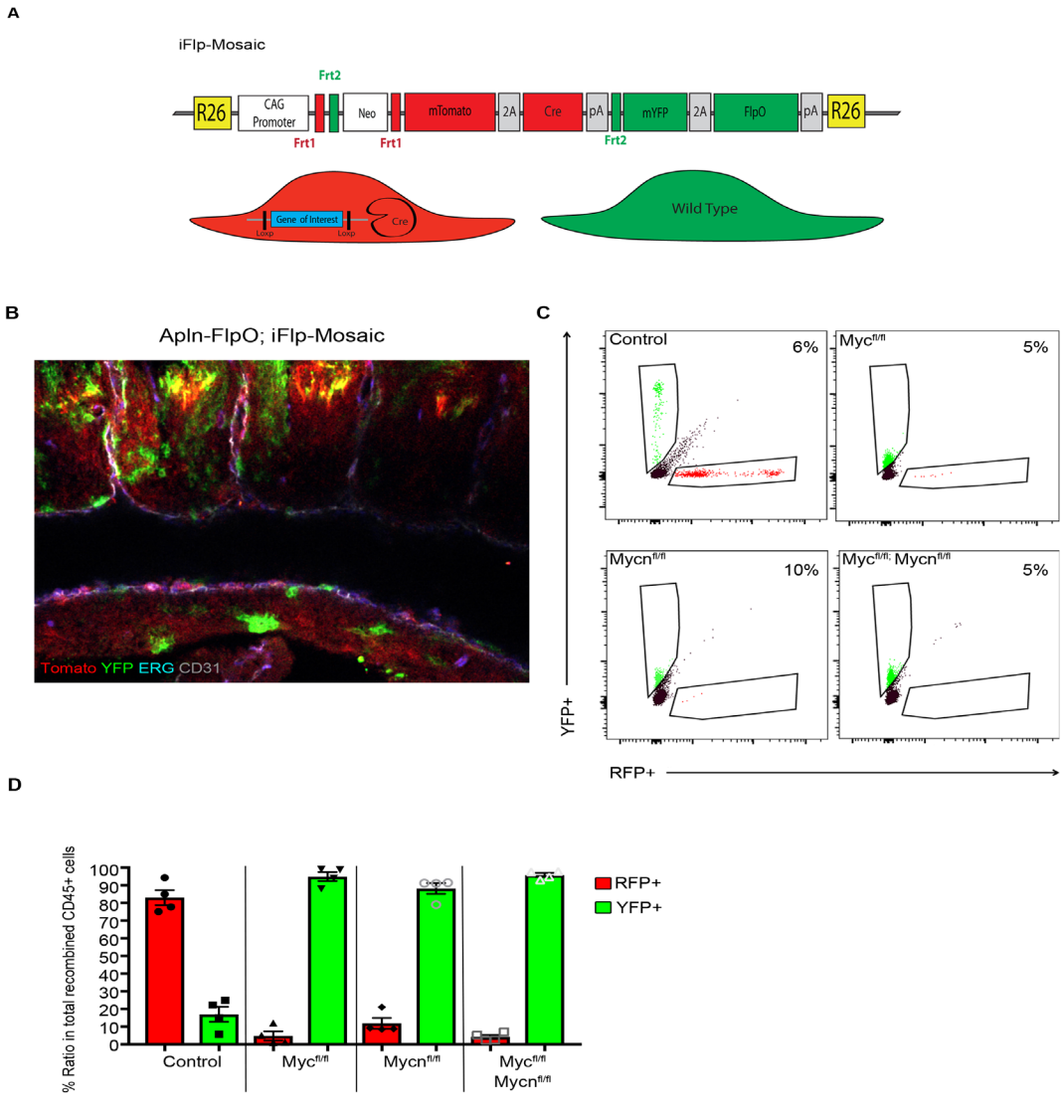

Figure 19 Blood analysis of iFlp-Mosaic adults with early Myc or Mycn loss of function show no contribution to adult HSC system. A, Graphical scheme of the *iFlp-Mosaic* line illustrating the one of two mutually exclusive recombination events. Tomato cells have a constitutively active Cre that will recombine any floxed allele while YFP cells are considered WT labeled cells. **B,** Representative image of Apln-FlpO; iFlp-Mosaics E10.5 DA with YFP and Tomato labeled ECs (ERG^+). **C,** Representative dot plot of cytometry analysis of Apln-FlpO; iFlp-Mosaic (Control; Top left), Apln-FlpO; iFlp-Mosaic; $Myc^{fl/fl}$ ($Myc^{fl/fl}$; Top right), Apln-FlpO; iFlp-Mosaic; $Mycn^{fl/fl}$ ($Myc^{fl/fl}$; bottom left), Apln-FlpO; iFlp-Mosaic; $Myc^{fl/fl}$; $Mycn^{fl/fl}$ ($Myc^{fl/fl}$; $Mycn^{fl/fl}$; Bottom right). All plots are plotted YFP^+ versus RFP^+ and all YFP^+ cells are pseudocolored in Green while RFP^+ are pseudocolored in Red. **D,** Quantification of the percent ratio of RFP versus YFP in the total recombined $CD45^+$ cells of the total blood for (n= 4 adults) each group.

Altogether, these results indicate that the early loss of Mycn, but not Myc, is disadvantageous for EHT and the development of early HSPCs. The loss of Myc does not directly impact EHT but mainly the subsequent hematopoietic stem cell differentiation or expansion. Therefore, the need for Mycn may only be transient during EHT. We found that besides the EHT defects, sustained loss of Mycn in adult LT-HSCs leads to irregularities in the adult hematopoetic system.

4.12 Single Cell Transcriptomic analysis of ECs, EHT, and HSCs

A recent publication on single-cell RNA-sequencing of various mouse embryo aortic cell types has indicated that it is possible to determine molecular events controlling EHT by analyzing the TF networks activated in each cell type (Baron et al., 2018). Using the published datasets available in the Gene Expression Omnibus repository (series record GSE112642), we reanalyzed the raw data to validate our data and further investigate Notch signaling in the various cell type present during definitive hematopoiesis.

We were able to produce a similar clustering identification with the exception that we had a total of 9 cell clusters (C0-C8) in the final tSNE (Figure 20A). Cluster C1 is mostly all classified HE cell types and C0 is a mixture of Endothelial (Non-HE) ($Cdh5^+$, Gfi^-, $c\text{-}kit^-$) cells and HE cells. Cluster C2 are a mixture of cells that are classified as HE ($Cdh5^+$, Gfi^+, $ckit^-$) and EHT. Cluster C3 and C4 are composed of EHT cells ($Cdh5^+$, $Gfi1^+$, $c\text{-}kit^+$). On the other side Cluster C5 and C6 are composed of Pre-HSC type II and type I ($c\text{-}kit^+$, $Cdh5^+$, $CD45^+$ and $c\text{-}kit^+$, $Cdh5^+$, $CD45^-$; respectively) and Cluster C7 and C8 are classified as Yolk Sac cells ($c\text{-}kit^+$) (Figure 20B).

Figure 20C is a two-dimension representation of the PCA to try and find a structure between the different clusters. The separation of the cluster represents how different the clusters are in variable parameters including differences/patterns in gene expression and differentiation potential, or the inverse, lineage commitment potential. Two known endothelial (Cdh5) and HSC (Rac2) genes where analyzed to determine in which cluster is this gene highly expressed. As expected, *Cdh5* is highly expressed in clusters C0 and C1, or the clusters that contain both endothelial and HE cells (Figure 20D). On the other hand, *Rac2* is highly expressed in clusters C6-C8, or those cells which are considered of hematopoietic lineage (Figure 20E).

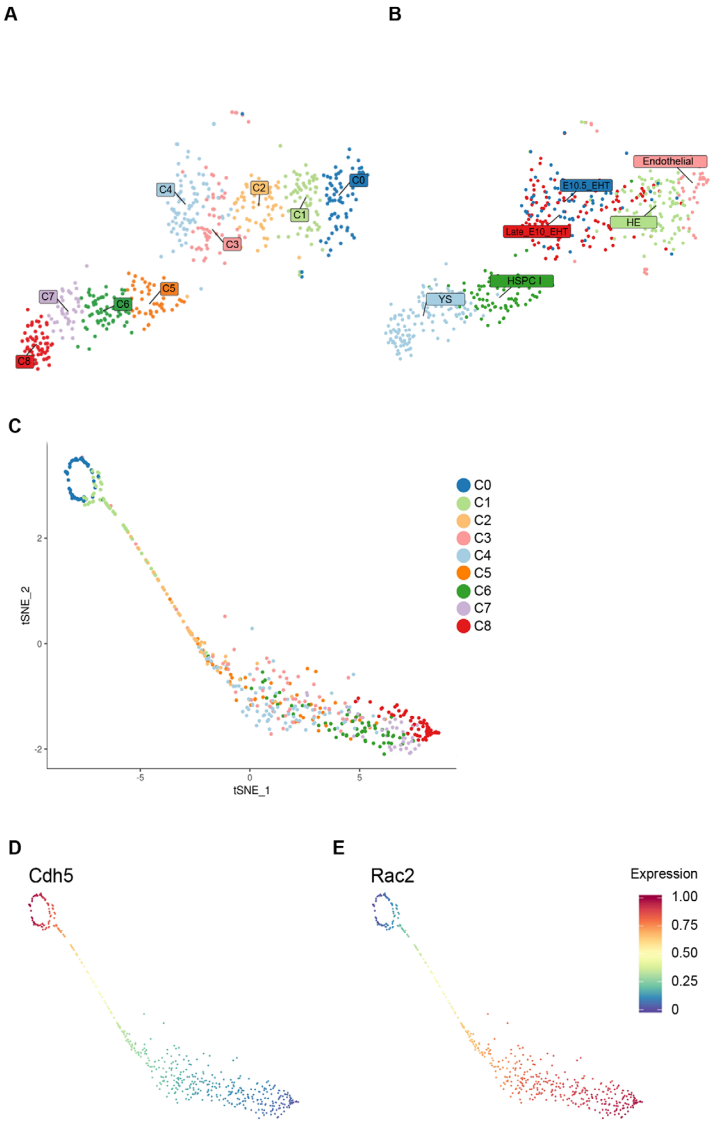

Figure 20 Single cell Transcriptomic analysis of Endothelial and Hematopoietic cells of E10 and E11 embryos. A, Representative image of the clusters and their name generated by the analysis (C0-C8). **B,** Representative image of the different cells types present within clusters (A). **C,** Chart of two- dimension analysis of the differentiation potential (tSNE_1) and population differences (tSNE_2) of each cell of the 9 clusters. **D,** Expression intensity of Cdh5 in the different clusters plotted in the two-dimension. **E,** Expression intensity of Rac2 in the different clusters plotted in the two-dimension. Expression intensity meaning is noted on the legend on the right.

We then analyzed the top 20 genes expressed in cells within cluster C4. Amongst the top 5 genes that appeared, *Mycn* is the second most expressed gene (Figure 21A). Figure 21B shows plots of the three most expressed genes in C4 in relation to all the cells in the analysis. Both *Ifitm1* and *Mycn* are only highly expressed in C2, C3 and C4- clusters that have a great proportion of cells identified as EHT. A gene expression comparison was also analyzed to identify the top 20 genes differentially expressed in C4 (EHT) versus C0 (arterial EC)(Figure 21C). Once again, within the top 5 genes highly differentially expressed we find *Mycn.* *Gpr56*, a known gene necessary for definitive hematopoietic development in the AGM, (Rao et al., 2015; Solaimani Kartalaei et al., 2015) is also highly expressed in

EHT cells as compared to ECs.

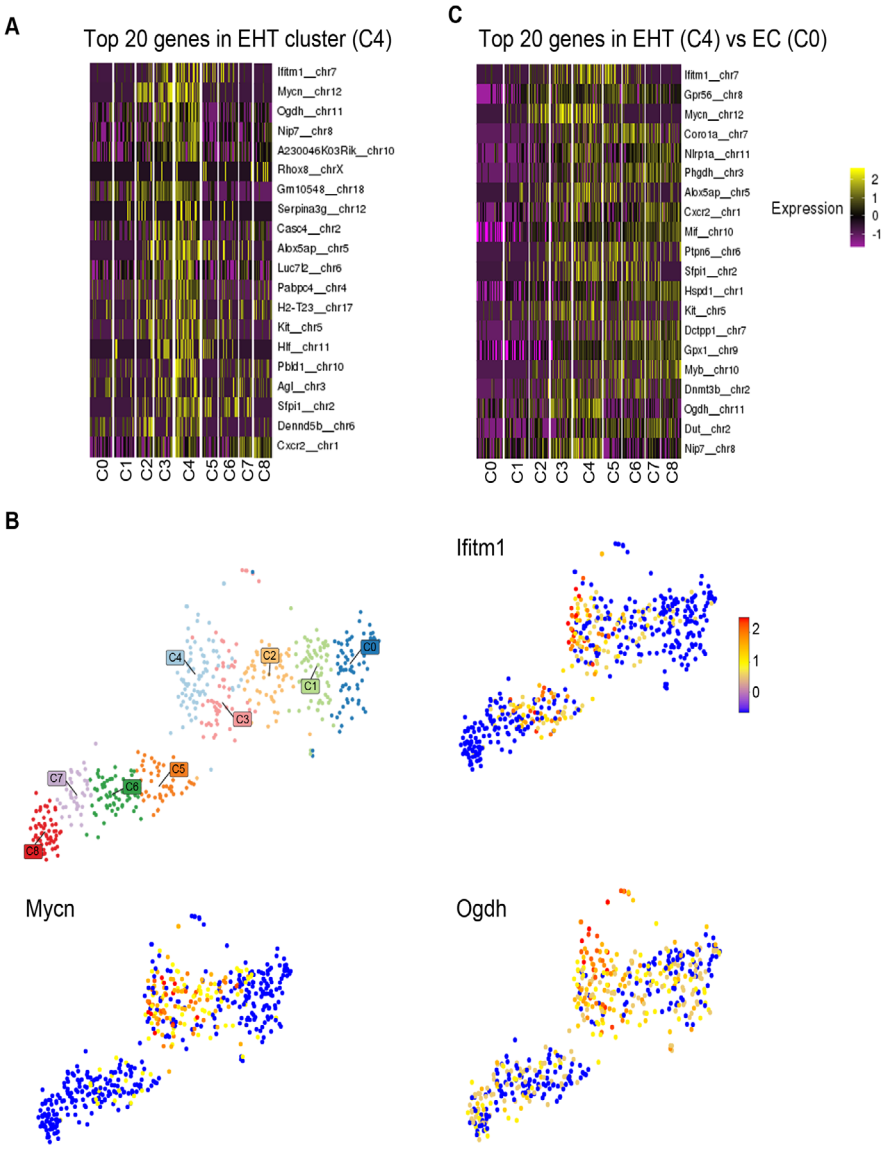

Figure 21 Mycn is one of the most highly expressed gene in the EHT (C4) cluster. A, List of the top 20 genes in the EHT (C4) cluster compared to all the other clusters (C0-C3, C5-C8). Intensity of the expression of each gene within the clusters is highlighted on the left. **B,** Representative image of the different cells types present within clusters (Top left) and the intensity of the expression of each gene (Ifitm1, Mycn, and Ogdh) in each cell. Expression intensity meaning is noted on the legend on the top right. **C,** List of the top 20 genes expressed in cluster C4 (EHT) versus cluster C0 (Endothelial cells). Intensity of the expression of each gene within the clusters is highlighted on the left. Expression intensity meaning is noted on the legend on the right.

The gene expression trends on selected genes were computed across trajectories by fitting a generalized additive model. The trajectories were then clustered on a heatmap representation (Figure 22A). Many of the genes that were analyzed included many that were also referenced in the original article (*Ptprc, Sfpi1, Runx1, Mpo, Myb, Gpr5, Dnmt3b, Rac2, Lyl1, Zfpm1, Mt1, Ikzf2, Gfi1, Gata2, Vwf, Elk3, Mecom, Cdh5, Jun,* and *Dnmt3a*). Since most of the genes are associated with either endothelial or hematopoietic cells, the

list of genes from the original paper helped guide the confidence associated with the results. All of the genes that were used reproduced the same trend on the heatmap. Additionally, the genes associated with endothelial identity were more highly expressed in the EC population (as seen in light blue and dark blue in the pseudotime chart underneath the heatmap of Figure 22A) and have intense red expression on the left hand side of the heatmap. Genes associated with hematopoietic identity (colored pink and red in the pseudotime mosaic) were highly expressed on the right hand side of the heatmap.

We structured the data to show a simplistic line trend of gene expression whereby as one follows the line from left to right, the cells identity goes from endothelial to hematopoitetic. Figure 22B shows the gene expression trend through pseudotime of genes associated with the arterial endothelium. For example, Cdh5, an endothelial gene, is highly expressed in ECs and decreases in expression as a cell adopts a more hematopoietic identity. The same trend is seen in *Gata2, Gja5*, and *Sox17*. Inversely, there are genes that increase as an EC adopts an HSC identity. This is seen in the 4 genes (*Rac2, Runx1, Myb,* and *Gpr56*) in Figure 22C. We were interested in the trend of genes associated with the Notch signaling pathway (Figure 22D) and found them to decrease through pseudotime. This data fits perfectly with the hypothesis that Notch signaling must decrease in a cell-autonomous manner in order for fate change to occur.

We were also interested in genes that were more dynamic, meaning, genes that are more highly expressed in the EHT phases (a population represented as shades of green in pseudotime). Here, we focused on the expression of *Mycn* since the LOF data suggested a transient need for Mycn during the definitive hematopoiesis process. As expected, *Mycn* peaked in the period associated with EHT (Figure 22A, E). To validate that *Myc* did not follow the same pattern as *Mycn* we analyzed its expression through pseudotime and determined that *Myc* followed the pattern that most resembles those seen in the HSC specific gene trend of Figure 22C. Therefore, *Myc* expression occurs after EHT while *Mycn* is only expressed during EHT.

Manic Fringe, an enzyme that can modify Notch receptor signaling by influencing the affinity for its ligands, was previously hypothesized to have a role during the process of dHSC (Gama-Norton et al., 2016). We therefore analyzed its expression and found it to be highly expressed in the HE and EHT cell population (Figure 22A, E). The trend was very similar to *Mycn,* although its expression peaks before that of *Mycn* and also subsequently decreases in expression in the hematopoietic cells. We also checked the expression of the other two fringe proteins, Lunatic Fringe (Lfng) and Radical Fringe (Rfng), and saw that their expression was low in all cell clusters compared to that of Mfng (not shown). Therefore, we conclude that Mfng is likely the only Fringe playing a role in the HE during definitive hematopoiesis.

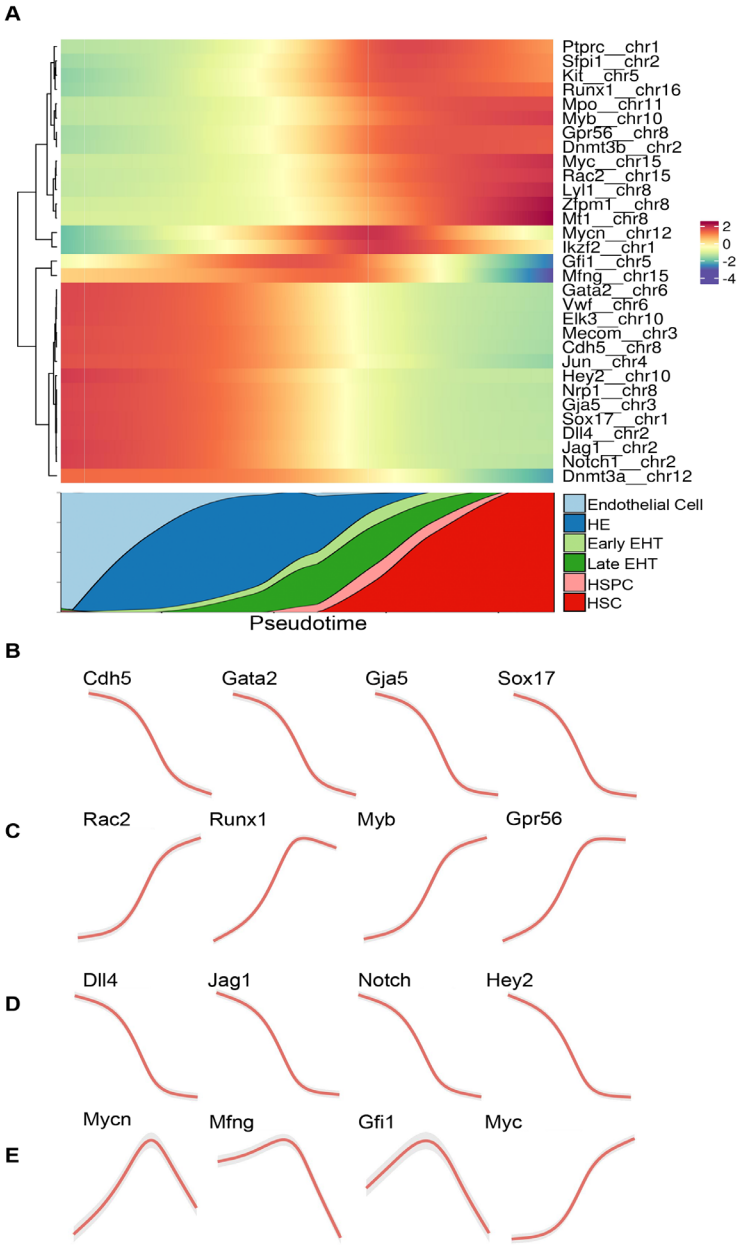

Figure 22 Dynamic expression of Manic Fringe and Mycn through pseudotime as cell progress from Endothelial to Hematopoietic. A, Representative heatmap analysis of several genes and their respective changes over pseudotime. Expression intensity meaning for the heatmap is indicated on the legend in the top right. Below the heatmap is a representative image of the various cell types (legend on the bottom right) to indicate which population the various intensities correspond to over pseudotime. **B,** Simple line representation of the trend of various arterial endothelial genes (*Cdh5, Gata2, Gja5, Sox17*) across pseudotime. **C,** Simple line representation of the trend of various hematopoietic associated genes (*Rac2, Runx1, Myb, Gpr56*) across pseudotime. **D,** Simple line representation of the trend of various Notch associated genes (*Dll4, Jag1, Notch1, Hey2*) across pseudotime. **E,** Simple line representation of the trend of various genes that change dynamically (*Mycn, Mfng, Gfi1*, and *Myc*) over pseudotime.

We also wanted to investigate if there were any differences in the expression levels of *Dll4* and *Jag1* in the dorsal endothelium. We found that although the expression of both ligands decrease overtime when following the same pseudotime trend established in previous

analysis, *Jag1* is more highly expressed in the endothelium as compared to *Dll4* (Figure 23A). These results correlate very well with our *Mfng*$^{EC\text{-}iGOF}$ data.

The laboratory is also very interested in the role of Notch in proliferation. Therefore, we decided to use the single cell RNA transcriptomics to analyze the proliferative dynamics and status of these DA cells. Cyclin-dependent kinase (Cdk) and their inhibitors (Cdkn1) are the core proteins regulating the transition of cells throughout the cell cycle, and therefore we analyzed the gene expression per cluster of *cdk1, cdk2* and *cdk3* to get insight into the proliferative dynamics of the cells. Cdk3, a protein mainly expressed in the G0-phase of the cell cycle, was not detected at the RNA level. This suggests that the cells are not in a quiescent state. *Cdk1* showed increased expression when going from the EC to HSC cell type while the *Cdk2* expression had higher expression in the HE/EHT intermediates (Figure 23B). We also checked expression levels of three different cdk inhibitors: *Cdkn1a (p21), Cdkn1b (p27)*, and *Cdkn1c (p57*). Only Cdkn1c was highly expressed in all cell types except for HSCs. Interestingly, the strongest expression was seen in the HE/EHT intermediate cell types. P57 is a tight-binding inhibitor of the G1-cyclin-CDK complexes during proliferation, thereby arresting the cells in the G1 phase (Matsuoka et al., 1995). Odc1, a regulator of proliferation through the regulation of polyamines, shows an increase in expression as cells undergo transition towards HSC fate. This suggests that ECs progressively adopt a more proliferative identity as cells undergo transition. This was further explored by analyzing two different proliferative gene data sources.

A published gene list of G1/S specific gene expression profile (Tirosh et al., 2016) was cross-checked with our transcriptomics gene list to determine if cells in C4 (or EHT cells) were more enriched with pro-proliferative genes as compared to C0 (ECs). This gene list includes*: pcna, mcm5, tyms, fen1, mcm2, mcm4, rrm1, ung, gins2, mcm6, cdca7, dtl, prim1, uhrf1, mlf1ip, hells, rfc2, nasp, rad51ap1, gmnn, wdr76, slbp, ubr7, pold3, msh2, atad2, rad51, rrm2, cdc45, cdc6, exo1, tipin, dscc1, blm, casp8ap2, usp1, clspn, pola1, chaf1b, brip1,* and *e2f8.* When comparing the two clusters, C4 has statistically higher reads in the G1/S phase genes as compared to the C0 cluster (Figure 23C). Using data from the lab, we analyzed a GSEA study of an RNA seq from E14.5 fetal hearts with loss of Dll4 in the endothelium with enrichment in E2F Target genes. These genes included: *pold1, kif18b, msh2, spag5, myc, cdc25b, mybl2, kif2c, mcm2, nup107, plk1, espl1, dnmt1, pold3, trip13, racgap1, aurka, tacc3, ncapd2, mcm4, melk, mlh1, brca1, bub1b, dlgap5, kpna2, mcm3, nup205, mcm5, dck, atad2, rrm2,* and *mthfd2*. When checking this list of pro-proliferative genes that are increased upon loss of Notch signaling in ECs in our cell types, again cluster C4 had higher reads as compared to C0 (Figure 23D). Altogether, this data suggests that in the EC to EHT-HSC transition, there is a general entry or boost of cell-cycle that then places the cells in a proliferative state. The proliferative state is refined and tightly controlled by the

presence of p57. Therefore, though the cells are in a more proliferative state, they do not begin to complete the cell-cycle or undergo mitosis until they become HSPC-HSC.

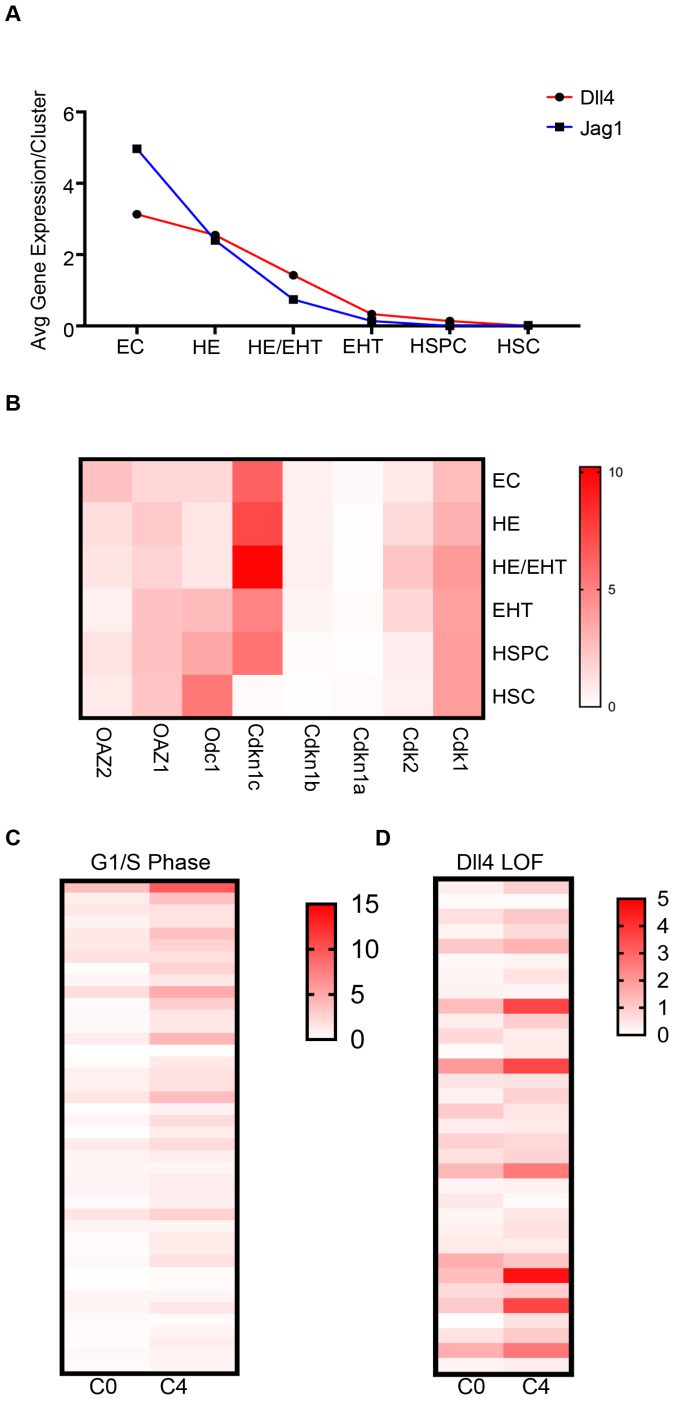

Figure 23 EHT cluster shows increased proliferative markers as compared to arterial ECs. **A,** Line plot chart of Notch ligands genes: Dll4 (Red line) and Jag1 (Blue line). The chart indicates the average gene expression of each gene versus cell type. **B,** Heatmap representation of the average gene expression per cluster of various proliferative genes. **C,** Heatmap analysis comparing the average gene expression of G1/S Phase specific genes in C1and C0. **D,** Heatmap analysis comparing the average gene expression of genes enriched in the Dll4 LOF fetal heart analysis in C1versus C0. EC= Endothelial Cells; HE= Hemogenic Endothelium; EHT= Endothelial-to-Hematopoietic transition; HSPC= Hematopoietic Stem Progenitor Cells; HSC= Hematopoietic Stem Cell. Legends to the right of the heatmaps indicate the representative gene expression based on the intensity of the RFP color.

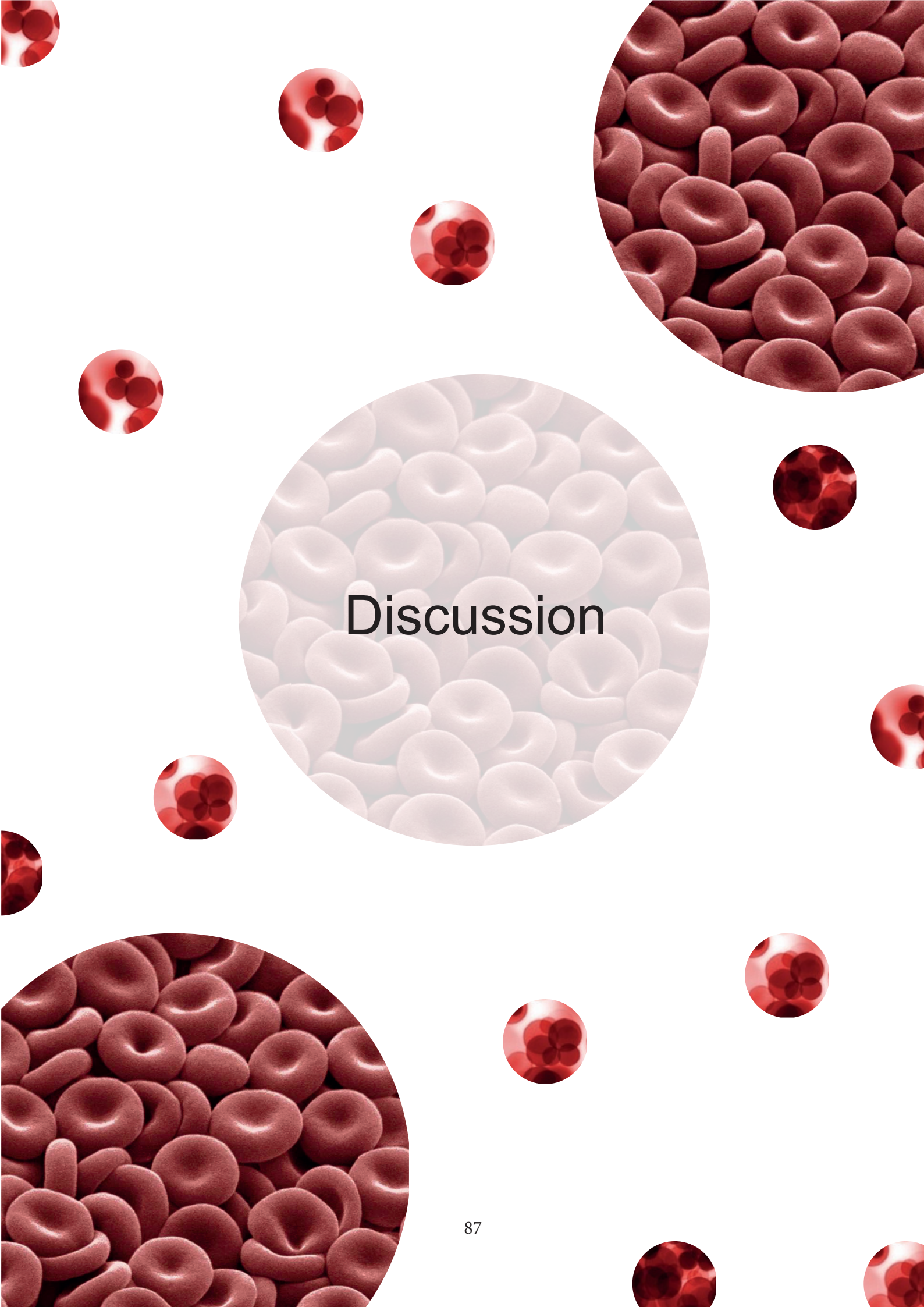

Discussion

DISCUSSION

Increased Notch activation in DA ECs reduces the generation of HSPCs

It has been shown that the induction of Notch activity in all cells of a zebrafish embryo following a heat shock inducible strategy increases the expression of the hemogenic gene *runx1* and the hematopoietic gene *cmyb* (Burns et al., 2005). Additionally, it has been shown that ectopic Notch overexpression can convert a venous structure into an arterial vessel and a potential hematopoietic niche (Burns et al., 2005; Lawson et al., 2001). *In vitro* work with human pluripotent stem cells has shown that Notch activation potentiates EHT initiation (Uenishi et al., 2018). Therefore, Notch activation was thought to induce HSPC development. However, in mice, the overexpression of NICD lacking its native PEST domain results in embryonic lethality by E9.5 with embryos presenting angiogenic remodeling, cardiac development, and hematopoietic lineage defects (Venkatesh et al., 2008). In this work, we have used a new mouse model that overexpresses NICD, with its native PEST domain (NICD-PEST), specifically in Tie2-Cre^{+} ECs, resulting in an increase in Notch signaling that more closely relates to the physiological Notch signaling levels. This can be confirmed by the lethality of mutant embryos at later stages (E15.5) and not E9.5. A similar experimental approach was never executed before in zebrafish or in mice, and that may explain the disparity of results obtained. Even though the arterial fate, and perhaps the subsequent HE niche, has been shown to be induced by ectopic activation of Notch signaling in zebrafish capillaries or veins, our data clearly shows that sustained activation of Notch in the endothelium of the mouse aorta blocks HSC development by blocking early EHT stages within the DA (further described below).

In agreement with our results, another publication has observed decreased number of HSC in FL of E12.5 mouse embryos upon strong but patchy overactivation of Notch in ECs (Tang et al., 2013). In addition, it was shown by *ex situ* cellular FACS profiling and clonal expansion assays that cells taken from embryos with a strong increase in Notch signaling in Tie2-Cre^{+} ECs have fewer hematopoietic-forming colonies (putative HSPCs). However, the overexpression of N1ICD (without the native PEST domain) model used in these studies is often toxic and blocks the proliferation and differentiation of most cells (unpublished results from our lab) and causes severe cardiovascular defects. In contrast to these studies, our *N1CDP$^{iEC\text{-}GOF}$* embryos have a relatively normal cardiovascular development which enabled us to perform 3D imaging of the E10.5 DA and conclude that increased Notch activity in the DA endothelium leads to a severe loss of progenitors right at the peak time of HSPC generation.

Notch activation in DA impairs the generation of the hemogenic endothelium and results in less EHT events

It has been shown that Notch signaling functions genetically upstream of Runx1 in the HE during EHT. In zebrafish, *runx1* is highly expressed in ECs with high Notch activation (Burns et al., 2005; Kobayashi et al., 2014) and Gata2, the direct induced transcriptional target of Notch, is required upstream of Runx1 before EHT can occur (Chen et al., 2009; Kissa and Herbomel, 2010; Nottingham et al., 2007). This dynamic relation led to the suggestion of a simple Notch->Gata2->Runx1 EHT pathway.

However, the GFP reporters used for mapping Notch activation in zebrafish are too stable to reflect the actual levels of Notch activation during EHT. Furthermore, arterial ECs are known to have very high levels of Notch signaling before EHT even occurs. This is seen in zebrafish and mouse embryos, whereby specification of the arterial system occurs through the expression of the Notch ligands, receptors and the canonical target genes *hey2 and hey1* and loss of these genes impairs arteriogenesis (Quillien et al., 2014; Rowlinson and Gering, 2010; Weinstein et al., 1995; Zhong et al., 2001) (Fischer et al., 2004; Kokubo et al., 2005). We observed that *N1ICDP*$^{EC\text{-}iGOF}$ mouse embryos have a significant decrease in the number of $CD31^{+}Runx1^{+}$ cells in the floor of the DA and that most ECs with high Notch activity do not co-express Runx1. We therefore propose that even though Notch activity is essential to form arteries, which precedes Runx1 expression and hemogenic conversion, Notch needs to be downregulated in pre-defined arterial ECs for Runx1 to be expressed and for EHT to occur. Interestingly, a recent publication in zebrafish embryos has also challenged previous zebrafish results by suggesting that *dll4* is repressed in the HE in a Runx1-dependent fashion suggesting that Notch signaling decreases in the HE (Bonkhofer et al., 2019). Here, we do not see high coexpression of GFP and runx1 and therefore believe high levels of Notch can also repress runx1 and decrease HE potential. Perhaps high runx1 expression can further re-enforce the decreased Notch levels during EHT.

If Gata2 is downstream of Notch activation and Runx1 is downstream of Gata2, why is Runx1 not upregulated in our *N1ICDP*$^{EC\text{-}iGOF}$ model? It has been shown that Notch/Rbpj activity can simultaneously induce the expression of *Gata2* and the downstream Notch target *Hes1*. Hes1 is part of a negative feedback loop that directly inhibits *Gata2* expression (Guiu et al., 2013). Therefore, high Notch signaling can generate higher than normal *Hes1* expression consequently suppressing *Gata2* and downstream *Runx1* expression leading to a block in HE specification. Interestingly, loss of both *Hes1/ Hes5* result in formation of large hematopoietic clusters – a phenotype attributed to increased *Gata2* expression (Guiu et al., 2013). Essentially, we can propose that high Notch signaling reduces hemogenic potenital through increased *Hes1* expression leading to less HE specification.

Our data suggest that overactivation of Notch strengthens the arterial endothelial program and does not allow the hemogenic program to develop. We believe this is the case because it has been shown that the silencing of the endothelial program is critical for cells to be able to adopt a hematopoietic identity (Swiers et al., 2013). Since our Tie2-Cre dependent genetic manipulations occur first in all ECs, we cannot be certain of what would be the consequence of activating Notch in already pre-specified Runx1^{+} HE cells. Would these cells revert to arterial ECs or continue their hematopoietic expansion? Further experiments would be needed to address these questions, for example use the *Runx1-Mer-Cre-Mer* (Samokhvalov et al., 2007) allele with our *N1ICDP*$^{EC\text{-}iGOF}$ allele to drive the increased Notch signaling specifically in Runx1^{+} HE. Even though most DA ECs with increased Notch activity do not express Runx1, it is interesting that a small percentage of these become Runx1^{+} and are able to bud out from the DA floor. Although the frequency of Notch high (GFP^{+}) budding cells was significantly lower than budding cells that were GFP^{-}, we did not compare the relative fluoresent intensity of EC/GFP^{+} versus HPSC/GFP^{+}. We suspect GFP intensity would be lower in those few budding GFP^{+} cells thereby suggeseting they had lower levels of Notch activation as compared to their EC neighbor.

During normal hematopoietic cluster formation in both mouse and chicken, Notch activity was shown to be specifically downregulated in the clusters but maintained in the aortic endothelium (Del Monte et al., 2007; Richard et al., 2013). Specifically, *Hes1* is shown to progressively decrease in expression in murine HSPCs as they mature in early definitive hematopoiesis (Richard et al., 2013). Recent scRNAseq data has also revealed that the expression of Notch ligands, receptors and canonical downstream targets is significantly lower during EHT (Baron et al., 2018). We also see the need for the downregulation of Notch for EHT but we still do not know how loss of Notch signaling is established in some DA ECs in the AGM.

Manic Fringe inhibits Jagged1/Notch signaling to induce EHT

Deletion of Jagged1 specifically in ECs of Tie2-Cre; Jag1$^{fl/fl}$ embryos resulted in a similar phenotype to what was previously reported in full Jagged1 KO (Jag1$^{-/-}$) mice (Gama-Norton et al., 2015; Robert-Moreno et al., 2008), further confirming the endothelial origin of the EHT defects observed in these mutants. Additionally, *jag1a* is known to be required in zebrafish for HSC formation (Espin-Palazon et al., 2014). However, early publications in mice did not thoroughly quantify how Notch signaling levels are affected upon loss of Jag1 in the endothelium. Here, we checked the levels of Dll4 in the DA and observed a 57% increase in Dll4 staining in embryos with Jag1 LOF. Since *Dll4* expression is known to be induced in

ECs by many pathways, including the Notch pathway (Benedito et al., 2009), we suspect higher Notch siganling in the DA upon loss of Jag1. These results are in accordance with Gama-Norton et al., (2015), who showed that active NICD signals are more frequent in the endothelium of $Jag1^{-/-}$ embryos as compared to $Jag1^{+/+}$, and that treatment of c-kit+ cells with Jagged1 ligands seem to attenuate Dll4/Notch signaling. Conversely, although Robert-Moreno et al., (2008) did not report on the status of Notch signaling in their $Jag1^{-/-}$ mutant embryos, they do report a decrease in *Runx1* expression frequency in the endothelium, similar to what we see in $N1ICDP^{EC\text{-}iGOF}$ embryos. Altogether, ours and the published results suggest that loss of Jagged1 in the DA endothelium leads to an increase in Notch activation. However, it is not yet clear how this occurs mechanistically. How can a Notch ligand (Jagged1) be an inhibitor of Notch signaling during EHT in DA ECs?

Several studies done in flies and mice have shown that the glycosyltransferases Fringes can modify the Notch receptors in such a way that they enhance Delta/Notch signaling and inhibit the Jagged ligands ability to signal (Bruckner et al., 2000; Kageyama et al., 2007; Kim et al., 1995; Marklund et al., 2010; Moloney et al., 2000; Panin et al., 2002; Yang et al., 2005). The exact mechanism is still controversial and under discussion with suggested mechanisms including changing the binding affinity of Delta/Jagged ligands or even changing the ligand-receptor pulling force and downstream signaling ability (Bray, 2016; Sjoqvist and Andersson, 2019). Yet, it is clear that Fringe modification of the Notch extracellular domain alters the ligands binding to the receptor (Hou et al., 2012; Kakuda and Haltiwanger, 2017; Taylor et al., 2014; Xu et al., 2007; Yang et al., 2005). Normally Fringe modification increases binding affinity of the receptor to Delta-family ligands, however, there are occasions where there is enhancement in binding of the Notch receptors to Jagged-family ligands creating a reduced Notch activation (Hicks et al., 2000; Taylor et al., 2014). It is also clear that this function of Fringe depends on the relative expression levels of the ligands, the receptors and fringes themselves.

In the DA endothelium, the main Notch ligands are Dll4 and Jagged1, and the main receptors are Notch1 and Notch4 (Robert-Moreno et al., 2005). Dll4 and Jagged1 have been shown to have opposing signaling abilities and functions in ECs during angiogenesis due to the presence of Fringes (Benedito et al., 2009). Embryos with loss of Manic Fringe (Mfng) do not have any obvious developmental phenotype (Moran et al., 2009a). However, all three fringes do play a role during B and T-cell differentiation by modulating Notch activity, therefore, they play an essential role in HSC development (Song et al., 2016). No data is available on the potential role of the three mammalian Fringes in the AGM although they were shown to be expressed in the vasculature, including in the DA, particularly Mfng and Lfng (Benedito et al., 2009; Gridley, 2010). Since Mfng/Lfng double KO mice are alive and form blood (Moran et al., 2009b), it is possible that the requirement for their functions

during EHT is only transient or that their functions are necessary but not essential for all EHT events that occur throughout the DA. Importantly, Jagged1 mutants do not die of blood defects, but rather because of embryonic and yolk sac vascular defects (Xue et al., 1999). Just as Jagged1 LOF mutants have a decrease but not a complete loss of HSPCs (Robert-Moreno et al., 2008), it is possible that Lfng/Mfng have a significant defect in EHT but the formation of the first HSPCs is compatible with the generation of enough HSPCs for adult hematopoiesis. During the timeframe of this thesis, we did not have access to mice with full loss of Mfng or Mfng/Lfng function. However, we did analyse embryos with an increase in Mfng expression in ECs. *Mfng*$^{iEC\text{-}OE}$ embryos had an increase in the number of c-Kit^{+} cells present in the DA at E10.5 and significantly lower Dll4 immunofluorescence in the tissue. Since Fringes are known to promote Delta-Notch signaling and inhibit Jagged1-Notch signaling, this overall decrease in Notch signaling after Mfng overexpression can only be explained if the gain in Dll4 signaling in the endothelium of the AGM of these mutants is masked by the more pronounced loss of Jagged1 signaling. For this to happen, Jagged1 ligand expression should be higher than Dll4 in the DA AGM. Indeed, analysis of published scRNAseq data (Baron et al., 2018) revealed that aorta ECs express more Jagged1 mRNA than Dll4. Furthermore, previous publications in zebrafish embryos has also shown that *jag1a* transcripts are highly expressed in ECs of the AGM region (although comparative expression of dll4 were not done) (Espin-Palazon et al., 2014). Therefore, we believe Manic Fringe is driving the initial decrease in Notch activity of EHT cells, most probably by modifying EGF repeats on the extracellular domain of the receptor.

It is also very interesting that we found Mfng expression to be dynamic across pseudotime in the single cell transcriptomics analysis published by Baron et al (2018). Mfng expression peaks specifically in the HE and substantially decreases in expression in the HSPC and HSC population. Curiously, Mfng expression pattern over pseudotime is grouped together with that of Gfi1. *Gfi1* expression is present in a subset of Runx1^{+} cells but it is shown to be downstream of Runx1 in the emergence of HSPCs in the DA (Thambyrajah et al., 2016a; Thambyrajah et al., 2016b; Wilson et al., 2010) and is shown to specifically define the HE population that will undergo EHT in the AGM. Recently, *in vitro* data in mouse embryonic stem cells have shown that Runx1 dosage affects HE differentiation (Lie et al., 2018), and therefore, could be the reason behind the heterogeneity of *Gfi1* expression in the Runx1^{+} HE. More single cell analysis must be done to determine how *Gfi1, Runx1,* and *Manic Fringe* are expressed in individual cells of the HE. However, our experimental data and the published scRNAseq data suggests that cells that will undergo EHT (Gfi1^{+}) will upregulate Manic Fringe, the protien which may be the inducer of a decrease in cell-autonomous Notch signaling. The cell-autonomous decrease in Notch signaling subsequently increases *Mycn* expression to correctly progress the cell towards a hematopoietic fate. We believe this cascade of events and signaling dynamic is imperative for EHT to occur.

Genes deregulated after mosaic loss of Notch signaling provide an indication of its biological function in the DA

Although the focus of this thesis is on the role of Notch in the differentiation of the HE, we also wanted to explore other molecular events including cell-cycle and proliferation. We had observed that budding HSPCs in the DA stained for Ki67^{+}, a proliferative marker, more than the underlying arterial endothelium (see Figure 14D). Since Myc is highly associated with cellular proliferation (Bretones et al., 2015; Zaytseva and Quinn, 2017), we wanted to explore the expression of *Myc* in ECs of the DA. Our data shows that DA ECs with Notch LOF have decreased expression of *Myc*. The results should come as no surprise as Notch directly induces the expression of *Myc* in HSCs to promote proliferation and self-renewal (Satoh et al., 2004; Sharma et al., 2006; Weng et al., 2006), and therefore should be downregulated in these cells. Also, previous genome-wide analysis revealed that Notch1/RBPJ binding can be found upstream of the *Myc* gene in human and murine T-lymphoblastic leukemia cells, showing that Notch regulates Myc in HSCs (Wang et al., 2011). Yet, why are HSPCs of the DA highly proflierative when they have low Notch signaling? In an attempt to reconcile how there could be a proliferative signal in EHT/budding cells without Myc we studied the expression of a close family member, Mycn. It is generally assumed that Myc and Mycn play redundant roles, given their similar protein structure, and because *Mycn* expression can compensate for loss of Myc if inserted into its gene promoter (Malynn et al., 2000). In Mycn-to-Myc replaced mice, Mycn can rescue the embryonic lethality associated with loss of Myc, producing mice that appear to be normal and healthy albeit smaller compared to WT mice (Malynn et al., 2000). Therefore, we wanted to explore both *Myc* and *Mycn* expression as we believed they could be involved in the proliferative status of the budding HSPCs.

Loss of Myc and Mycn is embryonically lethal but only Mycn is necessary during early hematopoietic development

The Myc family members, c-myc (Myc), Mycn and Mycl, are basic helix-loop-helix leucine zipper TFs implicated in many biological processes including proliferation, angiogenesis, cell growth, apoptosis, and differentiation (Hurlin, 2013; Zaytseva and Quinn, 2017). Mycl appears to be completely dispensable for all embryogenesis (Blackwell et al., 1993; Blackwood and Eisenman, 1991). However, loss of either Myc or Mycn is embryonically lethal by E10.5 and E12.5, respectively, with lethality mostly attributed to underdeveloped hearts and abnormalities in neural tube development (Charron et al., 1992; Davis et al., 1993; Sawai et al., 1993; Stanton et al., 1992; Trumpp et al., 2001). Other publications have also noted impaired vasculogenesis and angiogenesis (Baudino et al., 2002). Interestingly, Myc compensatory increase does occur in Mycn deficient mice (Stanton et al., 1992) and

vice-versa in Myc deficient mice (Trumpp et al., 2001), yet the increase is not enough to rescue lethality. Mice with endothelial specific loss of Myc did form major vessels, such as the DA, but presented defects in the development of the hematopoietic lineage (Dubois et al., 2008; He et al., 2008). However, both authors show slight variances in how loss of Myc affects the developing hematopoietic system. He and colleagues suggest a loss of HE in the aorta at E10.5 yet the analysis was low in quality and resolution as their data really suggests a loss of HSPCs and CD45^{+} HSCs, rather than loss of the HE; indeed no markers of HE were ever analyzed (He et al., 2008). Dubois et al. analyzed both mature and immature markers of HSC and saw a substantial decrease in CD45^{+} (mature) HSCs and an increase in stem/progenitor cells at E10.5 (Dubois et al., 2008). We attempted to analyze how endothelial loss of Myc affects hematopoietic fate *in vivo* with more resolution and specifically studying the AGM niche. Our data suggests that early loss of Myc does not affect HSPC development in the AGM at E10.5. We believe that earlier results showing loss of HSPCs in the DA was due to low resolution of the clusters themselves and lack of proper c-Kit labeling.

Interestingly, upon loss of Myc in the vasculature *Mycn* expression does not increase, therefore regulation of Myc and Mycn in the vasculature is different to that in overall development (Dubois et al., 2008; He et al., 2008). To my knowledge, there are no publications on the endothelial specific loss of Mycn in the context of the DA. Therefore, during my thesis, we sought to discover if endothelial loss of Mycn would affect the developing HSPC system in the DA at E10.5. We saw that unlike *Myc*^{iDEC}, embryos with loss of Mycn showed a drastic reduction in the number of c-Kit^{+} HSPCs present in the DA at E10.5 (see Figure 16 and 17). Therefore, we conclude that Mycn, not Myc, is essential for EHT and for the development of the dHSC during early embryonic development. We checked ECs with overactivation of Notch from the *N1CDP*$^{iEC\text{-}GOF}$ line and saw mainly decreased levels of *Mycn*. Our results suggests that Notch activation must decrease in the endothelium to allow for the increase in *Mycn* expression and this mechanism allows EHT to occur. To determine if there was any known link between Mycn and Notch we looked into any known publication of Rbpj/Notch1 binding sites near Mycn but could not find any publications. Interestingly, *MYCN* and *MYC* may regulate each other's expression, as seen in the human neuroblastoma (NA) model where increased activity of MYC represses MYCN in stage4-NA tumors and vice versa is seen in MYCN amplified tumors (Westermann et al., 2008), as well as in other studies (Huang and Weiss, 2013). Possible regulatory mechanism of Mycn will be discussed further in the next coming sections, however, I would like to first discuss a glaring inconsistency in the compensatory relationship between Mycn and Myc during development.

Previously, I discussed how replacing the Myc gene locus with Mycn results in the normal development of the adult mice (Malynn et al., 2000). However, it is shown that Myc null

mice have increased *Mycn* RNA levels (2x more) than their control counterpart and yet still suffer embryonic lethality at E10.5 (Trumpp et al., 2001). It is imperative to do a similar experiment as conducted by Malynn et al., (2000), replace the Mycn locus with the Myc gene, and determine if Myc can compensate for loss of Mycn. This experiment could conclusively determine if these proteins can compensate for each other.

Perhaps the reason Mycn increases upon loss of Myc and vice versa is not due to compensation attempts but rather because of their distinct spatiotemporal regulation? In development, Mycn is mostly found in the forebrain, hindbrain, and kidney while Myc is more generally expressed in many organs including the aforementioned ones but more highly expressed in the thymus, spleen, and liver (Huang and Weiss, 2013; Zimmerman et al., 1986). Additionally, Myc expression pattern suggests that it is important for cellular proliferation while Mycn and Mycl expression is more relevant for differentiation (Huang and Weiss, 2013; King et al., 2016). Admittedly, further analysis of both Myc and Mycn is needed to understand the interplay between the two proteins as I find it hard to understand how two mouse proteins that are 35% similar in sequence could completely compensate for each other and yet show such distinct cellular mechanisms (DePinho et al., 1986).

Mycn is transiently expressed during EHT and may be the critical mediator of the differentiation process

Mycn is expressed in several tissues during early embryonic development including: developing gut, kidney, lung, heart and central nervous system (Stanton et al., 1992; Tanaka et al., 1999). Given its expression in many different tissues and the early embryonic lethality associated with its loss, the role of Mycn in early hematopoiesis could have been easily missed. However, recent work *in vivo* showing that overexpression of Mycn (along with Meis1) in mature murine blood cells can reprogram them into induced HSCs possessing clonal multilineage differentiation potential (Riddell et al., 2014), suggests that Mycn plays a major role in the stem-like identity of HSCs. Indeed, although *Myc* and *Mycn* are equally expressed in HSCs of the BM (King et al., 2016; Laurenti et al., 2008), as HSCs differentiate into the different lineages of the hematopoietic tissue, *Mycn* expression substantially decreases while *Myc* expression remains relatively stable (Laurenti et al., 2008; King et al., 2016). Our functional analysis when combined with the unbiased scRNAseq data recently published by Baron and colleagues (2018) has shown how Mycn may be one of the key mediators of EHT. Here, we see that *Mycn* expression is low in ECs, peaks in single cells during EHT and then subsequently decreases in HSPCs (Figure 22). Interestingly, the Mycn peak in expression occurs right after a *Mfng* expression peak, appearing when EHT cells are under low Notch activity, as we discussed above. This is very much in line with

our qRT-PCR analysis of arterial ECs with low Notch signaling, in which *Mycn* expression is upregulated 6-fold. Therefore, our data strongly suggests that the peak in *Mycn* expression during EHT is dependent on the preceding increase in Mfng and decrease in Jagged1/ Notch signaling. Interestingly, *Myc* expression is inverse to that of *Mycn* across pseudotime and the expression pattern of *Myc* follows the same pattern as known hematopoietic genes *Rac2* and *Lyl1* (Figure 22). Therefore, we can see a dynamic and sequential need for Mycn and Myc during and after EHT. But, several questions are still open to discussion. What can be the potential role of Mycn during EHT? Why Myc cannot compensate for the loss of Mycn? What leads to the decrease in *Mycn* expression after EHT? And what causes the increase in *Myc* expression in the subsequent HSPC and HSC populations?

As mentioned earlier, full KO of Mycn is embryonically lethal and leads to an obvious defect in neural development. Additionally, hypomorophic mutations in Mycn can delay the early lethality of the mice but mice still expire before birth (Moens et al., 1992; Moens et al., 1993; Nagy et al., 1998), suggesting that threshold levels of Mycn is essential for its function. Mice null for Mycn specifically in the neuronal progenitors have diminished number of progenitors suggesting that Mycn regulates cell cycle (Knoepfler et al., 2002; Yoshida, 2018). Indeed, upon stabilization of Mycn in Huwe1-deficient HSCs, transcripts of cell-cycle progression targets were upregulated (King et al., 2016). Additionally, Mycn is known to promote expansion of undifferentiated limb bud mesenchyme at E10.5 (Ota et al., 2007). All of the above correlates with our single transcriptomics data analysis whereby EHT clusters (C4), which have almost exclusively high expression of *Mycn* compared to all the other clusters, also had more expression of E2F targets genes and G1/S enriched genes (Figure 23). Therefore, Mycn could be exerting a proliferative boost in the HE→EHT cells as evident not only by the transcriptomics analysis, but also due to the high Ki67 staining in budding cells of the DA.

In neuroblastoma models, upregulated MYCN activates pluripotency genes *KLF2, KLF4, LIF*, and *LIN28B* (Cotterman and Knoepfler, 2009). Since self-renewal ability of Myc and Mycn KO mouse ESCs is due to the inability of the cells to progress through S-Phase and G2/M checkpoints (Varlakhanova et al., 2010), and Mycn is highly associated with blocking differentiation while inducing pluripotency (Huang and Weiss 2013), perhaps the role of Mycn during EHT is similar. Maybe Mycn is necessary in the HE to prime the cells towards pluripotency, permitting these cells to be more plastic in endothelial identity and permitting them to respond to the other signaling pathways (BMP4, VEGF, Hh) crucial for AGM HSC development at E10.5 (Crisan et al., 2016; Dzierzak and Bigas, 2018; Medvinsky et al., 2011). This plastic phenotype goes in line with the high proliferative signature of these cells as length of G1 during cell cycle is associated with proliferation versus differentiation decisions (Ruijtenberg and van den Heuvel, 2016).

Furthermore, both proteins can reprogram fibroblasts into induced pluripotent stem (iPS) cells (Nakagawa and Yamanaka, 2010; Varlakhanova et al., 2010). However, the molecular cascade that they induce diverge to produce specific outcomes. For example, in a medulloblastoma tumor model, MYCN promotes a Sonic Hedgehog (SHH)-dependent transformation of medulloblastoma cells while MYC promotes a SHH-independent malignancy (Roussel and Robinson, 2013). Authors suggest that this data would mean that MYCN can transform cells in an already committed lineage while MYC can drive cancer stem cell functionality (Huang and Weiss 2013).

Divergent downstream events may be the reason why both proteins cannot fully compensate for the loss of the other. Indeed the Mycn null mouse embryos had severe defects in the central nervous system and embryonic death despite the endogenous upregulation of Myc (Stanton et al., 1992). Are downstream targets for both genes distinct? Tumors with amplified MYCN have a distinct gene expression profile compared to neuroblastomas with overexpression of MYC (Rickman et al., 2018). Additionally, *in vitro* data has shown slight differential binding affinities of Myc, Mycn, and Mycl in small cell lung cancer models, and MYC, MYCN, and MYCL are all affected in a mutually exclusive manner (Bragelmann et al., 2017). Therefore, although it is assumed that Myc and Mycn are redundant, the data overwhelmingly suggests that there are functional differences between the Myc family members and compensation is tissue and context dependent.

Not only am I interested in the role of Mycn and Myc during EHT, but I am also interested in how the dynamic expression of these genes function to seamlessly guide ECs through EHT and HSPC proliferation. As mentioned previously, *Mycn* is highly expressed in the EHT cells while *Myc* is highly expressed in the HSPCs of the DA. I tried to find if there are any published data on *Mycn* and *Myc* expression pattern that follow a similar trajectory during development and found that limb bud mesenchyme is similar to that seen in the DA (Zhou et al., 2011). The authors found that *Mycn* and *Myc* are sequentially expressed in the developing limb, with *Mycn* playing a role in producing the mesenchymal cells that will give rise to the chondrocyte and osteoblast progenitors, while *Myc* controls the proliferating chondrocytes and the number of cells that become mature (Zhou et al., 2011). Perhaps, Mycn and Myc are doing very similar sequential functions in the ECs of the DA: Mycn could be driving the HE cells towards EHT (by the proliferative priming mechanism suggested above) and once cells become HSPCs in the DA lumen, then Myc is in charge of expanding these cells and driving maturation (Pre-HSC type I→ Pre-HSC type II).

How are Myc and Mycn regulated?

Besides what was previously mentioned, not much is known about the developmental regulation of Mycn *in vivo;* however, work done in the cancer field may shed light into the possible regulation of Mycn during dHSPC formation in the DA. In human neuroblastoma, the stability of MYCN is highly regulated by Aurora A and Fbxw-7, whereby the former stabilizes MYCN and the latter promotes its degradation (Otto et al., 2009). Fbxw-7 is an ubiquitin ligase similar in role to the previously mentioned Huwe1 (Rickman et al., 2018). Upon cell cycle entry, cyclin dependent complexes activate E2F TFs to induce the S-phase of the cell cycle (Huang and Weiss 2013). E2F factors bind to the promoter of *MYCN* inducing its expression, which will lead to the increase in cyclin D2 (CDK2), a direct target of Mycn (Huang and Weiss 2013; Rickman et al., 2018). Previous work from our laboratory has seen that retina ECs with loss of Notch signaling upregulate E2F TFs and MAPK activity (Pontes-Quero et al., 2019), which also induces upregulation of *Mycn* expression in these cells (unpublished). Similarly, we also see high E2F targets genes in our transcriptomics analysis of EHT cells (Figure 23).

During the progression of the cycle (from G2→M), Mycn becomes phosphorylated by Cdk1 and Gsk3, leading to its degradation by Fbxw-7 (Rickman et al., 2018; Ruiz-Perez et al., 2017). It is also found that MYCN could negatively regulate its stability in the tumor context through p53. P53, a tumor suppressor that leads to G1 cell cycle arrest, can be activated by MYCN which in turn has been shown to be able to inactivate Aurora A thereby allowing the degradation of MYCN (Chiang, 2012). Interestingly, we see high expression of Cdkn1c or p57 in HE/EHT cells (Figure 23) which during T-cell development is upstream of p53 (Jayapal and Kaldis, 2014). During normal T-cell development, p57 regulates E2F1 to control E2F target gene expression and p53 activity to produce threshold activation of both pathways. Additionally, although p27 KO mice develop a normal hematopoietic system (Matsumoto et al., 2011; Takahashi et al., 2000), many studies have identified both kinase inhibitors to be important for proliferation, differentiation, apoptosis, and aging of hematopoietic cells (Dumble et al., 2007; Liu et al., 2009; Lotem and Sachs, 1993). Therefore, it is not outside the realm of possibility that the signaling pathways previously described in tumor models could be occurring in EHT cells to modulate Mycn activity, inducing its expression increase and then its subsequent protein degradation. However, more research is needed to fine-tune the pathway mechanism during development.

The most difficult to explain is the switch between Mycn and Myc from EHT→HSPC. Developing HSCs become Notch independent during the emergence of the hematopoietic system in the embryo. Here, we also see that the Notch signaling pathway is downregulated in HSPCs, and yet we see an increase in Myc expression. Since Myc is a direct target of

Notch (Song et al., 2016), how is it that *Myc* expression is increasing in HSPCs in the absence of Notch? It has been shown that ERK and AKT pathways can also regulate *Myc* expression (Chambard et al., 2007). Indeed, ERK signaling is essential for HSC development in zebrafish (Wang et al., 2013) but unfortunatly, Myc was not analyzed in the zebrafish embryo, leading us to only speculate that the connection between ERK and Myc expression may be involved in the proliferation of the HSPCs in the DA. On the other hand, although HSPCs become Notch independent as they go from Pre-HSC Type I to Type II (Souihol et al., 2016) and ,as a whole population, they have lower expression of downstream Notch gene targets, it is possible that a small portion of cells still have active Notch signaling. Indeed, we did see some c-Kit^{+} cells in the DA that were positive for N1CD signaling (not shown here), although we could not do co-staining experiments to see if they also had high Myc expression. Therefore, Notch signaling (be it by Notch1 or Notch2) could be activating low level Myc expression in HSPCs to facilitate the proliferation of some cells.

Working Model

Based on our results we have generated the following model:

Under physiological conditions, Notch signaling must decrease in the endothelial cell that will undergo endothelial to hematopoietic transition. We believe that *Manic Fringe* expression increases in those hemogenic endothelial cells that are fine-tuning EHT selectivity through upregulation of Gfi1. The modification of the Notch extracellular domain by Manic Fringe then increases receptor affinity for Jag1, the ligand more highly expressed in the arterial endothelium. This will lead to a decrease in *Hey2* expression and an increase in *Mycn* expression. Decreased Notch signaling and upregulation of Mycn further causes a decreases in endothelial identity (downregulating Sox17 and Gja5). The cell begins upregulating hematopoietic markers such as c-Kit and CD41 thereby undergoing the process of EHT and budding into the lumen of the DA.

Overactivation of Notch sustains high Notch activity in the HE and consequently prohibits the increase in *Mycn* expression. Cells without *Mycn* expression therefore do not undergo transition. The high Notch activity increases *Dll4* expression and *Hey2* converting the HE into more of an arterial endothelium thereby prohibiting functional EHT.

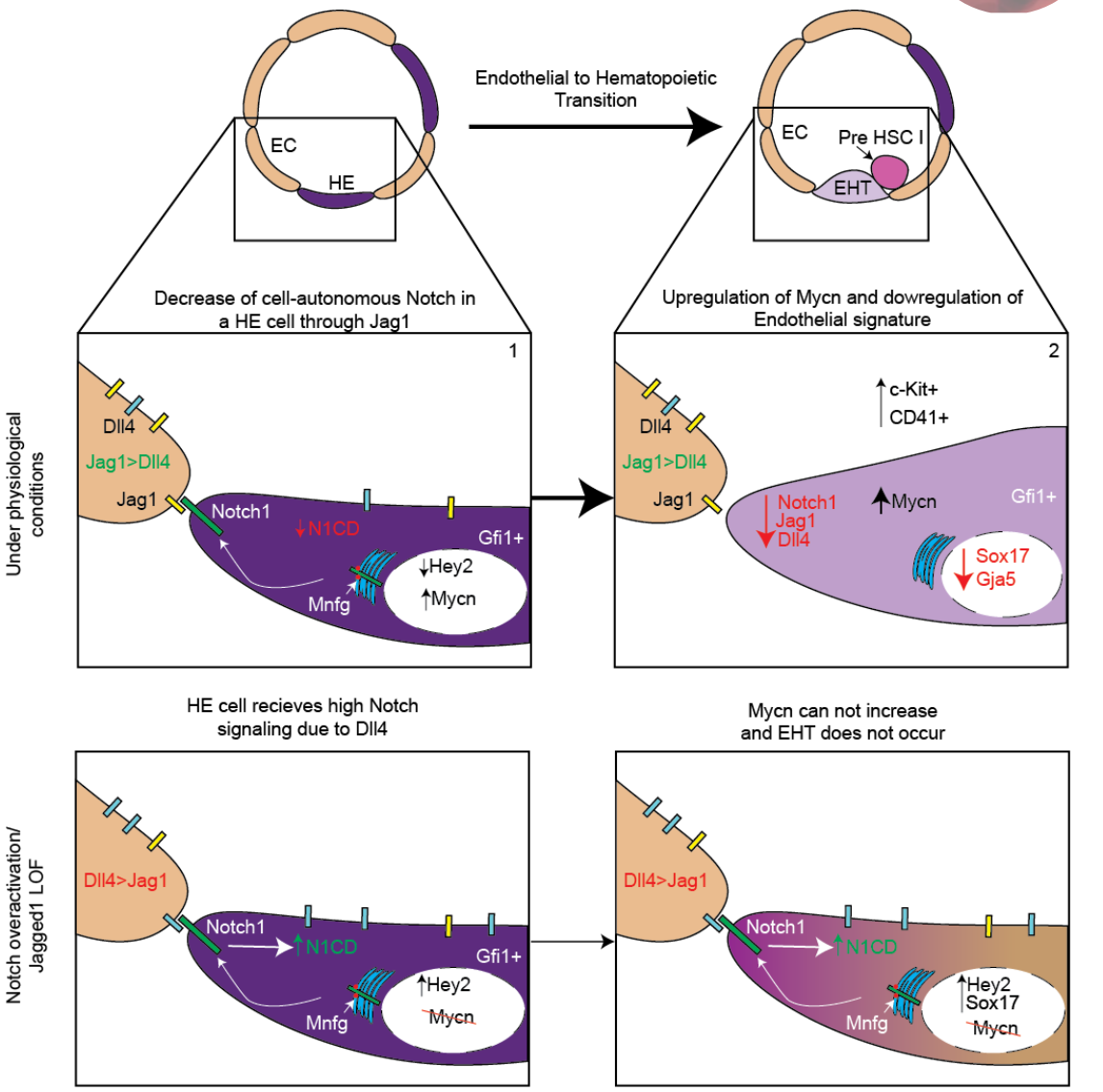

Figure 24 Working Model for the regulation of EHT by Notch and Mycn. A subset of ECs in the dorsal aorta will have higher Mfng expression, which glycosylates the Notch receptors in that cell. This leads to a reduction of Jagged1-to-Notch signaling ability and in increase in Dll4-Notch signaling ability. However, the overall Notch signaling input is decreased due to higher levels of Jagged1 than Dll4. A decrease in cell-autonomous Notch signaling in the hemogenic endothelial (HE) cell will lead to the upregulation of Mycn. As Mycn levels increase, the endothelial signature (Notch1 and its ligands, Sox17 and Gja5) decreases and the hematopoietic progenitors signature (c-kit, CD41) increases leading to endothelial-to-hematopoietic transition (EHT). Induction of Notch LOF after formation of arterial ECs, promotes this process. Notch overactivation or loss of Jag1 in aorta ECs, leads to higher Dll4-Notch signaling in the HE cell and therefore Mycn expression cannot increase. This leads to the maintenance of the endothelial signature and to the failure of EHT.

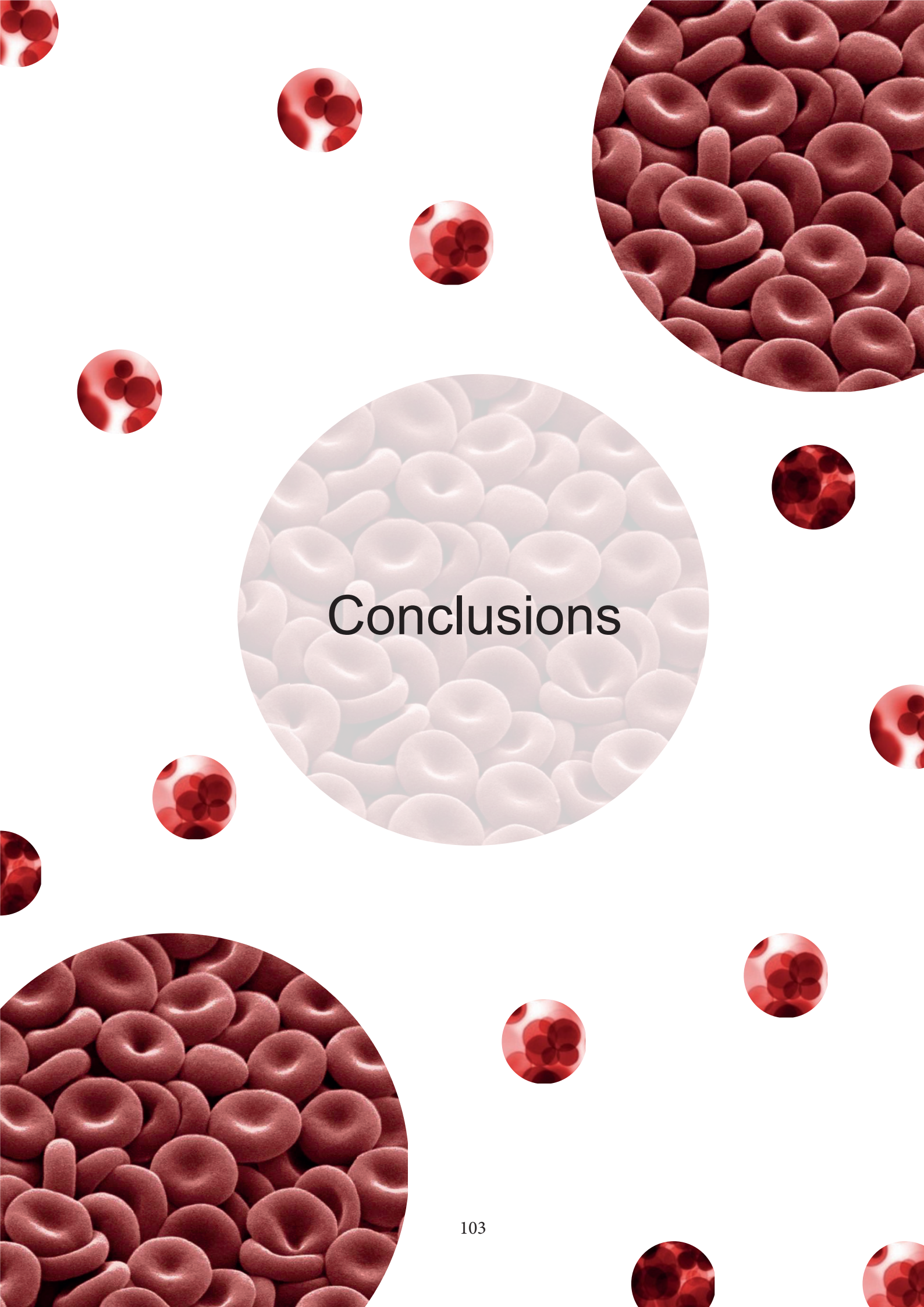

Conclusions

CONCLUSIONS

1) Overactivation of Notch leads to fewer hemogenic endothelial cells and decreased development of HSPCs in the Dorsal Aorta.
2) Inducible Notch genetic mosaic analysis shows that endothelial cells with lower Notch signaling contribute more frequently to the HSPC population of the Dorsal Aorta.
3) Loss of Jagged1 in the endothelium of the Dorsal Aorta increases arterial Notch signaling which blocks the development of HSPCs.
4) Manic Fringe, a negative regulator of Jagged1-Notch signaling, is transiently and highly expressed in hemogenic endothelium.
5) Overexpression of Manic Fringe in the Dorsal Aorta leads to decreased Notch signaling, an increase in endothelial to hematopoietic transition, and higher number of HSPCs.
6) Endothelial cells with Notch loss-of-function have increased expression of cell-cycle markers and hematopoietic differentiation genes, including Mycn.
7) Dorsal Aorta endothelial cells with early loss of Mycn do not contribute to the formation of the adult hematopoietic system.
8) In contrast to Mycn, Myc is dispensable for endothelial to hematopoietic transition, and is only required for the later stages of hematopoietic development.
9) Mycn is essential for the development or maintenance of the adult hematopoietic system.
10) Cells undergoing endothelial to hematopoietic transition must decrease their level of Notch signaling, in order to lose their quiescent arterial endothelium characteristics, and gain a proliferative hematopoietic fate.

CONCLUSIONES

1) La sobreactivación de Notch provoca una disminución de células hemogénicas en el endotelio y de progenitores hematopoyéticos en la aorta dorsal.
2) El análisis de ratones mosaico para Notch demuestra que las células endoteliales con pérdida de función de Notch contribuyen en mayor medida a la población HSPC de la aorta dorsal.
3) La pérdida de Jagged1 en el endotelio de la aorta dorsal aumenta la señalización de Notch en la arteria y bloquea el desarrollo de los progenitores hematopoyéticos.
4) Manic Fringe, un regulador negativo de la señalización Jagged1-Notch, se expresa de forma transitoria y elevada en el endotelio hemogénico.
5) La sobreexpresión de Manic Fringe en la aorta dorsal provoca un aumento de la población de células progenitoras hematopoyéticas y disminuye la señalización de Notch.
6) Las células endoteliales con pérdida de función de Notch presentan un incremento de la expresión de genes de proliferación y diferenciación, como Mycn.
7) Las células endoteliales de la aorta dorsal con pérdida temprana de Mycn no contribuyen a la formación del sistema hematopoyético adulto.
8) A diferencia de Mycn, Myc es prescindible para la transición de células endoteliales a hematopoyéticas y solo se requiere para las etapas posteriores del desarrollo hematopoyético.
9) Mycn es esencial para el desarrollo o mantenimiento del sistema hematopoyético en adultos.
10) Para que se produzca la transición de células endoteliales a hematopoyéticas, estas deben disminuir su nivel de señalización de Notch, para perder sus características endoteliales arteriales quiescentes, y obtener una identidad hematopoyética proliferativa.

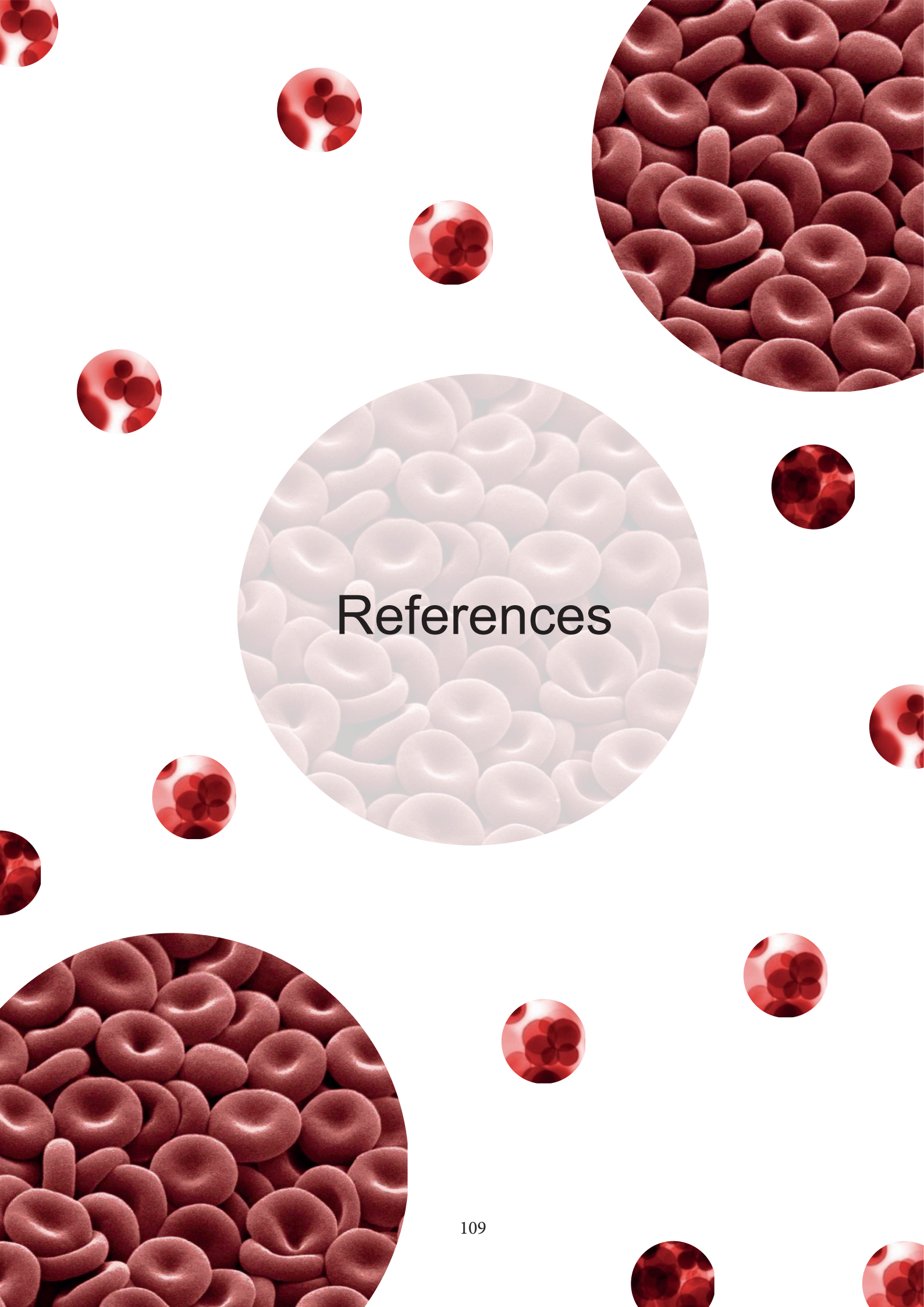

References

References

Adamo, L., and Garcia-Cardena, G. (2012). The vascular origin of hematopoietic cells. Dev Biol *362*, 1-10.

Adams, R.H. (2003). Molecular control of arterial-venous blood vessel identity. J Anat *202*, 105-112.

Ambler, C.A., Nowicki, J.L., Burke, A.C., and Bautch, V.L. (2001). Assembly of trunk and limb blood vessels involves extensive migration and vasculogenesis of somite-derived angioblasts. Dev Biol *234*, 352-364.

Babovic, S., and Eaves, C.J. (2014). Hierarchical organization of fetal and adult hematopoietic stem cells. Exp Cell Res *329*, 185-191.

Bakhuraysah, M.M., Siatskas, C., and Petratos, S. (2016). Hematopoietic stem cell transplantation for multiple sclerosis: is it a clinical reality? Stem Cell Res Ther *7*, 12.

Bansal, R., van Baarlen, J., Storm, G., and Prakash, J. (2015). The interplay of the Notch signaling in hepatic stellate cells and macrophages determines the fate of liver fibrogenesis. Sci Rep *5*, 18272.

Baron, C.S., Kester, L., Klaus, A., Boisset, J.C., Thambyrajah, R., Yvernogeau, L., Kouskoff, V., Lacaud, G., van Oudenaarden, A., and Robin, C. (2018). Single-cell transcriptomics reveal the dynamic of haematopoietic stem cell production in the aorta. Nat Commun *9*, 2517.

Batsivari, A., Rybtsov, S., Souilhol, C., Binagui-Casas, A., Hills, D., Zhao, S., Travers, P., and Medvinsky, A. (2017). Understanding Hematopoietic Stem Cell Development through Functional Correlation of Their Proliferative Status with the Intra-aortic Cluster Architecture. Stem Cell Reports *8*, 1549-1562.

Baudino, T.A., McKay, C., Pendeville-Samain, H., Nilsson, J.A., Maclean, K.H., White, E.L., Davis, A.C., Ihle, J.N., and Cleveland, J.L. (2002). c-Myc is essential for vasculogenesis and angiogenesis during development and tumor progression. Genes Dev *16*, 2530-2543.

Benedito, R., Roca, C., Sorensen, I., Adams, S., Gossler, A., Fruttiger, M., and Adams, R.H. (2009). The notch ligands Dll4 and Jagged1 have opposing effects on angiogenesis. Cell *137*, 1124-1135.

Bergiers, I., Andrews, T., Vargel Bolukbasi, O., Buness, A., Janosz, E., Lopez-Anguita, N., Ganter, K., Kosim, K., Celen, C., Itir Percin, G.*, et al.* (2018). Single-cell transcriptomics reveals a new dynamical function of transcription factors during embryonic hematopoiesis. Elife *7*.

Bertrand, J.Y., Chi, N.C., Santoso, B., Teng, S., Stainier, D.Y., and Traver, D. (2010). Haematopoietic stem cells derive directly from aortic endothelium during development. Nature *464*, 108-111.

Bigas, A., and Espinosa, L. (2012). Hematopoietic stem cells: to be or Notch to be. Blood *119*, 3226-3235.

Blackwell, T.K., Huang, J., Ma, A., Kretzner, L., Alt, F.W., Eisenman, R.N., and Weintraub, H. (1993). Binding of myc proteins to canonical and noncanonical DNA sequences. Mol Cell Biol *13*, 5216-5224.

Blackwood, E.M., and Eisenman, R.N. (1991). Max: a helix-loop-helix zipper protein that forms a sequence-specific DNA-binding complex with Myc. Science *251*, 1211-1217.

Boisset, J.C., van Cappellen, W., Andrieu-Soler, C., Galjart, N., Dzierzak, E., and Robin, C. (2010). In vivo imaging of haematopoietic cells emerging from the mouse aortic endothelium. Nature *464*, 116-120.

Bonkhofer, F., Rispoli, R., Pinheiro, P., Krecsmarik, M., Schneider-Swales, J., Tsang, I.H.C., de Bruijn, M., Monteiro, R., Peterkin, T., and Patient, R. (2019). Blood stem cell-forming haemogenic endothelium in zebrafish derives from arterial endothelium. Nat Commun *10*, 3577.

Bos, F.L., Hawkins, J.S., and Zovein, A.C. (2015). Single-cell resolution of morphological changes in hemogenic endothelium. Development *142*, 2719-2724.

Bragelmann, J., Dammert, M.A., Dietlein, F., Heuckmann, J.M., Choidas, A., Bohm, S., Richters, A., Basu, D., Tischler, V., Lorenz, C.*, et al.* (2017). Systematic Kinase Inhibitor Profiling Identifies CDK9 as a Synthetic Lethal Target in NUT Midline Carcinoma. Cell Rep *20*, 2833-2845.

Bray, S.J. (2016). Notch signalling in context. Nat Rev Mol Cell Biol *17*, 722-735.

Bretones, G., Delgado, M.D., and Leon, J. (2015). Myc and cell cycle control. Biochim Biophys Acta *1849*, 506-516.

Bruckner, K., Perez, L., Clausen, H., and Cohen, S. (2000). Glycosyltransferase activity of Fringe modulates Notch-Delta interactions. Nature *406*, 411-415.

Burns, C.E., Traver, D., Mayhall, E., Shepard, J.L., and Zon, L.I. (2005). Hematopoietic stem cell fate is established by the Notch-Runx pathway. Genes Dev *19*, 2331-2342.

Chambard, J.C., Lefloch, R., Pouyssegur, J., and Lenormand, P. (2007). ERK implication in cell cycle regulation. Biochim Biophys Acta *1773*, 1299-1310.

Charron, J., Malynn, B.A., Fisher, P., Stewart, V., Jeannotte, L., Goff, S.P., Robertson, E.J., and Alt, F.W. (1992). Embryonic lethality in mice homozygous for a targeted disruption of the N-myc gene. Genes Dev *6*, 2248-2257.

Chen, M.J., Yokomizo, T., Zeigler, B.M., Dzierzak, E., and Speck, N.A. (2009). Runx1 is required for the endothelial to haematopoietic cell transition but not thereafter. Nature *457*, 887-891.
Chiang, C.M. (2012). p53-Aurora A mitotic feedback loop regulates cell cycle progression and genomic stability. Cell Cycle *11*, 3719-3720.
Ciau-Uitz, A., and Patient, R. (2016). The embryonic origins and genetic programming of emerging haematopoietic stem cells. FEBS Lett *590*, 4002-4015.
Clarke, R.L., Yzaguirre, A.D., Yashiro-Ohtani, Y., Bondue, A., Blanpain, C., Pear, W.S., Speck, N.A., and Keller, G. (2013). The expression of Sox17 identifies and regulates haemogenic endothelium. Nat Cell Biol *15*, 502-510.
Cotterman, R., and Knoepfler, P.S. (2009). N-Myc regulates expression of pluripotency genes in neuroblastoma including lif, klf2, klf4, and lin28b. PLoS One *4*, e5799.
Crisan, M., Solaimani Kartalaei, P., Neagu, A., Karkanpouna, S., Yamada-Inagawa, T., Purini, C., Vink, C.S., van der Linden, R., van Ijcken, W., Chuva de Sousa Lopes, S.M.*, et al.* (2016). BMP and Hedgehog Regulate Distinct AGM Hematopoietic Stem Cells Ex Vivo. Stem Cell Reports *6*, 383-395.
Cumano, A., Ferraz, J.C., Klaine, M., Di Santo, J.P., and Godin, I. (2001). Intraembryonic, but not yolk sac hematopoietic precursors, isolated before circulation, provide long-term multilineage reconstitution. Immunity *15*, 477-485.
Davis, A.C., Wims, M., Spotts, G.D., Hann, S.R., and Bradley, A. (1993). A null c-myc mutation causes lethality before 10.5 days of gestation in homozygotes and reduced fertility in heterozygous female mice. Genes Dev *7*, 671-682.
Davis, R.L., and Turner, D.L. (2001). Vertebrate hairy and Enhancer of split related proteins: transcriptional repressors regulating cellular differentiation and embryonic patterning. Oncogene *20*, 8342-8357.
de Bruijn, M.F., Ma, X., Robin, C., Ottersbach, K., Sanchez, M.J., and Dzierzak, E. (2002). Hematopoietic stem cells localize to the endothelial cell layer in the midgestation mouse aorta. Immunity *16*, 673-683.
Dejana, E., Hirschi, K.K., and Simons, M. (2017). The molecular basis of endothelial cell plasticity. Nat Commun *8*, 14361.
Del Monte, G., Grego-Bessa, J., Gonzalez-Rajal, A., Bolos, V., and De La Pompa, J.L. (2007). Monitoring Notch1 activity in development: evidence for a feedback regulatory loop. Dev Dyn *236*, 2594-2614.
del Toro, R., Prahst, C., Mathivet, T., Siegfried, G., Kaminker, J.S., Larrivee, B., Breant, C., Duarte, A., Takakura, N., Fukamizu, A.*, et al.* (2010). Identification and functional analysis of endothelial tip cell-enriched genes. Blood *116*, 4025-4033.
DePinho, R.A., Legouy, E., Feldman, L.B., Kohl, N.E., Yancopoulos, G.D., and Alt, F.W. (1986). Structure and expression of the murine N-myc gene. Proc Natl Acad Sci U S A *83*, 1827-1831.
Duarte, A., Hirashima, M., Benedito, R., Trindade, A., Diniz, P., Bekman, E., Costa, L., Henrique, D., and Rossant, J. (2004). Dosage-sensitive requirement for mouse Dll4 in artery development. Genes Dev *18*, 2474-2478.
Dubois, N.C., Adolphe, C., Ehninger, A., Wang, R.A., Robertson, E.J., and Trumpp, A. (2008). Placental rescue reveals a sole requirement for c-Myc in embryonic erythroblast survival and hematopoietic stem cell function. Development *135*, 2455-2465.
Dumble, M., Moore, L., Chambers, S.M., Geiger, H., Van Zant, G., Goodell, M.A., and Donehower, L.A. (2007). The impact of altered p53 dosage on hematopoietic stem cell dynamics during aging. Blood *109*, 1736-1742.
Durand, C., Robin, C., Bollerot, K., Baron, M.H., Ottersbach, K., and Dzierzak, E. (2007). Embryonic stromal clones reveal developmental regulators of definitive hematopoietic stem cells. Proc Natl Acad Sci U S A *104*, 20838-20843.
Dzierzak, E., and Bigas, A. (2018). Blood Development: Hematopoietic Stem Cell Dependence and Independence. Cell Stem Cell *22*, 639-651.
Eilken, H.M., Nishikawa, S., and Schroeder, T. (2009). Continuous single-cell imaging of blood generation from haemogenic endothelium. Nature *457*, 896-900.
Esner, M., Meilhac, S.M., Relaix, F., Nicolas, J.F., Cossu, G., and Buckingham, M.E. (2006). Smooth muscle of the dorsal aorta shares a common clonal origin with skeletal muscle of the myotome. Development *133*, 737-749.
Espin-Palazon, R., Stachura, D.L., Campbell, C.A., Garcia-Moreno, D., Del Cid, N., Kim, A.D., Candel, S., Meseguer, J., Mulero, V., and Traver, D. (2014). Proinflammatory signaling regulates hematopoietic stem cell emergence. Cell *159*, 1070-1085.
Fernandez-Chacon, M., Casquero-Garcia, V., Luo, W., Francesca Lunella, F., Ferreira Rocha, S., Del Olmo-Cabrera, S., and Benedito, R. (2019). iSuRe-Cre is a genetic tool to reliably induce and report Cre-dependent genetic modifications. Nat Commun *10*, 2262.

Fischer, A., Schumacher, N., Maier, M., Sendtner, M., and Gessler, M. (2004). The Notch target genes Hey1 and Hey2 are required for embryonic vascular development. Genes Dev *18*, 901-911.
Gale, N.W., Dominguez, M.G., Noguera, I., Pan, L., Hughes, V., Valenzuela, D.M., Murphy, A.J., Adams, N.C., Lin, H.C., Holash, J., *et al.* (2004). Haploinsufficiency of delta-like 4 ligand results in embryonic lethality due to major defects in arterial and vascular development. Proc Natl Acad Sci U S A *101*, 15949-15954.
Gama-Norton, L., Ferrando, E., Ruiz-Herguido, C., Liu, Z., Guiu, J., Islam, A.B., Lee, S.U., Yan, M., Guidos, C.J., Lopez-Bigas, N., *et al.* (2015). Notch signal strength controls cell fate in the haemogenic endothelium. Nat Commun *6*, 8510.
Gama-Norton, L., Ferrando, E., Ruiz-Herguido, C., Liu, Z., Guiu, J., Islam, A.B., Lee, S.U., Yan, M., Guidos, C.J., Lopez-Bigas, N., *et al.* (2016). Corrigendum: Notch signal strength controls cell fate in the haemogenic endothelium. Nat Commun *7*, 10978.
Gao, W., Sweeney, C., Walsh, C., Rooney, P., McCormick, J., Veale, D.J., and Fearon, U. (2013). Notch signalling pathways mediate synovial angiogenesis in response to vascular endothelial growth factor and angiopoietin 2. Ann Rheum Dis *72*, 1080-1088.
Grego-Bessa, J., Luna-Zurita, L., del Monte, G., Bolos, V., Melgar, P., Arandilla, A., Garratt, A.N., Zang, H., Mukouyama, Y.S., Chen, H., *et al.* (2007). Notch signaling is essential for ventricular chamber development. Dev Cell *12*, 415-429.
Gridley, T. (2010). Notch signaling in the vasculature. Curr Top Dev Biol *92*, 277-309.
Gritz, E., and Hirschi, K.K. (2016). Specification and function of hemogenic endothelium during embryogenesis. Cell Mol Life Sci *73*, 1547-1567.
Guiu, J., Shimizu, R., D'Altri, T., Fraser, S.T., Hatakeyama, J., Bresnick, E.H., Kageyama, R., Dzierzak, E., Yamamoto, M., Espinosa, L., *et al.* (2013). Hes repressors are essential regulators of hematopoietic stem cell development downstream of Notch signaling. J Exp Med *210*, 71-84.
Hadland, B.K., Huppert, S.S., Kanungo, J., Xue, Y., Jiang, R., Gridley, T., Conlon, R.A., Cheng, A.M., Kopan, R., and Longmore, G.D. (2004). A requirement for Notch1 distinguishes 2 phases of definitive hematopoiesis during development. Blood *104*, 3097-3105.
Han, J.K., Chang, S.H., Cho, H.J., Choi, S.B., Ahn, H.S., Lee, J., Jeong, H., Youn, S.W., Lee, H.J., Kwon, Y.W., *et al.* (2014). Direct conversion of adult skin fibroblasts to endothelial cells by defined factors. Circulation *130*, 1168-1178.
He, C., Hu, H., Braren, R., Fong, S.Y., Trumpp, A., Carlson, T.R., and Wang, R.A. (2008). c-myc in the hematopoietic lineage is crucial for its angiogenic function in the mouse embryo. Development *135*, 2467-2477.
Hellstrom, M., Phng, L.K., Hofmann, J.J., Wallgard, E., Coultas, L., Lindblom, P., Alva, J., Nilsson, A.K., Karlsson, L., Gaiano, N., *et al.* (2007). Dll4 signalling through Notch1 regulates formation of tip cells during angiogenesis. Nature *445*, 776-780.
Henig, I., and Zuckerman, T. (2014). Hematopoietic stem cell transplantation-50 years of evolution and future perspectives. Rambam Maimonides Med J *5*, e0028.
Hicks, C., Johnston, S.H., diSibio, G., Collazo, A., Vogt, T.F., and Weinmaster, G. (2000). Fringe differentially modulates Jagged1 and Delta1 signalling through Notch1 and Notch2. Nat Cell Biol *2*, 515-520.
Hierlmeier, S., Eyrich, M., Wolfl, M., Schlegel, P.G., and Wiegering, V. (2018). Early and late complications following hematopoietic stem cell transplantation in pediatric patients - A retrospective analysis over 11 years. PLoS One *13*, e0204914.
Hou, X., Tashima, Y., and Stanley, P. (2012). Galactose differentially modulates lunatic and manic fringe effects on Delta1-induced NOTCH signaling. J Biol Chem *287*, 474-483.
Huang, M., and Weiss, W.A. (2013). Neuroblastoma and MYCN. Cold Spring Harb Perspect Med *3*, a014415.
Hur, J., Choi, J.I., Lee, H., Nham, P., Kim, T.W., Chae, C.W., Yun, J.Y., Kang, J.A., Kang, J., Lee, S.E., *et al.* (2016). CD82/KAI1 Maintains the Dormancy of Long-Term Hematopoietic Stem Cells through Interaction with DARC-Expressing Macrophages. Cell Stem Cell *18*, 508-521.
Hurlin, P.J. (2013). Control of vertebrate development by MYC. Cold Spring Harb Perspect Med *3*, a014332.
Jaffredo, T., Bollerot, K., Sugiyama, D., Gautier, R., and Drevon, C. (2005). Tracing the hemangioblast during embryogenesis: developmental relationships between endothelial and hematopoietic cells. Int J Dev Biol *49*, 269-277.
Jaffredo, T., Lempereur, A., Richard, C., Bollerot, K., Gautier, R., Canto, P.Y., Drevon, C., Souyri, M., and Durand, C. (2013). Dorso-ventral contributions in the formation of the embryonic aorta and the control of aortic hematopoiesis. Blood Cells Mol Dis *51*, 232-238.
Jayapal, S.R., and Kaldis, P. (2014). p57(Kip2) regulates T-cell development and lymphoma. Blood *123*, 3370-3371.
Kageyama, R., Masamizu, Y., and Niwa, Y. (2007). Oscillator mechanism of Notch pathway in the segmentation

clock. Dev Dyn *236*, 1403-1409.
Kakuda, S., and Haltiwanger, R.S. (2017). Deciphering the Fringe-Mediated Notch Code: Identification of Activating and Inhibiting Sites Allowing Discrimination between Ligands. Dev Cell *40*, 193-201.
Kato, Y. (2011). The multiple roles of Notch signaling during left-right patterning. Cell Mol Life Sci *68*, 2555-2567.
Kim, J., Irvine, K.D., and Carroll, S.B. (1995). Cell recognition, signal induction, and symmetrical gene activation at the dorsal-ventral boundary of the developing Drosophila wing. Cell *82*, 795-802.
King, B., Boccalatte, F., Moran-Crusio, K., Wolf, E., Wang, J., Kayembe, C., Lazaris, C., Yu, X., Aranda-Orgilles, B., Lasorella, A.*, et al.* (2016). The ubiquitin ligase Huwe1 regulates the maintenance and lymphoid commitment of hematopoietic stem cells. Nat Immunol *17*, 1312-1321.
Kissa, K., and Herbomel, P. (2010). Blood stem cells emerge from aortic endothelium by a novel type of cell transition. Nature *464*, 112-115.
Knoepfler, P.S., Cheng, P.F., and Eisenman, R.N. (2002). N-myc is essential during neurogenesis for the rapid expansion of progenitor cell populations and the inhibition of neuronal differentiation. Genes Dev *16*, 2699-2712.
Kobayashi, I., Kobayashi-Sun, J., Kim, A.D., Pouget, C., Fujita, N., Suda, T., and Traver, D. (2014). Jam1a-Jam2a interactions regulate haematopoietic stem cell fate through Notch signalling. Nature *512*, 319-323.
Kokubo, H., Miyagawa-Tomita, S., and Johnson, R.L. (2005). Hesr, a mediator of the Notch signaling, functions in heart and vessel development. Trends Cardiovasc Med *15*, 190-194.
Kovall, R.A., Gebelein, B., Sprinzak, D., and Kopan, R. (2017). The Canonical Notch Signaling Pathway: Structural and Biochemical Insights into Shape, Sugar, and Force. Dev Cell *41*, 228-241.
Krebs, L.T., Starling, C., Chervonsky, A.V., and Gridley, T. (2010). Notch1 activation in mice causes arteriovenous malformations phenocopied by ephrinB2 and EphB4 mutants. Genesis *48*, 146-150.
Krebs, L.T., Xue, Y., Norton, C.R., Shutter, J.R., Maguire, M., Sundberg, J.P., Gallahan, D., Closson, V., Kitajewski, J., Callahan, R.*, et al.* (2000). Notch signaling is essential for vascular morphogenesis in mice. Genes Dev *14*, 1343-1352.
Kumano, K., Chiba, S., Kunisato, A., Sata, M., Saito, T., Nakagami-Yamaguchi, E., Yamaguchi, T., Masuda, S., Shimizu, K., Takahashi, T.*, et al.* (2003). Notch1 but not Notch2 is essential for generating hematopoietic stem cells from endothelial cells. Immunity *18*, 699-711.
Lampreia, F.P., Carmelo, J.G., and Anjos-Afonso, F. (2017). Notch Signaling in the Regulation of Hematopoietic Stem Cell. Curr Stem Cell Rep *3*, 202-209.
Lancrin, C., Mazan, M., Stefanska, M., Patel, R., Lichtinger, M., Costa, G., Vargel, O., Wilson, N.K., Moroy, T., Bonifer, C.*, et al.* (2012). GFI1 and GFI1B control the loss of endothelial identity of hemogenic endothelium during hematopoietic commitment. Blood *120*, 314-322.
Lancrin, C., Sroczynska, P., Stephenson, C., Allen, T., Kouskoff, V., and Lacaud, G. (2009). The haemangioblast generates haematopoietic cells through a haemogenic endothelium stage. Nature *457*, 892-895.
Laurenti, E., Varnum-Finney, B., Wilson, A., Ferrero, I., Blanco-Bose, W.E., Ehninger, A., Knoepfler, P.S., Cheng, P.F., MacDonald, H.R., Eisenman, R.N.*, et al.* (2008). Hematopoietic stem cell function and survival depend on c-Myc and N-Myc activity. Cell Stem Cell *3*, 611-624.
Lawson, N.D., Scheer, N., Pham, V.N., Kim, C.H., Chitnis, A.B., Campos-Ortega, J.A., and Weinstein, B.M. (2001). Notch signaling is required for arterial-venous differentiation during embryonic vascular development. Development *128*, 3675-3683.
Lawson, N.D., Vogel, A.M., and Weinstein, B.M. (2002). sonic hedgehog and vascular endothelial growth factor act upstream of the Notch pathway during arterial endothelial differentiation. Dev Cell *3*, 127-136.
le Noble, F., Moyon, D., Pardanaud, L., Yuan, L., Djonov, V., Matthijsen, R., Breant, C., Fleury, V., and Eichmann, A. (2004). Flow regulates arterial-venous differentiation in the chick embryo yolk sac. Development *131*, 361-375.
Liakhovitskaia, A., Rybtsov, S., Smith, T., Batsivari, A., Rybtsova, N., Rode, C., de Bruijn, M., Buchholz, F., Gordon-Keylock, S., Zhao, S.*, et al.* (2014). Runx1 is required for progression of CD41+ embryonic precursors into HSCs but not prior to this. Development *141*, 3319-3323.
Lie, A.L.M., Marinopoulou, E., Lilly, A.J., Challinor, M., Patel, R., Lancrin, C., Kouskoff, V., and Lacaud, G. (2018). Regulation of RUNX1 dosage is crucial for efficient blood formation from hemogenic endothelium. Development *145*.
Limbourg, F.P., Takeshita, K., Radtke, F., Bronson, R.T., Chin, M.T., and Liao, J.K. (2005). Essential role of endothelial Notch1 in angiogenesis. Circulation *111*, 1826-1832.
Liu, Y., Elf, S.E., Miyata, Y., Sashida, G., Liu, Y., Huang, G., Di Giandomenico, S., Lee, J.M., Deblasio, A., Menendez, S.*, et al.* (2009). p53 regulates hematopoietic stem cell quiescence. Cell Stem Cell *4*, 37-48.
Livet, J., Weissman, T.A., Kang, H., Draft, R.W., Lu, J., Bennis, R.A., Sanes, J.R., and Lichtman, J.W. (2007).

Transgenic strategies for combinatorial expression of fluorescent proteins in the nervous system. Nature *450*, 56-62.
Lizama, C.O., Hawkins, J.S., Schmitt, C.E., Bos, F.L., Zape, J.P., Cautivo, K.M., Borges Pinto, H., Rhyner, A.M., Yu, H., Donohoe, M.E.*, et al.* (2015). Repression of arterial genes in hemogenic endothelium is sufficient for haematopoietic fate acquisition. Nat Commun *6*, 7739.
Lotem, J., and Sachs, L. (1993). Hematopoietic cells from mice deficient in wild-type p53 are more resistant to induction of apoptosis by some agents. Blood *82*, 1092-1096.
Maekawa, Y., Tsukumo, S., Okada, H., Kishihara, K., and Yasutomo, K. (2003). Breakdown of peripheral T-cell tolerance by chronic interleukin-15 elevation. Transplantation *76*, 415-420.
Maillard, I., Weng, A.P., Carpenter, A.C., Rodriguez, C.G., Sai, H., Xu, L., Allman, D., Aster, J.C., and Pear, W.S. (2004). Mastermind critically regulates Notch-mediated lymphoid cell fate decisions. Blood *104*, 1696-1702.
Malynn, B.A., de Alboran, I.M., O'Hagan, R.C., Bronson, R., Davidson, L., DePinho, R.A., and Alt, F.W. (2000). N-myc can functionally replace c-myc in murine development, cellular growth, and differentiation. Genes Dev *14*, 1390-1399.
Marklund, U., Hansson, E.M., Sundstrom, E., de Angelis, M.H., Przemeck, G.K., Lendahl, U., Muhr, J., and Ericson, J. (2010). Domain-specific control of neurogenesis achieved through patterned regulation of Notch ligand expression. Development *137*, 437-445.
Matsumoto, A., Takeishi, S., Kanie, T., Susaki, E., Onoyama, I., Tateishi, Y., Nakayama, K., and Nakayama, K.I. (2011). p57 is required for quiescence and maintenance of adult hematopoietic stem cells. Cell Stem Cell *9*, 262-271.
Matsuoka, S., Edwards, M.C., Bai, C., Parker, S., Zhang, P., Baldini, A., Harper, J.W., and Elledge, S.J. (1995). p57KIP2, a structurally distinct member of the p21CIP1 Cdk inhibitor family, is a candidate tumor suppressor gene. Genes Dev *9*, 650-662.
McGarvey, A.C., Rybtsov, S., Souilhol, C., Tamagno, S., Rice, R., Hills, D., Godwin, D., Rice, D., Tomlinson, S.R., and Medvinsky, A. (2017). A molecular roadmap of the AGM region reveals BMPER as a novel regulator of HSC maturation. J Exp Med *214*, 3731-3751.
McGill, M.A., and McGlade, C.J. (2003). Mammalian numb proteins promote Notch1 receptor ubiquitination and degradation of the Notch1 intracellular domain. J Biol Chem *278*, 23196-23203.
Medvinsky, A., Rybtsov, S., and Taoudi, S. (2011). Embryonic origin of the adult hematopoietic system: advances and questions. Development *138*, 1017-1031.
Michalicka, M., Boisjoli, G., Jahan, S., Hovey, O., Doxtator, E., Abu-Khader, A., Pasha, R., and Pineault, N. (2017). Human Bone Marrow Mesenchymal Stromal Cell-Derived Osteoblasts Promote the Expansion of Hematopoietic Progenitors Through Beta-Catenin and Notch Signaling Pathways. Stem Cells Dev *26*, 1735-1748.
Moens, C.B., Auerbach, A.B., Conlon, R.A., Joyner, A.L., and Rossant, J. (1992). A targeted mutation reveals a role for N-myc in branching morphogenesis in the embryonic mouse lung. Genes Dev *6*, 691-704.
Moens, C.B., Stanton, B.R., Parada, L.F., and Rossant, J. (1993). Defects in heart and lung development in compound heterozygotes for two different targeted mutations at the N-myc locus. Development *119*, 485-499.
Moloney, D.J., Panin, V.M., Johnston, S.H., Chen, J., Shao, L., Wilson, R., Wang, Y., Stanley, P., Irvine, K.D., Haltiwanger, R.S.*, et al.* (2000). Fringe is a glycosyltransferase that modifies Notch. Nature *406*, 369-375.
Moran, J.L., Shifley, E.T., Levorse, J.M., Mani, S., Ostmann, K., Perez-Balaguer, A., Walker, D.M., Vogt, T.F., and Cole, S.E. (2009a). Manic fringe is not required for embryonic development, and fringe family members do not exhibit redundant functions in the axial skeleton, limb, or hindbrain. Dev Dyn *238*, 1803-1812.
Moran, J.L., Shifley, E.T., Levorse, J.M., Mani, S., Ostmann, K., Perez-Balaguer, A., Walker, D.M., Vogt, T.F., and Cole, S.E. (2009b). Manic fringe is not required for embryonic development, and fringe family members do not exhibit redundant functions in the axial skeleton, limb, or hindbrain. Dev Dyn *238*, 1803-1812.
Muller, A.M., Medvinsky, A., Strouboulis, J., Grosveld, F., and Dzierzak, E. (1994). Development of hematopoietic stem cell activity in the mouse embryo. Immunity *1*, 291-301.
Nagy, A., Moens, C., Ivanyi, E., Pawling, J., Gertsenstein, M., Hadjantonakis, A.K., Pirity, M., and Rossant, J. (1998). Dissecting the role of N-myc in development using a single targeting vector to generate a series of alleles. Curr Biol *8*, 661-664.
Nakagawa, M., Ichikawa, M., Kumano, K., Goyama, S., Kawazu, M., Asai, T., Ogawa, S., Kurokawa, M., and Chiba, S. (2006). AML1/Runx1 rescues Notch1-null mutation-induced deficiency of para-aortic splanchnopleural hematopoiesis. Blood *108*, 3329-3334.
Nakagawa, M., and Yamanaka, S. (2010). Reprogramming of somatic cells to pluripotency. Adv Exp Med Biol *695*, 215-224.
Nikolova-Krstevski, V., Yuan, L., Le Bras, A., Vijayaraj, P., Kondo, M., Gebauer, I., Bhasin, M., Carman, C.V.,

and Oettgen, P. (2009). ERG is required for the differentiation of embryonic stem cells along the endothelial lineage. BMC Dev Biol *9*, 72.
North, T., Gu, T.L., Stacy, T., Wang, Q., Howard, L., Binder, M., Marin-Padilla, M., and Speck, N.A. (1999). Cbfa2 is required for the formation of intra-aortic hematopoietic clusters. Development *126*, 2563-2575.
Noseda, M., Chang, L., McLean, G., Grim, J.E., Clurman, B.E., Smith, L.L., and Karsan, A. (2004). Notch activation induces endothelial cell cycle arrest and participates in contact inhibition: role of p21Cip1 repression. Mol Cell Biol *24*, 8813-8822.
Nottingham, W.T., Jarratt, A., Burgess, M., Speck, C.L., Cheng, J.F., Prabhakar, S., Rubin, E.M., Li, P.S., Sloane-Stanley, J., Kong, A.S.J.*, et al.* (2007). Runx1-mediated hematopoietic stem-cell emergence is controlled by a Gata/Ets/SCL-regulated enhancer. Blood *110*, 4188-4197.
Oka, C., Nakano, T., Wakeham, A., de la Pompa, J.L., Mori, C., Sakai, T., Okazaki, S., Kawaichi, M., Shiota, K., Mak, T.W.*, et al.* (1995). Disruption of the mouse RBP-J kappa gene results in early embryonic death. Development *121*, 3291-3301.
Ota, S., Zhou, Z.Q., Keene, D.R., Knoepfler, P., and Hurlin, P.J. (2007). Activities of N-Myc in the developing limb link control of skeletal size with digit separation. Development *134*, 1583-1592.
Ottersbach, K. (2019). Endothelial-to-haematopoietic transition: an update on the process of making blood. Biochem Soc Trans *47*, 591-601.
Otto, T., Horn, S., Brockmann, M., Eilers, U., Schuttrumpf, L., Popov, N., Kenney, A.M., Schulte, J.H., Beijersbergen, R., Christiansen, H.*, et al.* (2009). Stabilization of N-Myc is a critical function of Aurora A in human neuroblastoma. Cancer Cell *15*, 67-78.
Padron-Barthe, L., Temino, S., Villa del Campo, C., Carramolino, L., Isern, J., and Torres, M. (2014). Clonal analysis identifies hemogenic endothelium as the source of the blood-endothelial common lineage in the mouse embryo. Blood *124*, 2523-2532.
Panin, V.M., Shao, L., Lei, L., Moloney, D.J., Irvine, K.D., and Haltiwanger, R.S. (2002). Notch ligands are substrates for protein O-fucosyltransferase-1 and Fringe. J Biol Chem *277*, 29945-29952.
Pardanaud, L., Altmann, C., Kitos, P., Dieterlen-Lievre, F., and Buck, C.A. (1987). Vasculogenesis in the early quail blastodisc as studied with a monoclonal antibody recognizing endothelial cells. Development *100*, 339-349.
Pardanaud, L., Luton, D., Prigent, M., Bourcheix, L.M., Catala, M., and Dieterlen-Lievre, F. (1996). Two distinct endothelial lineages in ontogeny, one of them related to hemopoiesis. Development *122*, 1363-1371.
Park, C., Kim, T.M., and Malik, A.B. (2013). Transcriptional regulation of endothelial cell and vascular development. Circ Res *112*, 1380-1400.
Park, H.W., Chang, J.W., Yang, Y.S., Oh, W., Hwang, J.H., Kim, D.G., and Paek, S.H. (2015). The Effect of Donor-Dependent Administration of Human Umbilical Cord Blood-Derived Mesenchymal Stem Cells following Focal Cerebral Ischemia in Rats. Exp Neurobiol *24*, 358-365.
Peeters, M., Ottersbach, K., Bollerot, K., Orelio, C., de Bruijn, M., Wijgerde, M., and Dzierzak, E. (2009). Ventral embryonic tissues and Hedgehog proteins induce early AGM hematopoietic stem cell development. Development *136*, 2613-2621.
Pontes-Quero, S., Fernandez-Chacon, M., Luo, W., Lunella, F.F., Casquero-Garcia, V., Garcia-Gonzalez, I., Hermoso, A., Rocha, S.F., Bansal, M., and Benedito, R. (2019). High mitogenic stimulation arrests angiogenesis. Nat Commun *10*, 2016.
Pontes-Quero, S., Heredia, L., Casquero-Garcia, V., Fernandez-Chacon, M., Luo, W., Hermoso, A., Bansal, M., Garcia-Gonzalez, I., Sanchez-Munoz, M.S., Perea, J.R.*, et al.* (2017). Dual ifgMosaic: A Versatile Method for Multispectral and Combinatorial Mosaic Gene-Function Analysis. Cell *170*, 800-814 e818.
Quillien, A., Moore, J.C., Shin, M., Siekmann, A.F., Smith, T., Pan, L., Moens, C.B., Parsons, M.J., and Lawson, N.D. (2014). Distinct Notch signaling outputs pattern the developing arterial system. Development *141*, 1544-1552.
Rao, T.N., Marks-Bluth, J., Sullivan, J., Gupta, M.K., Chandrakanthan, V., Fitch, S.R., Ottersbach, K., Jang, Y.C., Piao, X., Kulkarni, R.N.*, et al.* (2015). High-level Gpr56 expression is dispensable for the maintenance and function of hematopoietic stem and progenitor cells in mice. Stem Cell Res *14*, 307-322.
Reya, T., Morrison, S.J., Clarke, M.F., and Weissman, I.L. (2001). Stem cells, cancer, and cancer stem cells. Nature *414*, 105-111.
Richard, C., Drevon, C., Canto, P.Y., Villain, G., Bollerot, K., Lempereur, A., Teillet, M.A., Vincent, C., Rossello Castillo, C., Torres, M.*, et al.* (2013). Endothelio-mesenchymal interaction controls runx1 expression and modulates the notch pathway to initiate aortic hematopoiesis. Dev Cell *24*, 600-611.
Rickman, D.S., Schulte, J.H., and Eilers, M. (2018). The Expanding World of N-MYC-Driven Tumors. Cancer Discov *8*, 150-163.
Riddell, J., Gazit, R., Garrison, B.S., Guo, G., Saadatpour, A., Mandal, P.K., Ebina, W., Volchkov, P., Yuan,

G.C., Orkin, S.H., *et al.* (2014). Reprogramming committed murine blood cells to induced hematopoietic stem cells with defined factors. Cell *157*, 549-564.
Rittie, L., and Fisher, G.J. (2005). Isolation and culture of skin fibroblasts. Methods Mol Med *117*, 83-98.
Robert-Moreno, A., Espinosa, L., de la Pompa, J.L., and Bigas, A. (2005). RBPjkappa-dependent Notch function regulates Gata2 and is essential for the formation of intra-embryonic hematopoietic cells. Development *132*, 1117-1126.
Robert-Moreno, A., Guiu, J., Ruiz-Herguido, C., Lopez, M.E., Ingles-Esteve, J., Riera, L., Tipping, A., Enver, T., Dzierzak, E., Gridley, T., *et al.* (2008). Impaired embryonic haematopoiesis yet normal arterial development in the absence of the Notch ligand Jagged1. EMBO J *27*, 1886-1895.
Rossant, J., and Tam, P.P.L. (2002). Mouse development : patterning, morphogenesis, and organogenesis (San Diego: Academic Press).
Roussel, M.F., and Robinson, G.W. (2013). Role of MYC in Medulloblastoma. Cold Spring Harb Perspect Med *3*.
Rowlinson, J.M., and Gering, M. (2010). Hey2 acts upstream of Notch in hematopoietic stem cell specification in zebrafish embryos. Blood *116*, 2046-2056.
Ruijtenberg, S., and van den Heuvel, S. (2016). Coordinating cell proliferation and differentiation: Antagonism between cell cycle regulators and cell type-specific gene expression. Cell Cycle *15*, 196-212.
Ruiz-Perez, M.V., Henley, A.B., and Arsenian-Henriksson, M. (2017). The MYCN Protein in Health and Disease. Genes (Basel) *8*.
Sahara, M., Hansson, E.M., Wernet, O., Lui, K.O., Spater, D., and Chien, K.R. (2014). Manipulation of a VEGF-Notch signaling circuit drives formation of functional vascular endothelial progenitors from human pluripotent stem cells. Cell Res *24*, 820-841.
Samokhvalov, I.M., Samokhvalova, N.I., and Nishikawa, S. (2007). Cell tracing shows the contribution of the yolk sac to adult haematopoiesis. Nature *446*, 1056-1061.
Samokhvalov, I.M., Thomson, A.M., Lalancette, C., Liakhovitskaia, A., Ure, J., and Medvinsky, A. (2006). Multifunctional reversible knockout/reporter system enabling fully functional reconstitution of the AML1/Runx1 locus and rescue of hematopoiesis. Genesis *44*, 115-121.
Sanchez-Martin, M., and Ferrando, A. (2017). The NOTCH1-MYC highway toward T-cell acute lymphoblastic leukemia. Blood *129*, 1124-1133.
Sato, Y. (2013). Dorsal aorta formation: separate origins, lateral-to-medial migration, and remodeling. Dev Growth Differ *55*, 113-129.
Satoh, Y., Matsumura, I., Tanaka, H., Ezoe, S., Sugahara, H., Mizuki, M., Shibayama, H., Ishiko, E., Ishiko, J., Nakajima, K., *et al.* (2004). Roles for c-Myc in self-renewal of hematopoietic stem cells. J Biol Chem *279*, 24986-24993.
Sawai, S., Shimono, A., Hanaoka, K., and Kondoh, H. (1991). Embryonic lethality resulting from disruption of both N-myc alleles in mouse zygotes. New Biol *3*, 861-869.
Sawai, S., Shimono, A., Wakamatsu, Y., Palmes, C., Hanaoka, K., and Kondoh, H. (1993). Defects of embryonic organogenesis resulting from targeted disruption of the N-myc gene in the mouse. Development *117*, 1445-1455.
Sharma, V.M., Calvo, J.A., Draheim, K.M., Cunningham, L.A., Hermance, N., Beverly, L., Krishnamoorthy, V., Bhasin, M., Capobianco, A.J., and Kelliher, M.A. (2006). Notch1 contributes to mouse T-cell leukemia by directly inducing the expression of c-myc. Mol Cell Biol *26*, 8022-8031.
Sjoqvist, M., and Andersson, E.R. (2019). Do as I say, Not(ch) as I do: Lateral control of cell fate. Dev Biol *447*, 58-70.
Solaimani Kartalaei, P., Yamada-Inagawa, T., Vink, C.S., de Pater, E., van der Linden, R., Marks-Bluth, J., van der Sloot, A., van den Hout, M., Yokomizo, T., van Schaick-Solerno, M.L., *et al.* (2015). Whole-transcriptome analysis of endothelial to hematopoietic stem cell transition reveals a requirement for Gpr56 in HSC generation. J Exp Med *212*, 93-106.
Song, Y., Kumar, V., Wei, H.X., Qiu, J., and Stanley, P. (2016). Lunatic, Manic, and Radical Fringe Each Promote T and B Cell Development. J Immunol *196*, 232-243.
Souilhol, C., Lendinez, J.G., Rybtsov, S., Murphy, F., Wilson, H., Hills, D., Batsivari, A., Binagui-Casas, A., McGarvey, A.C., MacDonald, H.R., *et al.* (2016). Developing HSCs become Notch independent by the end of maturation in the AGM region. Blood *128*, 1567-1577.
Spangrude, G.J. (1994). Biological and clinical aspects of hematopoietic stem cells. Annu Rev Med *45*, 93-104.
Stanton, B.R., Perkins, A.S., Tessarollo, L., Sassoon, D.A., and Parada, L.F. (1992). Loss of N-myc function results in embryonic lethality and failure of the epithelial component of the embryo to develop. Genes Dev *6*, 2235-2247.
Sudo, T., Yokota, T., Oritani, K., Satoh, Y., Sugiyama, T., Ishida, T., Shibayama, H., Ezoe, S., Fujita, N.,

Tanaka, H.*, et al.* (2012). The endothelial antigen ESAM monitors hematopoietic stem cell status between quiescence and self-renewal. J Immunol *189*, 200-210.
Susaki, E.A., Tainaka, K., Perrin, D., Kishino, F., Tawara, T., Watanabe, T.M., Yokoyama, C., Onoe, H., Eguchi, M., Yamaguchi, S.*, et al.* (2014). Whole-brain imaging with single-cell resolution using chemical cocktails and computational analysis. Cell *157*, 726-739.
Swiers, G., Baumann, C., O'Rourke, J., Giannoulatou, E., Taylor, S., Joshi, A., Moignard, V., Pina, C., Bee, T., Kokkaliaris, K.D.*, et al.* (2013). Early dynamic fate changes in haemogenic endothelium characterized at the single-cell level. Nat Commun *4*, 2924.
Takahashi, K., Nakayama, K., and Nakayama, K. (2000). Mice lacking a CDK inhibitor, p57Kip2, exhibit skeletal abnormalities and growth retardation. J Biochem *127*, 73-83.
Tanaka, M., Chen, Z., Bartunkova, S., Yamasaki, N., and Izumo, S. (1999). The cardiac homeobox gene Csx/Nkx2.5 lies genetically upstream of multiple genes essential for heart development. Development *126*, 1269-1280.
Tang, Y., Bai, H., Urs, S., Wang, Z., and Liaw, L. (2013). Notch1 activation in embryonic VE-cadherin populations selectively blocks hematopoietic stem cell generation and fetal liver hematopoiesis. Transgenic Res *22*, 403-410.
Taylor, P., Takeuchi, H., Sheppard, D., Chillakuri, C., Lea, S.M., Haltiwanger, R.S., and Handford, P.A. (2014). Fringe-mediated extension of O-linked fucose in the ligand-binding region of Notch1 increases binding to mammalian Notch ligands. Proc Natl Acad Sci U S A *111*, 7290-7295.
Thambyrajah, R., Mazan, M., Patel, R., Moignard, V., Stefanska, M., Marinopoulou, E., Li, Y., Lancrin, C., Clapes, T., Moroy, T.*, et al.* (2016a). GFI1 proteins orchestrate the emergence of haematopoietic stem cells through recruitment of LSD1. Nat Cell Biol *18*, 21-32.
Thambyrajah, R., Patel, R., Mazan, M., Lie, A.L.M., Lilly, A., Eliades, A., Menegatti, S., Garcia-Alegria, E., Florkowska, M., Batta, K.*, et al.* (2016b). New insights into the regulation by RUNX1 and GFI1(s) proteins of the endothelial to hematopoietic transition generating primordial hematopoietic cells. Cell Cycle *15*, 2108-2114.
Tirosh, I., Izar, B., Prakadan, S.M., Wadsworth, M.H., 2nd, Treacy, D., Trombetta, J.J., Rotem, A., Rodman, C., Lian, C., Murphy, G.*, et al.* (2016). Dissecting the multicellular ecosystem of metastatic melanoma by single-cell RNA-seq. Science *352*, 189-196.
Trumpp, A., Refaeli, Y., Oskarsson, T., Gasser, S., Murphy, M., Martin, G.R., and Bishop, J.M. (2001). c-Myc regulates mammalian body size by controlling cell number but not cell size. Nature *414*, 768-773.
Tsai, F.Y., Keller, G., Kuo, F.C., Weiss, M., Chen, J., Rosenblatt, M., Alt, F.W., and Orkin, S.H. (1994). An early haematopoietic defect in mice lacking the transcription factor GATA-2. Nature *371*, 221-226.
Uenishi, G.I., Jung, H.S., Kumar, A., Park, M.A., Hadland, B.K., McLeod, E., Raymond, M., Moskvin, O., Zimmerman, C.E., Theisen, D.J.*, et al.* (2018). NOTCH signaling specifies arterial-type definitive hemogenic endothelium from human pluripotent stem cells. Nat Commun *9*, 1828.
Varlakhanova, N.V., Cotterman, R.F., deVries, W.N., Morgan, J., Donahue, L.R., Murray, S., Knowles, B.B., and Knoepfler, P.S. (2010). myc maintains embryonic stem cell pluripotency and self-renewal. Differentiation *80*, 9-19.
Venkatesh, D.A., Park, K.S., Harrington, A., Miceli-Libby, L., Yoon, J.K., and Liaw, L. (2008). Cardiovascular and hematopoietic defects associated with Notch1 activation in embryonic Tie2-expressing populations. Circ Res *103*, 423-431.
Wakamatsu, Y., Maynard, T.M., Jones, S.U., and Weston, J.A. (1999). NUMB localizes in the basal cortex of mitotic avian neuroepithelial cells and modulates neuronal differentiation by binding to NOTCH-1. Neuron *23*, 71-81.
Wang, H., Zou, J., Zhao, B., Johannsen, E., Ashworth, T., Wong, H., Pear, W.S., Schug, J., Blacklow, S.C., Arnett, K.L.*, et al.* (2011). Genome-wide analysis reveals conserved and divergent features of Notch1/RBPJ binding in human and murine T-lymphoblastic leukemia cells. Proc Natl Acad Sci U S A *108*, 14908-14913.
Wang, H.U., Chen, Z.F., and Anderson, D.J. (1998). Molecular distinction and angiogenic interaction between embryonic arteries and veins revealed by ephrin-B2 and its receptor Eph-B4. Cell *93*, 741-753.
Wang, L., Liu, T., Xu, L., Gao, Y., Wei, Y., Duan, C., Chen, G.Q., Lin, S., Patient, R., Zhang, B.*, et al.* (2013). Fev regulates hematopoietic stem cell development via ERK signaling. Blood *122*, 367-375.
Weinstein, B.M., Stemple, D.L., Driever, W., and Fishman, M.C. (1995). Gridlock, a localized heritable vascular patterning defect in the zebrafish. Nat Med *1*, 1143-1147.
Weng, A.P., Millholland, J.M., Yashiro-Ohtani, Y., Arcangeli, M.L., Lau, A., Wai, C., Del Bianco, C., Rodriguez, C.G., Sai, H., Tobias, J.*, et al.* (2006). c-Myc is an important direct target of Notch1 in T-cell acute lymphoblastic leukemia/lymphoma. Genes Dev *20*, 2096-2109.
Westermann, F., Muth, D., Benner, A., Bauer, T., Henrich, K.O., Oberthuer, A., Brors, B., Beissbarth, T.,

Vandesompele, J., Pattyn, F., *et al.* (2008). Distinct transcriptional MYCN/c-MYC activities are associated with spontaneous regression or malignant progression in neuroblastomas. Genome Biol *9*, R150.
Wilkinson, A.C., Ishida, R., Kikuchi, M., Sudo, K., Morita, M., Crisostomo, R.V., Yamamoto, R., Loh, K.M., Nakamura, Y., Watanabe, M., *et al.* (2019). Long-term ex vivo haematopoietic-stem-cell expansion allows nonconditioned transplantation. Nature.
Wilkinson, R.N., Pouget, C., Gering, M., Russell, A.J., Davies, S.G., Kimelman, D., and Patient, R. (2009). Hedgehog and Bmp polarize hematopoietic stem cell emergence in the zebrafish dorsal aorta. Dev Cell *16*, 909-916.
Wilson, N.K., Timms, R.T., Kinston, S.J., Cheng, Y.H., Oram, S.H., Landry, J.R., Mullender, J., Ottersbach, K., and Gottgens, B. (2010). Gfi1 expression is controlled by five distinct regulatory regions spread over 100 kilobases, with Scl/Tal1, Gata2, PU.1, Erg, Meis1, and Runx1 acting as upstream regulators in early hematopoietic cells. Mol Cell Biol *30*, 3853-3863.
Xu, A., Haines, N., Dlugosz, M., Rana, N.A., Takeuchi, H., Haltiwanger, R.S., and Irvine, K.D. (2007). In vitro reconstitution of the modulation of Drosophila Notch-ligand binding by Fringe. J Biol Chem *282*, 35153-35162.
Xue, Y., Gao, X., Lindsell, C.E., Norton, C.R., Chang, B., Hicks, C., Gendron-Maguire, M., Rand, E.B., Weinmaster, G., and Gridley, T. (1999). Embryonic lethality and vascular defects in mice lacking the Notch ligand Jagged1. Hum Mol Genet *8*, 723-730.
Yang, L.T., Nichols, J.T., Yao, C., Manilay, J.O., Robey, E.A., and Weinmaster, G. (2005). Fringe glycosyltransferases differentially modulate Notch1 proteolysis induced by Delta1 and Jagged1. Mol Biol Cell *16*, 927-942.
Yoder, M.C. (2014). Inducing definitive hematopoiesis in a dish. Nat Biotechnol *32*, 539-541.
Yokomizo, T., and Dzierzak, E. (2010). Three-dimensional cartography of hematopoietic clusters in the vasculature of whole mouse embryos. Development *137*, 3651-3661.
Yokomizo, T., Ogawa, M., Osato, M., Kanno, T., Yoshida, H., Fujimoto, T., Fraser, S., Nishikawa, S., Okada, H., Satake, M., *et al.* (2001). Requirement of Runx1/AML1/PEBP2alphaB for the generation of haematopoietic cells from endothelial cells. Genes Cells *6*, 13-23.
Yoshida, G.J. (2018). Emerging roles of Myc in stem cell biology and novel tumor therapies. J Exp Clin Cancer Res *37*, 173.
You, L.R., Lin, F.J., Lee, C.T., DeMayo, F.J., Tsai, M.J., and Tsai, S.Y. (2005). Suppression of Notch signalling by the COUP-TFII transcription factor regulates vein identity. Nature *435*, 98-104.
Zape, J.P., Lizama, C.O., Cautivo, K.M., and Zovein, A.C. (2017). Cell cycle dynamics and complement expression distinguishes mature haematopoietic subsets arising from hemogenic endothelium. Cell Cycle *16*, 1835-1847.
Zaytseva, O., and Quinn, L.M. (2017). Controlling the Master: Chromatin Dynamics at the MYC Promoter Integrate Developmental Signaling. Genes (Basel) *8*.
Zhen, F., Lan, Y., Yan, B., Zhang, W., and Wen, Z. (2013). Hemogenic endothelium specification and hematopoietic stem cell maintenance employ distinct Scl isoforms. Development *140*, 3977-3985.
Zhong, T.P., Childs, S., Leu, J.P., and Fishman, M.C. (2001). Gridlock signalling pathway fashions the first embryonic artery. Nature *414*, 216-220.
Zhou, F., Li, X., Wang, W., Zhu, P., Zhou, J., He, W., Ding, M., Xiong, F., Zheng, X., Li, Z., *et al.* (2016). Tracing haematopoietic stem cell formation at single-cell resolution. Nature *533*, 487-492.
Zhou, Z.Q., Shung, C.Y., Ota, S., Akiyama, H., Keene, D.R., and Hurlin, P.J. (2011). Sequential and coordinated actions of c-Myc and N-Myc control appendicular skeletal development. PLoS One *6*, e18795.
Zimmerman, K.A., Yancopoulos, G.D., Collum, R.G., Smith, R.K., Kohl, N.E., Denis, K.A., Nau, M.M., Witte, O.N., Toran-Allerand, D., Gee, C.E., *et al.* (1986). Differential expression of myc family genes during murine development. Nature *319*, 780-783.

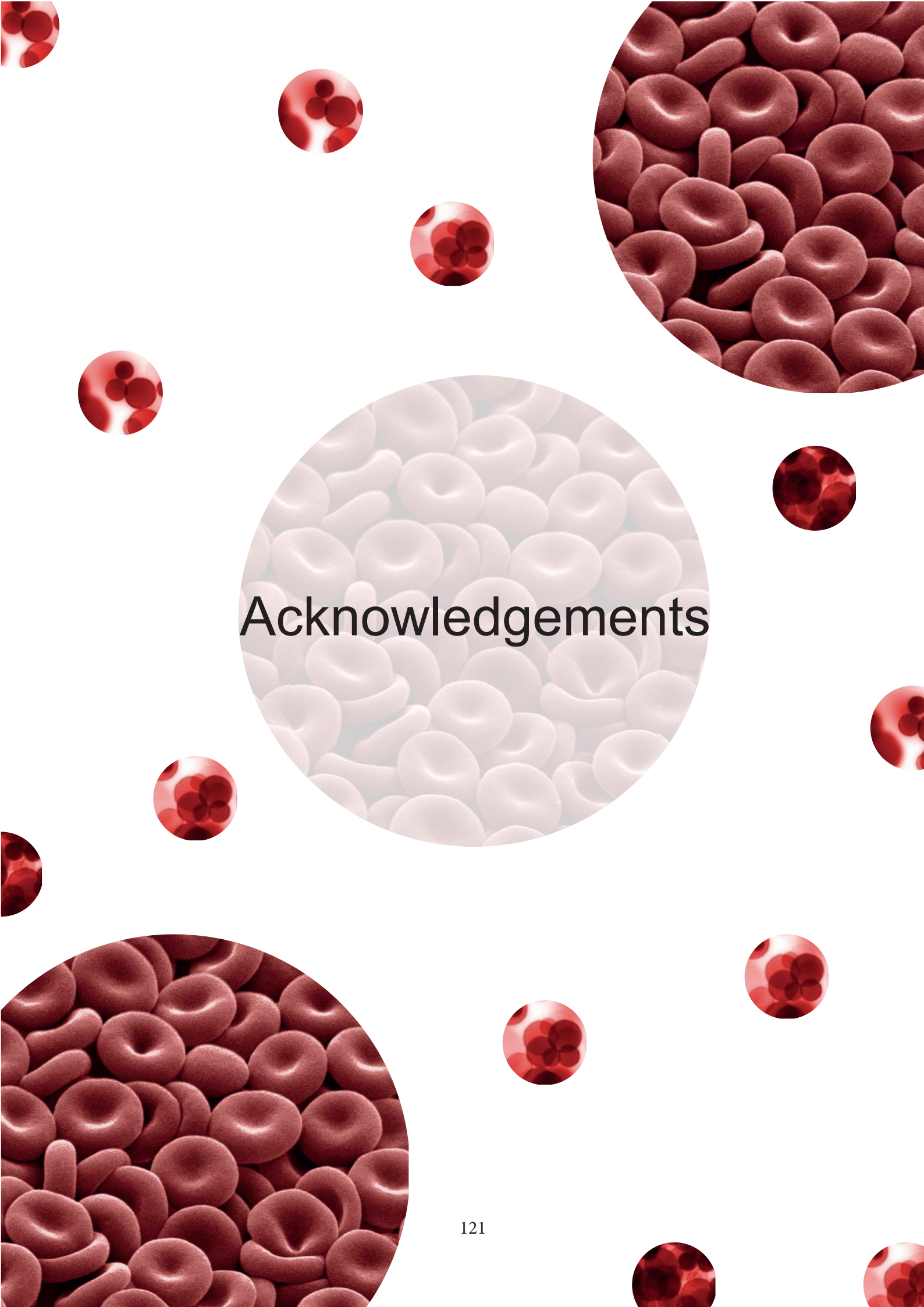

Acknowledgements

Acknowledgements

"Happiness can be found even in the darkest of times,
when one only remembers to turn on the light."
Dumbledore, Harry Potter

A Ph.D. experience can be full of darkness: dark corridors and dark rooms. I can't even count the amount of times I have been in the dim microscopy rooms, spending hours in what can only be considered the place that inspired Winterfell, taking the images that you see in this thesis. Or, walking down the halls whose motion-sensored lights only turn on when you are already half-way to your destination. The -2 corridor seems like a scene in the Walking Dead, and with my imagination, it was difficult trying not to imagine zombies coming towards me in the darkness. But perhaps the most haunting darkness is the one that happens all in our heads Let's admit it; the thesis is hard stuff! The amount of fails is always greater than the wins. The data doesn't make sense, or the plug check was negative, or the images are not crisp enough. The days are long and paradoxically there is not enough time to get that extra result that you need. This mental darkness can be depressing. But, as Dumbledore said, one must remember to turn on the light, and in my experience, I found that the people around me were that source of brightness. Here, I would like to acknowledge those who made sure I was never in the shadows.

First and foremost, to my family: To my mother and grandmother, this doctoral title is yours as much as it is mine. All of my achievements, all of my triumphs, all that I am, is because of you two. Thank you for every sacrifice you have ever done to provide for me. Thank you Mom for taking those extra shifts at work, thank you for getting me that Harry Potter book, thank you for getting me those science models of the human body, thank you for letting me move to a different country, and thank you for encouraging me to explore and see the world. Grandma, thank you for waking me up super early for school every day, thank you for making sure I ate all of my oatmeal, thank you for telling me to never settle, and thank you for letting me know that I can move mountains. I am able to stand where I am today because you two built an unshakeable foundation. In the random, chaotic assignment of beings, I am honored and blessed to have been born into our family. To my little brother, I am so proud of the man you are becoming. I know that anything you set your mind to will flourish into a beautiful reality. Don't be too hard on Ma and Grandma, they always mean well. To my bestie Giuli, who is basically family, thank you for the marathon phone sessions and basically for being my free therapist throughout the years. I'm so glad that we have remained close after all these years (even our horrible boatride in Indonesia was not enough to make me question ever knowing you). Vivi, my amazing flatmate, thank you for helping me grow as a woman. I would not be so informed of the world, so ready to take a stance on what I find important, nor so cultured if it weren't for you.

To my group: Thank you **Rui** for the opportunity to work in your laboratory; I have learned so much. To the members in my group, past and present: **Sofia**, although you are years younger than me, you took so much care of me. I am so happy to have seen you progress through life and see you get married and have your beautiful baby boy! **Irene**, my little rebel, you are such a feisty one, we need more people like you to question the world and make it better. **Maca**, your optimism is one I could never understand, but that energy helped at times when I needed extra encouragement. **Wen**, sweet Wencito, thank you for your "interesting" theories throughout the years. **Ivana,** remember the art of slowing down, you run so fast all I see is a blur. Thanks for listening to my mycn hypothesis and helping me create fun experiments to try. **Carlos,** you are the funniest and smartest guy I know; we really missed you in the laboratory. **Aroa,** you should be a private investigator, how are your theories always right? **Nestor,** my Peruvian brother, say perhaps to finally bringing me that tupper I have been begging years for. **Veronica**, thanks for always laughing at my jokes and complimenting me on my English. **Mayank,** keep calm and carry on! **Sarita,** you were always so kind to me, thank you for daily encouragement. **Tania,** after all these years, you take a train to come down and see me on my special day. Thank you! **Luis,** hombre, you are a sweet man who provides advice and humor in any situation.

JLP group: **Marcos,** how can a giant be such a teddy bear? Thank you for your hugs and jokes and pranks and piggyback-rides (although I do not forgive you for dropping me that one time). I don't think this experience would have been complete without you. **Tamara,** little sister, I'm so glad that I was able to share so many moments with you in the short amount of time that I have known you. You are so sweet and loving and funny

and sarcastic, and I enjoyed knowing you. **Ana,** another younger person with an incredible sense of self-worth, you are amazing and smart and also sarcastic (I must have a thing for sarcastic people). I admire you so much! **Ale, Vanessa, Dimi, Vera, Rebeca**[2], **Quim (**silver fox**), Vitor, Donal, Luis,** and past member of the group, **Patri, Lao, Paula, and Gaetano** it was all so fun to be with you guys through Notch meetings, afterwork drinks, concerts, and the daily hussle and bussle of the lab.

MT group: **Ghislaine,** my French sista! Your incredible ability to pour love into people was so comforting. 95% of the time with you was spent dancing, singing, laughing, and dancing some more. Thank you for sharing your beautiful family with me; they became my family away from home. **Noelia**, a force to be reckoned with, you have taught me so much about putting my foot down and walking with confidence. If I wasn't dancing with Ghislaine, I was dancing with you. Thanks for all that exercise girls, go cardio!! **Rocio**, extra thanks to you for helping me with the mice. Without you, I don't think I would even have a project. **Susana, Lin, Sandra, Cristina, José, Ester, Morena, Vane, Bea, and Miguel** I enjoyed all of our time together. You are all amazing people and I am incredibly lucky to have spent these years by your side.

NM group: **Maria,** words are not sufficent enough to acknowledge how thankful I am to you. You really took me under your wing. You were there to help me move, you invited me into your home for Christmas every year, you never failed to remember my birthday. You are a treasure! It is not enough for everything you have done, but THANK YOU! **Carlos**, you never taught me how to box but the random play fights in the hallway made up for it.

MMF group: **Sergio**, **Julio,** and **Melisa,** my first friends from the 3S, 4 years with you guys wasn't enough. Thanks for the parties, the tattoo, the books, the encouragement, and the laughs. **Claudio**, hombre, you also really took care of me. Thank you for the mountain hikes (yes, even the one where I almost shattered my hips), the cervezas, and the chats we've had throughout these years. **Jesús, Antonio,** and **María,** thanks for putting up with my constant craziness in the 3S. I'm pretty sure I've had a major dance session with each of you in the afternoons when reggaeton was our only saving grace from insanity.

AB group: **Cris**, pequeña Sevillana, my memory of us is a mixture of latin music, crepes, and cocktails. **Cris,** I love your accent, everytime I was repeating it, I promise it was to try and adopt it myself. **Silvia,** you are a real sweetheart. **Mariya,** hermana ucrania, in the short time I have known you, you have become such a great friend. Girls thanks for the birthday dinners, the weekend celebrations, and the afterwork beers. The four of you are phenomenal!

JAC group: **Diana, Carla, Carmen**, and **Maria,** if we weren't bumping into each other in the bathroom than we were joking around in the nanodrop. Thanks for sharing your smiles. Every time I walked into the 3S I felt the instant warmth and happiness provided by you girls.

To friends **Magda**, **Simon,** and **Ian**, thanks for the encouragement and conversations, the dinners and the dance shows. I have fond memories of all of you!

Last and not least, to the units of CNIC:

Cellomics: **Raquel, Elena, Mariano**, and **Jose**, normally the prospect of trying to isolate ECs from E10.5 was a nightmare but once I passed those sliding glass doors, all of that melted away. Thanks for creating miracles and somehow always finding my cells, I still don't know how you did it.

Microscopy: **Valeria,** thank you for being so kind to my grandma when she came to visit; the coffee was delicious. And thank you for the work you put into getting the SP8, it was awesome working with it! **Elvira**, and **Veronica,** none of the images would have been possible without you two. Thank you for your patience when I thought the microscope was against me and for always being there to help get crisper images.

Animalario: **Sandra, Gonzalo,** and **Merche,** the unseen heros, thank you for always, ALWAYS, being on top of the mice. I know there were many times when I would forget to put a petition and you three were always so accomodating to help me do the experiments that I needed to do. Just like those in Microscropy and Cellomics, this project would have been pure imagination without you.

Vale.